ISABELLE CRISTINA OLIVEIRA NEVES

α-TOCOPHEROL ENCAPSULATION IN ORA-PRO-NOBIS (*Pereskia aculeata* Miller) MUCILAGE-WHEY PROTEIN ISOLATE MICROPARTICLES

LAVRAS – MG
2020

ISABELLE CRISTINA OLIVEIRA NEVES

α-TOCOPHEROL ENCAPSULATION IN ORA-PRO-NOBIS (*Pereskia aculeata* Miller) MUCILAGE-WHEY PROTEIN ISOLATE MICROPARTICLES

Tese apresentada à Universidade Federal de Lavras, como parte das exigências do Programa de Pós-Graduação em Ciência dos Alimentos, área de concentração em Ciência dos Alimentos, para a obtenção do título de Doutor.

Prof. Dr. Jaime Vilela de Resende
Orientador

Prof. Dra. Lizzy Ayra Alcântara Veríssimo
Coorientadora

Prof. Dr. Michael A. Rogers
Coorientador

LAVRAS – MG
2020

Ficha catalográfica elaborada pelo Sistema de Geração de Ficha Catalográfica da Biblioteca Universitária da UFLA, com dados informados pelo(a) próprio(a) autor(a).

Neves, Isabelle Cristina Oliveira.
α-Tocopherol encapsulation in ora-pro-nobis (*Pereskia aculeata* Miller) mucilage-whey protein isolate microparticles. Brasil. / Isabelle Cristina Oliveira Neves,. - 2020.
85 p. : il.

Orientador: Jaime Vilela de Resende.
Coorientador: Lizzy Ayra Alcântara Veríssimo, Michael A. Rogers
Tese (doutorado) - Universidade Federal de Lavras, 2020.
Bibliografia.

1. Encapsulation. 2. α-Tocopherol. 3. Bioaccessibility. I. Resende, Jaime Vilela de. II. Veríssimo, Lizzy Ayra Alcântara. III. Michael, Rogers. IV. Título.

ISABELLE CRISTINA OLIVEIRA NEVES

α-TOCOPHEROL ENCAPSULATION IN ORA-PRO-NOBIS (*Pereskia aculeata* Miller) MUCILAGE -WHEY PROTEIN ISOLATE MICROPARTICLES

ENCAPSULAMENTO DE α -TOCOFEROL EM MICROPARTÍCULAS PRODUZIDAS A PARTIR DE MUCILAGE DE ORA-PRO-NOBIS (*Pereskia aculeata* Miller) E ISOLADO PROTEICO DE SORO DE LEITE

Tese apresentada à Universidade Federal de Lavras, como parte das exigências do Programa de Pós-Graduação em Ciência dos Alimentos, área de concentração em Ciência dos Alimentos, para a obtenção do título de Doutor.

APROVADA em 17 de fevereiro de 2020.

Dr. Fabiano Freire Costa	UFJF
Dra. Lanamar de Almeida Carlos	UFSJ
Dra. Lizzy Ayra Alcântara Veríssimo	UFLA
Dra. Vanelle Maria da Silva	UFV

Prof. Dr. Jaime Vilela de Resende
Orientador

LAVRAS – MG
2020

AGRADECIMENTOS

Agradeço a Deus por nunca me deixar sozinha, por me guiar e sustentar todos os dias durante minha trajetória de estudos, possibilitando que eu concluísse mais essa etapa da minha vida. Graças à Ele por me iluminar e dar ânimo para que eu perseverasse até o fim.

Agradeço à Universidade Federal de Lavras (UFLA) e ao Departamento de Ciência dos Alimentos (DCA) pela oportunidade concedida para a realização da Pós-Graduação. À Coordenação de Aperfeiçoamento de Pessoal de Nível Superior (CAPES) e ao Conselho Nacional de Desenvolvimento Científico e Tecnológico (CNPq) pela concessão da bolsa de estudos. À Fundação de Amparo à Pesquisa do Estado de Minas Gerais (FAPEMIG) pelo auxílio financeiro à pesquisa.

Agradeço aos meus pais, Geraldo e Elda, por todo amor, carinho, compreensão e apoio incondicional que sempre me deram. Obrigada por se preocuparem se eu estava bem e por me acompanharem em cada mudança de cidade e república durante todos esses anos. Obrigada por guardarem marmitex com minhas comidas preferidas, que me salvaram sempre que eu não tinha comida pronta e nem queria cozinhar. Agradeço também à minha irmã Larissa por sempre me botar pra cima, acreditando que eu poderia trabalhar até na CIA se quisesse. Agradeço pelo companheirismo e por todas as risadas que tivemos juntas, enquanto discutíamos do nosso futuro após o fim dos nossos estudos. Agradeço às minhas avós, Marli e Marta, por sempre me incluírem em suas orações e por torcerem por minha felicidade, acima de tudo.

Agradeço às pessoas maravilhosas e super inteligentes do Laboratório de Refrigeração de Alimentos, Amanda, Ana Cristina, Adrise, Camilla, Larissa, Natália, Sergio, Sarita, Thamires e Yasmin por tornarem meus dias mais alegres e leves, por discutirem meus resultados comigo e me animarem quando os experimentos estavam dando errado. Em especial, quero agradecer ao Esquadrão Suicida (Amanda, Natália e Sérgio) por serem meus companheiros de todas as horas, por me chamarem pra sair e por me ajudarem em tudo o que precisei. Vocês sempre estarão comigo, independente de onde estivermos morando. Agradeço aos meus amigos que estavam distantes, Fernanda (Dita), Hiani, Jamille, Nátália, Samira, Izabela, Fernanda, Maria Elisa, Antonio Vinicius, Greissz, Yara, Paula Chequer e Thaís, mas que sempre conseguiam uma maneira de se fazerem presentes.

Agradeço ao meu orientador, professor Jaime Vilela de Resende por ter aberto as portas do seu laboratório para minha pesquisa, pela confiança, por toda atenção, conhecimento e orientação. À coorientadora Lizzy pelo carinho, por ter contribuído para melhoria do trabalho e por ter sempre disponibilidade para ajudar. Ao Dr. Michael Rogers, professor da University

of Guelph (Canadá), por ter me aceitado em seu grupo de pesquisa, por ter colocado à minha disposição todos os recursos do seu laboratório, e por todo conhecimento transmitido.

À Dra. Lanamar de Almeida Carlos, à Dra. Vanelle Maria da Silva e ao Dr. Fabiano Freire Costa, por terem aceitado participar da banca de defesa contribuindo para a melhoria do trabalho.

Obrigada a todos que contribuíram para concretização deste momento. Com vocês, minha jornada foi mais leve e feliz! Vamos juntos celebrar essa vitória!

“Porque Deus é o que opera em vós tanto o querer como o efetuar, segundo a sua boa vontade. Até aqui nos ajudou o Senhor.” (Filipenses 2:13; 1 Samuel 7:12)

RESUMO

Micropartículas de isolado proteico de soro de leite (WPI) e mucilagem de ora-pro-nobis (OPN) com α-tocoferol encapsulado foram preparadas utilizando óleo insaturado de cadeia longa (óleo de canola (CA)) ou óleo saturado de cadeia média (óleo de coco (CO)) como fase lipídica carreadora. As micropartículas foram produzidas pela liofilização de emulsões de CO- ou CA-em água, com várias proporções de WPI/OPN. Anteriormente à liofilização, as emulsões apresentaram comportamento Newtoniano ou pseudoplástico. Menores valores de diâmetro médio de gota (230,37 nm) e índice de polidispersidade (0,144), e maior módulo do potencial zeta (-49,63 mV) foram encontrados para tratamentos com menor conteúdo de OPN e preparados com CO. Os rendimentos de secagem para as emulsões liofilizadas variaram entre 74,1% e 87,1% m/m, dependendo da razão entre biopolímeros e se CA ou CO foi utilizado como carreador. As proporções de WPI:OPN (entre 23:1 e 7:1) e o tipo de fase oleosa (CO ou CA) não afetaram significativamente as propriedades físicas da micropartícula (como retenção de óleo, umidade e atividade de água). Maior densidade aparente de pó (0,22 $g \cdot cm^{-3}$) e eficiência de encapsulamento (79,8% m/m) foram obtidas pela liofilização de tratamentos contendo CO, comparadas às emulsões CA-em-água e com maiores concentrações de OPN. A rugosidade da superfície das micropartículas aumentou com o aumento da concentração de OPN, independente do óleo carreador utilizado, como observado pela microscopia eletrônica de varredura. Durante os 35 dias do teste de estabilidade, a retenção de α-tocoferol e a cinética de degradação diferiram entre CO e CA e dependeram da umidade relativa em que o pó foi armazenado. Picos de absorbância característicos a grupamentos encontrados na estrutura de proteínas, carboidratos, α-tocoferol e lipídeos (CA e CO) foram observados nos espectros da espectroscopia de infravermelho. A bioacessibilidade do α-tocoferol encapsulado foi maior quando utilizado CA WPI/OPN (23:1) (55,0±1,89%) em comparação com o CO WPI/OPN (23:1) (42,4±1,78%), enquanto a taxa de liberação de α-tocoferol e o tempo de indução foram estaticamente equivalentes para todos os tratamentos. Conclui-se que o tratamento CO WPI:OPN (23:1) foi o que apresentou melhor desempenho para uma possível aplicação industrial, uma vez que manteve alta retenção do bioativo durante o teste de estabilidade ao armazenamento e alta bioacessibilidade.

Palavras-chave: Vitamina E; Óleo de canola; Óleo de coco; Cinética de degradação; Comportamento isotérmico; Óleo transportador; Bioacessibilidade.

ABSTRACT

Microparticles of whey protein isolate (WPI) and ora-pro-nobis mucilage (OPN) encapsulated α-tocopherol were made using long-chain unsaturated (e.g., canola oil (CA)) or medium-chain saturated oil (e.g., coconut oil (CO)) as the carrier oil. Microparticles were produced from CO- or CA-in-water emulsions by freeze-drying emulsions with various ratios of WPI/OPN. Before freeze dying, emulsions exhibited Newtonian or shear-thinning behavior. Smaller values of mean droplet diameter (230.37 nm) and polydispersity index (0.144), and higher zeta potential modulus (-49.63 mV) were found for treatments with lower OPN content and prepared with CO. Drying yields for freeze-dried emulsions ranged between 74.1% to 87.1% w/w, depending on the biopolymers ratio and varied depending on whether CA or CO was used as the carrier. WPI:OPN ratios (between 23:1 and 7:1) nor oil phase (CO or CA) significantly affected the physical properties (e.g., oil retention, water content, and activity) of the dried powder between treatments. Higher powder bulk density (0.22 $g \cdot cm^{-3}$) and encapsulation efficiency (79.8% w/w) were obtained from freeze-drying CO, compared to CA-in-water emulsions and with higher concentrations of OPN. The surface roughness of the microparticles increased with increments in OPN concentration, regardless the carrier oil used, as observed by scanning electron microscopy. Over 35 days, α-tocopherol retention and degradation kinetics differed between CO and CA and was dependent on relative humidity. Absorbance peaks characteristic of groups found in the structure of proteins, carbohydrates, α-tocopherol and lipids (CA and CO) were observed in the infrared spectroscopy spectra. Bioaccessibility of encapsulated α-tocopherol was higher with CA WPI/OPN (23:1) (55.0±1.89%) compared to CO WPI/OPN (23:1) (42.4±1.78%), while the rate of α-tocopherol release and induction time for release were statically equal. It is concluded that the CO WPI:OPN (23:1) treatment was the one that presented the best performance for a possible industrial application, since it maintained high bioactive retention during the storage stability test and high bioaccessibility.

Keywords: Vitamin E; Canola oil; Coconut oil; Degradation kinetics; Isothermal behavior; Carrier oil; Bioaccessibility.

LISTA DE FIGURAS

PRIMEIRA PARTE

SEGUNDA PARTE

ARTIGO

SUPPLEMENTARY

LISTA DE TABELAS

SEGUNDA PARTE

ARTIGO

LISTA DE SIGLAS

ANOVA	Analysis of variance
CA	Canola oil
CO	Coconut oil
DVS	Dynamic vapor sorption
FTIR	Fourier Transform Infrared Spectroscopy
GAB	Guggenheim, Ander- son and de Boer
GI	Gastrointestinal
HPMC	Hydroxypropyl-methylcellulose
HPLC	High performance liquid chromatography
OPN	Ora-pro-nobis mucilage
OR	Oil retention
PDI	Polydispersity index
RDA	Recommended Dietary Allowance
RH	Relative humidity
RMSE	Root-mean-square error
SEM	Scanning electron microscopy
SIES	Small intestinal electrolyte solution
WPI	Whey protein isolate
TIM-1	TNO gastro-intestinal model

LISTA DE SÍMBOLOS

a_w	Water activity (dimensionless)
BD	Bulk density ($g \cdot cm^{-3}$)
C	Model constants (dimensionless)
$C(t)$	α-tocopherol (%) released as a function of time (min)
C_0	α-tocopherol concentration after powder production ($mg \cdot L^{-1}$)
C_{asymp}	Maximum α-tocopherol bioaccessibility (%)
C_T	α-tocopherol concentration as a function of time ($mg \cdot L^{-1}$)
d_i	Average droplet diameter (nm)
EE	Encapsulation efficiency (%)
K	Consistency index ($Pa \cdot s^n$)
k	First order rate constant ($days^{-1}$) – for half-life
k	Model constant (dimensionless) – for sorption isotherms
k	Rate constant (min^{-1}) – for bioaccessibility
m	Equilibrium moisture content (g water/100 g dry basis)
m	Mass (g) – for bulk density
m_0	Monolayer moisture content (g water/100 g dry basis)
n	Flow behavior index (dimensionless)
R^2	Coefficient of determination
SO	Non-encapsulated oil (g)
t	Time (days)
$t_{1/2}$	Half-life time (days)
t_c	Induction time (min)
TO	Total oil (g)
TR_{35}	α-tocopherol retention after 35 of storage (dimensionless)
V	Volume (cm^3)
γ	Shear rate (s^{-1})
ζ-potential	Zeta-potencial (mV)
η_{100}	Apparent viscosity at 100 s^{-1} ($mPa \cdot s$)
μ	Newtonian viscosity ($Pa \cdot s$)
τ	Shear stress (Pa)

SUMÁRIO

PRIMEIRA PARTE

1 INTRODUÇÃO GERAL

Em um cenário de constante competitividade nos setores alimentício, cosmético e farmacêutico, a utilização de moléculas bioativas encapsuladas na formulação de produtos funcionalizados segue em crescente tendência como uma forma de inovação. Compostos bioativos podem ser definidos como substâncias capazes de promover benefícios à saúde, por meio da prevenção ou retardamento do aparecimento de doenças, devido à sua ação antioxidante e/ou anti-inflamatória, por exemplo. Dentre os antioxidantes, destaca-se a vitamina E, sendo o α-tocoferol a forma biologicamente mais ativa desta vitamina. É relatado que seu consumo reduz os riscos associados a doenças cardiovasculares, minimiza efeitos de envelhecimento e reduz a probabilidade de ocorrência de doenças relacionadas à presença de radicais livres, como o câncer. Entretanto, na sociedade ocidental em que o consumo de alimentos ultra processados é predominante, a ingestão desta vitamina é menor do que a dose diária recomendada para adultos. Além disso, por ser uma vitamina lipofílica, sua incorporação em matrizes alimentares, que na sua maioria são hidrofílicas, torna-se um desafio. Sua inclusão em formulações de alimentos ultraprocessados, com objetivo de aumentar o valor nutricional, pode agregar valor ao produto e atrair a preferência do consumidor.

O microencapsulamento é uma técnica capaz de conferir maior estabilidade a um composto de interesse durante o período de estocagem por protegê-lo de condições adversas, tais como contato com oxigênio, luz, enzimas, umidade, valores de pH extremos, além de mascarar odor e sabor indesejáveis. Isto é alcançado por meio da formação de uma camada protetora em torno de um núcleo contendo o bioativo, que controla sua liberação e reduz a ocorrência de reações que podem alterar a estrutura molecular do soluto, eliminando sua atividade biológica. Emulsões são sistemas ideais para o encapsulamento de compostos anfifílicos e hidrofóbicos, como a vitamina E, pois facilitam a incorporação destas moléculas em meios aquosos. A seleção do material de parede apropriado e do núcleo depende da técnica de encapsulamento, propriedades físicas do material do núcleo e custo.

Óleos vegetais têm sido utilizados como principal fonte lipídica na alimentação por serem abundantes e com custo de extração acessível. O óleo de canola é formado, principalmente, de ácidos graxos insaturados de cadeia longa, enquanto o óleo de coco compõe-se de ácidos graxos saturados de cadeia média. Quando utilizadas como carreadores, as

características estruturais de seus triglicerídeos podem interferir na eficiência do encapsulamento, bem como na bioacessibilidade do bioativo encapsulado.

Não existe uma solução única no design de micropartículas e, embora seja possível usar um único polímero como material de parede, o encapsulamento utilizando múltiplos componentes é geralmente preferido. Neste caso, as diferentes propriedades atribuídas a cada polímero podem ser combinadas para projetar camadas protetoras mais eficientes em torno das substâncias bioativas. Uma diversidade de polímeros que pode ser utilizada na obtenção de micropartículas, entretanto, a utilização de matérias-primas de origem natural (ao invés de sintética), como os polissacarídeos e proteínas, tem sido preferida pelo consumidor, pois são atóxicos, apresentam custo acessível e são biodegradáveis.

As proteínas do soro do leite têm sido utilizadas em vários produtos processados, como bebidas, alimentos saudáveis, lácteos e fórmulas para bebês, contribuindo consideravelmente com a dose de proteínas ingerida. Além disso, por apresentarem capacidade gelificante, emulsificante e espumante, podem ser utilizadas no encapsulamento e liberação controlada de compostos bioativos. A mucilagem de ora-pro-nobis é extraída das folhas da espécie *Pereskia aculeata* Miller, que é um planta com origem no Brasil, de cultivo perene, fácil propagação e resistente a climas secos e, por isso, possui alto potencial de utilização. Aliado a isso, a mucilagem apresenta grandes quantidades de polissacarídeos (arabinogalactana) e de proteínas em sua estrutura, conferindo-lhe ação gelificante, emulsificante e espumante.

Após a produção e caracterização de micropartículas contendo um bioativo encapsulado, sua absorção pode ser analisada utilizando metodologias *in vitro* que simulam as condições do trato gastrointestinal superior humano em termos do ambiente fisiológico e eventos cinéticos. O modelo TNO TIM-1 é um sistema dinâmico automatizado que imita os principais eventos que ocorrem durante a digestão nos compartimentos do estômago e intestino delgado (duodeno, jejuno e íleo), como o movimento peristáltico do estômago e intestino, regulação do pH, temperatura, atividade enzimática, tempo de trânsito e liberação de secreções gastrointestinais. Desta maneira, é possível obter informações sobre a bioacessibilidade de compostos de forma realista, já que esse modelo foi validado e correlacionado estatisticamente com estudos *in vivo* em humanos. O conhecimento da fração bioacessível de um composto ativo, como o α-tocoferol, pode auxiliar na definição dos materiais de parede/núcleo ideais para sua incorporação em matrizes alimentares. Além disso, pode-se verificar se, de fato, o bioativo mantém-se íntegro e disponível para ser absorvido e utilizado no metabolismo, a fim de que se possa tirar proveito do benefício destas substâncias com atividade biológica.

Até o momento, não foram relatados estudos explorando os efeitos do óleo carreador sobre misturas de mucilagem de OPN e isolado proteico de soro de leite na microencapsulação de α-tocoferol. Com base neste contexto, este trabalho objetivou utilizar a mucilagem extraída das folhas de ora-pro-nobis combinada com isolado proteico de soro de leite como um material de parede alternativo para o microencapsulamento de α-tocoferol por liofilização, utilizando óleo de canola ou óleo de coco como veículo para solubilização do bioativo. Primeiramente, uma emulsão óleo em água foi produzida e caracterizada em termos de viscosidade, tamanho médio da gota e potencial zeta. Em seguida, as micropartículas obtidas pela secagem da emulsão por liofilização foram avaliadas quanto ao rendimento de secagem, eficiência de encapsulamento, retenção de óleo, densidade, conteúdo de umidade, atividade de água e morfologia. Por fim, os tratamentos que apresentaram melhores características de emulsão e pó foram submetidos a um teste de estabilidade acelerada por 35 dias, analisando-se a eficiência de encapsulamento, retenção de α-tocoferol, cinética de degradação, espectroscopia de infravermelho com transformada de Fourier e isotermas de sorção. A bioacessibilidade do α-tocoferol contido nestas micropartículas também foi estudada utilizando o equipamento TIM-1.

2 REFERENCIAL TEÓRICO

2.1 Microencapsulamento

O conceito de alimento tem mudado ao longo das últimas décadas. O maior acesso à informação em todos os campos do conhecimento tem levado o consumidor a ser mais exigente quanto àquilo que ingere. Como uma estratégia de inovação industrial, emerge a ideia de se fabricar alimentos que possuam propriedades funcionais, ou seja, que além de nutrir e fornecer energia ao organismo, também possam prevenir doenças e promover a saúde e bem estar (YE; GEORGES; SELOMULYA, 2018). A suplementação destes produtos pode ser realizada por meio da adição de ingredientes com atividade biológica, tais como minerais (CHURIO; VALENZUELA, 2018), vitaminas (CHAPEAU et al., 2017), ácidos graxos polinsaturados (ROJAS et al., 2019), bactérias probióticas (GONZÁLEZ-FERRERO; IRACHE; GONZÁLEZ-NAVARRO, 2018), peptídeos (MCCLEMENTS, 2018), fibras alimentares (LEON; AGUILERA; PARK, 2019), dentre outros. Tendo em vista que a maioria destas substâncias apresenta instabilidade ao calor, acidez, oxigênio, umidade e luz, surge a necessidade de se desenvolver procedimentos que otimizem a preservação destes compostos bioativos durante as etapas de processamento e período de estocagem do alimento (REHMAN et al., 2019). Assim, a microencapsulação apresenta-se como uma tecnologia alternativa para assegurar maior estabilidade aos bioativos, além de aumentar o valor nutricional, promover a liberação controlada do material, melhorar a incorporação de substâncias líquidas em sistemas secos, mascarar sabor e odores indesejáveis e prolongar a vida útil do alimento, sem exercer influência adversa em suas propriedades físicas, químicas ou funcionais (BALLESTEROS et al., 2017; YE; GEORGES; SELOMULYA, 2018).

A técnica de microencapsulamento baseia-se no empacotamento/ou aprisionamento de compostos com propriedades funcionais por um material de parede, resultando na formação de cápsulas com dimensões que podem variar de micrometros a milímetros (OZKAN et al., 2019). A molécula de interesse é comumente denominada material de núcleo, fase interna ou ativo, enquanto a barreira material, que forma a cápsula, é chamada de encapsulante, material de parede ou de cobertura (DAS PURKAYASTHA; MANHAR, 2016). Na indústria de alimentos, a substância ativa presente no núcleo da partícula deve ser uniformemente envolvida por um uma camada composta por materiais de grau alimentício capazes de separar a fase interna da matriz circundante (YE; GEORGES; SELOMULYA, 2018).

As partículas produzidas podem ser classificadas, em função de sua estrutura, como microesferas e microcápsulas, o que se relaciona com a localização do soluto de interesse (REHMAN et al., 2019). Nas primeiras, o soluto ativo é molecularmente disperso no polímero da matriz, de modo que não é possível observar um núcleo diferenciado, formando um sistema matricial ou monolítico (LETCHFORD; BURT, 2007; RAY; RAYCHAUDHURI; CHAKRABORTY, 2016). Já nas microcápsulas, a fase interna é rodeada por um invólucro polimérico, o que é comumente chamado de sistemas do tipo reservatório, pois o soluto é envolvido por uma membrana de espessura variável, isolando o núcleo do meio externo. Neste caso, o material ativo pode formar um ou mais núcleos, sendo denominados como mono ou polinuclear, respectivamente (JAFARI, 2017; SAMAKRADHAMRONGTHAI et al., 2019). Além disso, as cápsulas podem apresentar um invólucro duplo, onde cada parede possui características de solubilidade diferentes (KARACA; LOW; NICKERSON, 2015). A principal diferença entre as microcápsulas e as microesferas é que, nas microesferas, uma pequena fração do material ativo pode permanecer exposta à superfície, o que não ocorre nas microcápsulas (RAY; RAYCHAUDHURI; CHAKRABORTY, 2016). Estas diferenciações podem ser observadas na Figura 1 para um composto bioativo microencapsulado utilizando uma matriz polimérica como agente de cobertura.

Figura 1 − Tipos de encapsulados.

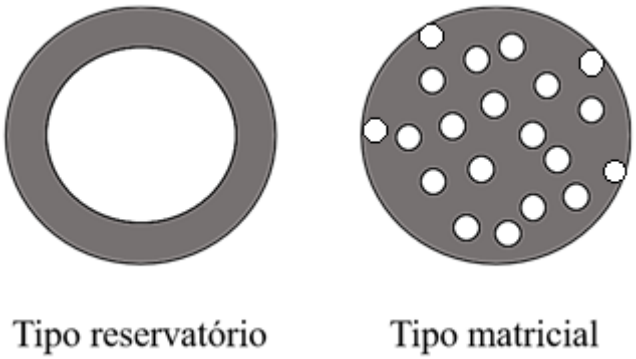

Fonte: Do Autor (2020).

Dependendo do método de fabricação das micropartículas, as técnicas de microencapsulamento podem ser classificadas em três grupos: métodos físicos (*spray-drying*, *spray-chilling*, liofilização, precipitação por fluido supercrítico e evaporação de solvente); métodos físico-químicos (coacervação, lipossomas e gelificação iônica); e método químicos (polimerização interfacial e inclusão molecular) (OZKAN et al., 2019; YE; GEORGES; SELOMULYA, 2018). A escolha do método a ser empregado depende da disponibilidade de

equipamentos, propriedades químicas e físicas do material a ser encapsulado e do material de parede, tamanho da partícula que se quer produzir, aplicação final das cápsulas, mecanismos de liberação desejados e custo (RIBEIRO; ESTEVINHO; ROCHA, 2019). As várias tecnologias empregadas dão origem a partículas com características diferentes em termos de tamanho e tipo de cápsula produzida. Entretanto, em geral, o método utilizado deve ser simples, reprodutível, rápido e fácil de transpor à escala industrial (CARVALHO; ESTEVINHO; SANTOS, 2016). Dentre estes métodos, destaca-se o processo de liofilização. Esta técnica baseia-se na desidratação por sublimação do solvente de um produto congelado, sob vácuo (BORA et al., 2018). Por este procedimento, pode-se realizar a secagem de uma emulsão formada a partir de um ativo coberto por uma membrana de agente encapsulante (BAN et al., 2020). As cápsulas obtidas pelo processo de liofilização são de excelente qualidade por não serem submetidas a altas temperaturas durante sua formação, evitando a degradação de compostos termo sensíveis, sem alteração da aparência do produto (OZKAN et al., 2019). Estudos recentes têm ressaltado as vantagens e benefícios de utilização da liofilização para secagem de produtos contendo materiais bioativos (ARAB et al., 2019; BALLESTEROS et al., 2017; BAN et al., 2020; DA CRUZ et al., 2019; GURSUL; KARABULUT; DURMAZ, 2019; SHADDEL et al., 2018; YAMASHITA et al., 2017).

2.1.1 Material de parede: hidrocoloides

O material utilizado no encapsulamento de substâncias é selecionado de acordo com as propriedades físicas e químicas do agente a ser encapsulado, da aplicação à qual se destinam as cápsulas e do método utilizado para formá-las (DE SOUZA SIMÕES et al., 2017). Esta escolha depende ainda de fatores como a não reatividade do material e proteção do ativo ao longo do período de armazenamento, do mecanismo de liberação do material encapsulado, suas propriedades reológicas, habilidade de emulsificar ou dispersar, e ser economicamente viável (SAMAKRADHAMRONGTHAI et al., 2019; YE; GEORGES; SELOMULYA, 2018). Os materiais encapsulantes devem possuir boas propriedades de formação de filme, baixa higroscopicidade, estabilidade durante a estocagem, proteção do núcleo do contato com oxigênio, luz e pH, baixa viscosidade em altas concentrações de sólidos, sabor e odor suaves, fácil reconstituição, baixo custo, e características de superfície (porosidade) que permitam a liberação adequada do núcleo (DE SOUZA SIMÕES et al., 2017; SHISHIR et al., 2018). Na prática, muitas vezes, pelo fato de um mesmo composto não englobar todas essas propriedades, usa-se uma mistura de polímeros para compor a barreira encapsulante (DE SOUZA SIMÕES

et al., 2017). Ter um entendimento claro das propriedades do ingrediente ativo e da composição do material de parede torna-se crucial para criação de um sistema de encapsulação eficaz e que proporcione estabilidade ao ingrediente microencapsulado até seu local de destino.

A diversidade de polímeros que podem ser utilizados na obtenção de micropartículas é grande, podendo ser biodegradáveis e não-biodegradáveis, solúveis ou insolúveis, naturais ou sintéticos (GUERRA-ROSAS et al., 2016). A utilização de matérias-primas de origem natural, como os polissacarídeos e proteínas, tem sido preferida pelo consumidor, pois são atóxicos e seguros à saúde, apresentam custo acessível, encontram-se disponíveis na natureza (ou podem ser sintetizados a partir de microrganismos) e são biodegradáveis (REHMAN et al., 2019). Desta maneira, tem-se optado pela investigação e desenvolvimento de produtos que utilizem ingredientes "*label-friendly*" e que possam ser aplicados em alimentos e bebidas de forma eficiente, a fim de substituir completamente, ou parcialmente, ingredientes sintéticos (ADJONU et al., 2014; OZTURK; MCCLEMENTS, 2016; YANG; MCCLEMENTS, 2013).

O termo hidrocoloides engloba um grupo heterogêneo de biomoléculas que são capazes de formar dispersões viscosas e/ou géis quando dispersos em água (SAHA; BHATTACHARYA, 2010). Estes polímeros de cadeia longa podem ser encontrados em produtos de origem animal, como as proteínas do leite (TAN; ZHONG; LANGRISH, 2020) ou quitosana (RUDKE et al., 2019), serem produzidos por microrganismos (MOHAPATRA et al., 2018) ou algas (ABDUL KHALIL et al., 2018), ou serem extraídos a partir de uma fonte vegetal, como de exsudados de plantas superiores, sementes, folhas, frutos e tubérculos (LIMA JUNIOR et al., 2013; MARTIN et al., 2017). Neste último caso, estas moléculas são chamadas de gomas ou mucilagens (CUNHA; PAULA; FEITOSA, 2009).

No caso do microencapsulamento de compostos hidrofóbicos, é comum proceder à secagem de emulsões óleo-em-água, a fim de conseguir incorporá-los em matrizes alimentares secas e hidrofílicas (PERES et al., 2016). Nestes sistemas, os hidrocoloides utilizados devem possuir em sua estrutura segmentos com grupamentos hidrofóbicos e hidrofílicos, como é o caso de proteínas e polissacarídeos associados à proteínas, para que sejam capazes de formar um filme protetor ao redor das gotículas da fase lipídica contendo o composto bioativo (LAM; NICKERSON, 2013). A formação desta emulsão envolve três etapas (FIGURA 2): (1) difusão do agente emulsificante pela fase contínua e sua adsorção na interface óleo-água; (2) rearranjo da estrutura do composto emulsificante de forma que seus grupos hidrofóbicos voltem-se para a fração lipídica e os segmentos hidrofílicos orientem-se para a fase contínua aquosa; e (3) interação molecular entre as cadeias dos agentes de superfície e consequente formação de um filme viscoelástico e coeso em torno das gotículas de óleo. Assim, percebe-se que os

hidrocoloides atuam diminuindo a tensão interfacial entre as fases, possibilitando a dispersão da fase descontínua imiscível e conferindo estabilidade ao sistema por certo período de tempo. Além disso, é importante ressaltar que é necessário fornecer energia ao sistema para que aja quebra e dispersão da fase descontínua na fase aquosa (HAKANSSON; RAYNER, 2018; LAM; NICKERSON, 2013; MCCLEMENTS, 2015).

Figura 2 − Esquema do processo de produção de emulsão óleo-em-água: (a) difusão do agente emulsificante para a interface óleo/água; (b) reorientação das moléculas na interface; (c) formação de um filme viscoelástico.

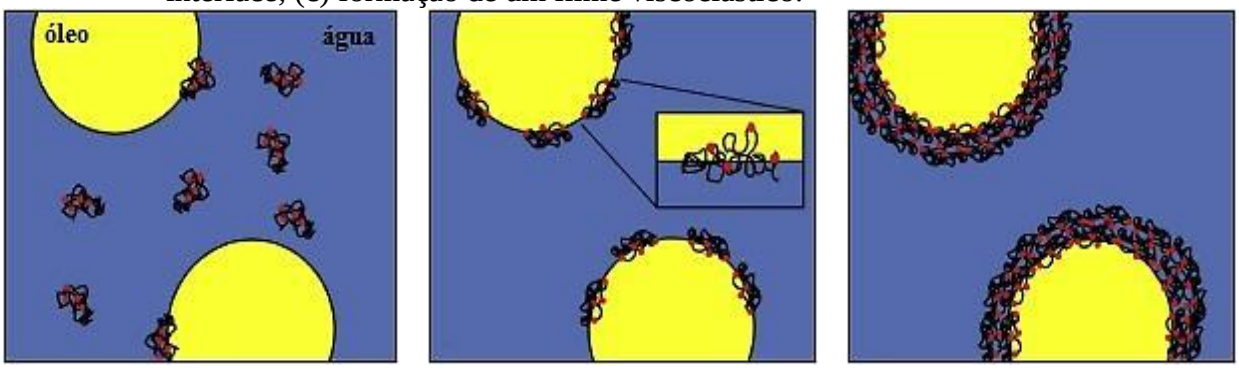

(a) (b) (c)

Fonte: Lam e Nickerson (2013).

A utilização de hidrocoloides que sejam extraídos a partir de fontes renováveis ou de resíduos agroindustriais é de grande interesse por parte da indústria. Desta forma, é possível inserir no mercado novos aditivos com funcionalidades específicas, além de contribuir para a preservação do meio ambiente (ZAMENI et al., 2015).

2.1.1.1 Proteínas de soro de leite

O soro de leite é considerado um coproduto lácteo decorrente da produção de queijos ou caseína, sendo composto por uma mistura heterogênea de proteínas, a saber: β-lactoglobulina (40-50% m/m), α-lactalbumina (12-15% m/m), imunoglobulinas (8% m/m), albumina de soro bovino (5% m/m), lactoferrina (1% m/m), lactoperoxidase (0,5% m/m), proteose-peptona e glicomacropeptídeo (12% m/m) (DEVI et al., 2017; MADUREIRA et al., 2007; QI; ONWULATA, 2011). Por serem prontamente solúveis em água, as proteínas do soro do leite são utilizadas em vários produtos processados, como bebidas, alimentos saudáveis, lácteos, produtos à base de carne, alimentos congelados e fórmulas para bebês, contribuindo consideravelmente com a dose de proteínas ingerida (SOUZA et al., 2019; TAN; ZHONG; LANGRISH, 2020).

O constante investimento no desenvolvimento de novos produtos e o aperfeiçoamento das tecnologias de separação e purificação das proteínas do soro permitiram a sua utilização pela indústria. De acordo com a legislação (MAPA, 2014), este ingrediente pode ser classificado quanto ao teor de proteína de leite presente, sendo denominado concentrado proteico de soro de leite quando a porcentagem de proteína estiver entre 35%-80% m/m; e isolado proteico de soro de leite para produtos com mais de 90% m/m de proteína (TSAI; WENG, 2019; USCATEGUI; VELÁSQUEZ; VALENCIA, 2018). Ambos ingredientes são produzidos industrialmente pelo processo de separação por membrana e concentração do soro de leite, seguida pela desidratação em *spray dryer* (GANJU; GOGATE, 2017; LIMA et al., 2019; YADAV et al., 2016).

As proteínas de soro de leite possuem diversas propriedades funcionais, tais como capacidade emulsificante, gelificante, capacidade de formação de filme e propriedades de superfície ativa, além de um alto valor nutricional (KELLY, 2019; SUHAG; NANDA, 2015). Desta forma, estudos recentes têm mostrado que as proteínas do soro de leite podem ser utilizadas no encapsulamento e liberação controlada de compostos bioativos, formando o material de parede como componente único ou em combinação com outros compostos veiculantes, apresentando alto rendimento de encapsulamento e cápsulas com alta estabilidade durante o armazenamento (BILEK; YILMAZ; ÖZKAN, 2017; DEVI et al., 2017; ESFANJANI; JAFARI; ASSADPOUR, 2017; SHISHIR et al., 2018; TAN; ZHONG; LANGRISH, 2020).

2.1.1.2 Mucilagem de ora-pro-nobis

A mucilagem de ora-pro-nobis é extraída das folhas da espécie *Pereskia aculeata* Miller, pertencente à família das Cactáceas (FIGURA 3) (DE CASTRO CAMPOS PINTO et al., 2015; TAKEITI et al., 2009). Esta é uma planta nativa brasileira com característica de trepadeira, é de fácil cultivo, propagação e resistente à climas secos e, por isso, possui alto potencial de utilização (MARTINEVSKI et al., 2013).

Figura 3 − Folhas de ora-pro-nobis (*Pereskia aculeata* Miller).

Fonte: Do Autor (2020).

As folhas de ora-pro-nobis não apresentam toxicidade e seu consumo tem sido associado ao aumento do valor nutricional das refeições, por apresentar elevado teor de proteínas (25% b.s) com alta digestibilidade (85%) e aminoácidos essenciais, como triptofano. Além disso, são ricas em minerais (como ferro, zinco, manganês, cálcio, fósforo, magnésio), fibras alimentares, vitaminas A e C, além de ácido fólico (SOUZA et al., 2016; TAKEITI et al., 2009). É relatado ainda a presença de ácidos fenólicos e flavonoides com capacidade antioxidante e compostos fito-químicos com atividade antimicrobiana (GARCIA et al., 2019).

As plantas da família das Cactáceas têm sido apontadas como uma fonte potencial de mucilagens, por apresentarem grandes quantidades de polissacarídeos e de proteínas em sua estrutura (PETERA et al., 2015). As folhas de ora-pro-nobis possuem alto teor de arabinogalactana, que se caracteriza como um biopolímero composto por uma cadeia principal de (1→4) β-D-galactopiranose com ramificações de galactose, arabinose, ramnose e ácido galacturônico na proporção de 5,4 : 8,3 : 1,8 : 1,0, respectivamente (LIMA JUNIOR et al., 2013; MARTIN et al., 2017). Esta arabinogalactana é considerada do tipo I por estar covalentemente associada a proteínas, sendo encontrada em paredes celulares de plantas superiores (MARTIN et al., 2017; MERCÊ et al., 2001). Este complexo proteoglicano está relacionado às propriedades funcionais da mucilagem de ora-pro-nobis, e possibilita sua incorporação em matrizes alimentares como ingrediente natural.

Estudos têm demonstrado as propriedades tecnológicas da mucilagem de ora-pro-nobis, apontando-a como uma fonte viável para aplicação industrial. É relatada sua capacidade de

formação de géis e emulsões, utilizando-se diferentes concentrações do hidrocoloide e temperaturas (CONCEIÇÃO et al., 2014; JUNQUEIRA et al., 2018; LIMA JUNIOR et al., 2013), na presença ou não de cloreto de sódio e sacarose e em diferentes valores de pH (JUNQUEIRA et al., 2019). Ainda, pode-se citar trabalhos que demonstram a capacidade da mucilagem de ora-pro-nobis em formar nanoemulsões de óleo-em-água por meio da sonicação ultrassônica (LAGO et al., 2019) e filmes biodegradáveis, quando associada com glicerol (OLIVEIRA et al., 2019). Foi avaliada também a inclusão da mucilagem em bebidas lácteas fermentadas, o que aumentou o teor proteico e a viscosidade do produto, bem como reduziu a sinérese (AMARAL et al., 2018). Desta maneira, é possível perceber que a utilização da mucilagem de ora-pro-nobis possui perspectiva de aplicação em diversas áreas da indústria de alimentos, sendo um hidrocoloide de versátil aplicação.

2.1.2 Material de núcleo: α-tocoferol

O desenvolvimento tecnológico nos campos da indústria de cosméticos, alimentos e farmacêutica tem permitido o isolamento de compostos bioativos, assim como o estudo de suas interações com o corpo humano (DE SOUZA SIMÕES et al., 2017). Compostos bioativos podem ser definidos como substâncias capazes de promover benefícios à saúde, por meio da prevenção ou retardamento do aparecimento de doenças, devido à sua ação antioxidante e/ou anti-inflamatória, por exemplo (EZHILARASI et al., 2013; HU; HUANG, 2013). Desta maneira, é importante que as propriedades funcionais destas substâncias sejam preservadas até o momento de sua utilização. Para tanto, na maior parte dos casos, os bioativos não são adicionados em seu estado puro às matrizes alimentares, devido à sua suscetibilidade à degradação física, química e enzimática, ou devido à baixa solubilidade em água (DE SOUZA SIMÕES et al., 2017). Assim, destaca-se a importância do encapsulamento desses compostos como uma forma de permitir sua incorporação em produtos alimentícios com alto teor de água, preservando sua biodisponibilidade e evitando os efeitos de degradação (DORDJEVIĆ et al., 2015; JOYE; DAVIDOV-PARDO; MCCLEMENTS, 2014).

Os antioxidantes são compostos considerados bioativos e, quando incorporados em matrizes alimentares, apresentam diversas propriedades funcionais como prevenção da deterioração por oxidação, aumento do valor nutricional e benefícios à saúde (ALVAREZ-SUAREZ et al., 2016; BALLESTEROS et al., 2017; OZKAN et al., 2019). Dentre os antioxidantes, destaca-se a vitamina E. Este bioativo tem sido utilizado em muitas aplicações cosméticas, médicas e como suplementação alimentar, por ser capaz de proteger as células

humanas contra os danos causados pela presença de radicais livres, sendo associado à minimização de efeitos de envelhecimento, prevenção de câncer, doenças cardiovasculares, assim como prevenção e tratamento da doença de Alzheimer e outras doenças neurológicas (EERMAN; BRODATY, 2004; SHARIPOVA et al., 2016; WANG et al., 2015).

A vitamina E é composta por um subconjunto de isoprenóides, que incluem quatro tocoferóis e quatro tocotrienóis (FIGURA 4). O α-tocoferol é a fração da vitamina E mais encontrada na natureza e de maior atividade biológica (REBOUL, 2017). Estes compostos são antioxidantes lipofílicos e são sintetizados apenas por organismos fotossintéticos, podendo ser encontrados em óleos vegetais (óleo de girassol), sementes (amêndoas), frutas e vegetais (tomates, espinafre) (DELLAPENNA, 2005). No entanto, devido à sua baixa disponibilidade, sensibilidade à luz, calor e oxigênio, e à baixa solubilidade em água, seu consumo pela população têm sido inferior à ingestão diária recomendada (10 mg) (ANVISA, 2005), tornando sua incorporação em sistemas alimentares aquosos um constante desafio a ser superado pela indústria de alimentos (SHARIF et al., 2017). Feng et al. (2009), demonstraram em seu estudo utilizando microemulsões produzidas com emulsificantes aniônicos que a microencapsulação de vitamina E pode aumentar sua biodisponibilidade.

Figura 4 − Conjunto das frações que compõe a vitamina E.

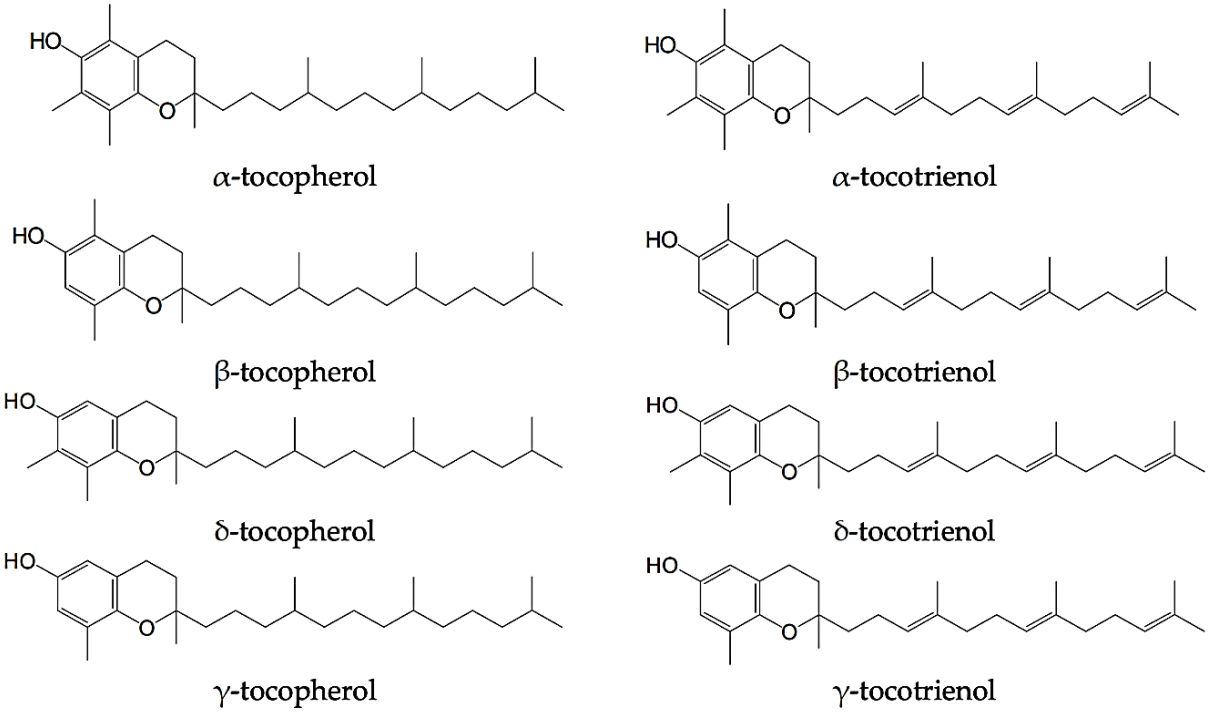

Fonte: Reboul (2017).

2.2 TIM-1

A digestão de alimentos pelo trato gastrointestinal humano é um processo que ocorre em várias etapas, com o objetivo de reduzir o alimento ingerido em compostos mais simples para que possam ser absorvidos e utilizados no funcionamento do organismo (MCDONALD; MACFARLANE, 2018). Técnicas *in vitro* que visam simular este processo devem considerar fatores que incluem as condições fisiológicas do estômago e intestino (temperatura, pH, enzimas digestivas, soluções de eletrólitos), motilidade gastrointestinal, secreção e esvaziamento do líquido digestivo, além do design das vilosidades gástricas e intestinais (LI et al., 2020).

O modelo TIM-1 (TNO gastro-intestinal model) foi desenvolvido pelo Departamento de Fisiologia da *TNO Nutrition and Food Research Institute* em Zeist, Holanda (MINEKUS et al., 1995). Este sistema é composto por um reator dinâmico multi-compartimental (FIGURA 5) que imita as condições *in vivo* de processos físicos, químicos e fisiológicos das etapas da digestão que ocorrem no trato gastrointestinal superior (WEI et al., 2019). Nesse equipamento, membranas de sílica gel flexíveis são alocadas em tubos de vidro transparente cheios de água, com intuito de reproduzir a movimentação do alimento no estômago, duodeno, jejuno e íleo, que é controlada alterando-se a pressão da água. Durante o trânsito gradual da refeição pelos compartimentos, diferentes frações da refeição são expostas a condições variáveis devido à secreção gradual de fluidos digestivos e à absorção de água e nutrientes. Os parâmetros fisiológicos e fluidos digestivos inseridos no trato gastrointestinal ao longo da simulação da digestão são regulados por um computador. Estes protocolos são desenvolvidos para uma configuração digestiva específica, e podem incluir parâmetros característicos para diferentes espécies (humanos, cachorros, porcos), idades (crianças, adultos e idosos), doenças, entre outros, por meio de dados obtidos em estudos *in vivo* (LI et al., 2020; MINEKUS, 2015; MINEKUS et al., 1995). Apesar do controle minucioso das condições que simulam os parâmetros fisiológicos da digestão, o uso do TIM-1 apresenta como desvantagens o alto custo para aquisição e manutenção do equipamento, a ausência de feedback do sistema nervoso central para liberação de hormônios específicos que controlam a motilidade gástrica e intestinal, e o fato de que não existem células que imitem a mucosa da parede do intestino, tornando impossível simular os processos fisiológicos de transporte ativo ou facilitado (BAO et al., 2019; BLANQUET et al., 2004).

Figura 5 − Representação esquemática do TIM-1. **A**. compartimento gástrico; **B**. esfíncter pilórico; **C**. compartimento do duodeno; **D**. válvula peristáltica; **E**. compartimento do jejuno; **F**. válvula peristáltica; **G**. compartimento do íleo; **H**. esfíncter ileocecal; **I**. secreção gástrica; **J**. secreção do duodeno; **K**. secreção de bicarbonato; **L**. pré-filtros; **M**. sistema de filtração; **N**. filtrado que representa a fração bioacessível; **O**. sistema de fibra dos filtros (seção transversal); **P**. eletrodos de pH; **Q**. sensores de nível; **R**. sensores de temperatura; **S.** sensores de pressão.

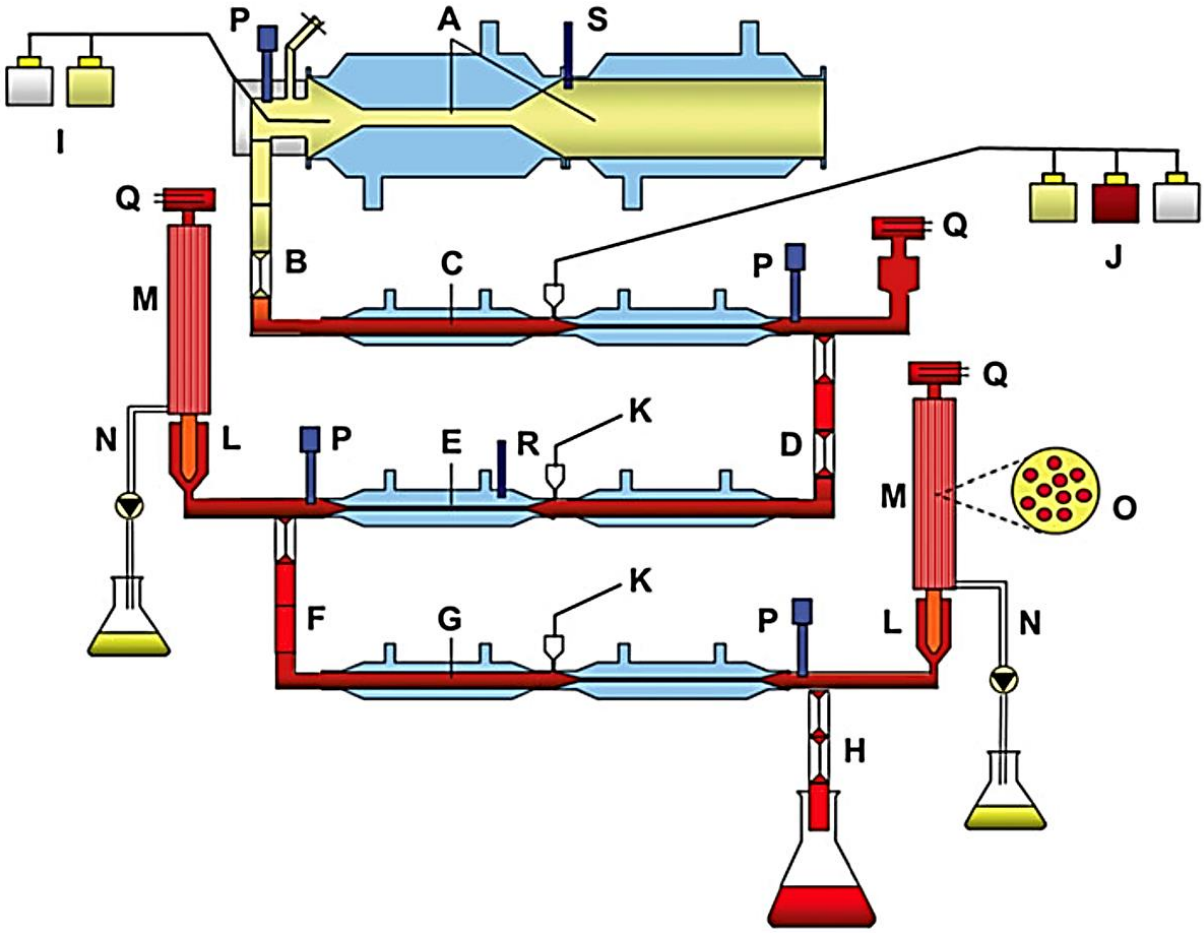

Fonte: Minekus (2015).

Os produtos resultantes da digestão são coletados por mangueiras conectadas aos compartimentos do jejuno e íleo. Substâncias solúveis em água são removidas por diálise através de membranas com um limite de massa molecular de 10 kDa. Já os compostos lipofílicos, por serem incorporados em micelas para serem absorvidos pelo organismo, são removidos através de um filtro com poros de 50 nm de raio, permitindo a passagem dessas estruturas que ficariam retidas no sistema anterior (MINEKUS, 2015).

O sistema digestivo artificial TIM-1 é um instrumento preciso e que apresenta reprodutibilidade nas análises, fornecendo informações sobre tempo de residência gástrico e intestinal, bioacessibilidade intestinal de compostos, bem como sobre a eliminação de amostras não absorvidas (TING et al., 2015a, b; WEI et al., 2019). Entende-se por bioacessibilidade

quando se utiliza o TIM-1 a quantidade de uma determinada substância liberada de uma matriz alimentar capaz de traspassar o sistema de membranas dos compartimentos representativos do jejuno e íleo, refletindo o que seria a disponibilidade para absorção intestinal desta substância quando na digestão *in vivo* (MINEKUS, 2015; RIBNICKY et al., 2014). A adição de compostos encapsulados a produtos alimentares pode, além de superar algumas perdas nutricionais que ocorrem frequentemente durante o processamento e armazenamento de alimentos, conferir proteção e permitir sua melhor absorção no intestino delgado até atingir a corrente sanguínea, aumentando a bioacessibilidade do composto (DE SOUZA SIMÕES et al., 2017; JOYE; DAVIDOV-PARDO; MCCLEMENTS, 2014).

Estudos de digestão *in vitro* utilizando o TIM-1 têm sido realizados para diversas matrizes alimentícias com objetivo de estimar a bioacessibilidade de uma diversidade de compostos, como por exemplo: antocianinas (RIBNICKY et al., 2014), corantes (WEI et al., 2019), açúcares em fibras alimentares (ALHASAWI et al., 2018), ácidos graxos poliinsaturados (DA SILVA et al., 2018), vitaminas (GALÁN et al., 2014; LIN et al., 2018), probióticos (URIOT et al., 2016), minerais (MORALES; MOYANO, 2010) e proteínas (VILLEMEJANE et al., 2016). Além disso, os resultados obtidos em estudos de simulação *in vitro* utilizando-se o TIM-1 têm sido estatisticamente validados e correlacionados com dados de avaliações *in vivo* em seres humanos (ANSON et al., 2011; DÉAT et al., 2009; EKLUND-JONSSON et al., 2008; LARSSON; MINEKUS; HAVENAAR, 1997; MARTEAU et al., 1997; SOULIMAN et al., 2006; TING et al., 2015a, b; VAN DE WIELE et al., 2007; VERWEI et al., 2006).

3 CONCLUSÃO GERAL

A crescente exigência do consumidor por alimentos que apresentem benefícios à saúde ao serem ingeridos tem feito com que novos produtos sejam desenvolvidos, com intuito de reforçar o valor nutricional do alimento. Desta maneira, o encapsulamento de substâncias tem sido utilizado como uma estratégia para incorporação de moléculas bioativas, como vitaminas e óleos, em matrizes alimentares, a fim de criar produtos com propriedades funcionalizadas e de maior valor agregado. O α-tocoferol é a forma biologicamente mais ativa da vitamina E, cuja ingestão está associada com a prevenção de doenças cardiovasculares e aquelas associadas à presença de radicais livres. Entretanto, seu consumo é deficiente em uma alimentação baseada em produtos ultraprocessados, o que cria a necessidade de sua incorporação neste tipo de alimento.

A microencapsulação é uma técnica que permite o revestimento de ingredientes por um material de parede com intuito de proteger e promover a liberação controlada de compostos bioativos e funcionais, prolongando a vida útil do produto. Devido ao apelo crescente por produtos que contenham apenas ingredientes saudáveis, o uso de emulsificantes naturais tem atraído considerável atenção no cenário industrial. Neste contexto, as proteínas de soro de leite têm sido amplamente utilizadas como material de parede em técnicas de encapsulamento, devido ao seu alto valor nutricional e por serem moléculas anfifílicas, o que permite o encapsulamento de compostos hidrofóbicos por métodos de emulsificação. A mucilagem extraída das folhas de ora-pro-nobis também tem se mostrado promissora para uso pela indústria por ser um polissacarídeo rico em arabinogalactana associado a proteínas, o que lhe confere propriedades emulsificantes e espessantes.

O estudo da bioacessibilidade de compostos incorporados em matrizes alimentícias torna-se possível por meio da utilização de sistemas que imitem as condições do trato gastrointestinal, como o TIM-1, um modelo de sistema automatizado dinâmico que simula de forma realista os eventos de digestão dos compartimentos do estômago e intestino delgado. Em geral, a tecnologia de microencapsulamento tem apresentado aplicações potenciais na indústria de alimentos, no entanto, pesquisas sobre a estabilidade durante armazenamento e a cinética de digestão de compostos bioativos encapsulados é fundamental para que, de fato, seus benefícios possam ser usufruídos pelo consumidor.

REFERÊNCIAS

ABDUL KHALIL, H. P. S. et al. A review of extractions of seaweed hydrocolloids: Properties and applications. **Express Polymer Letters**, v. 12, n. 4, p. 296–317, 2018.

ADJONU, R. et al. Whey protein peptides as components of nanoemulsions: A review of emulsifying and biological functionalities. **Journal of Food Engineering**, v. 122, n. 1, p. 15–27, 2014.

ALHASAWI, F. M. et al. Gastric viscosity and sugar bioaccessibility of instant and steel cut oat/milk protein blends. **Food Hydrocolloids**, v. 82, p. 424–433, 2018.

ALVAREZ-SUAREZ, J. M. et al. Activation of AMPK/Nrf2 signalling by Manuka honey protects human dermal fibroblasts against oxidative damage by improving antioxidant response and mitochondrial function promoting wound healing. **Journal of Functional Foods**, v. 25, p. 38–49, 2016.

AMARAL, T. N. et al. Blends of *Pereskia aculeata* Miller mucilage, guar gum, and gum Arabic added to fermented milk beverages. **Food Hydrocolloids**, v. 79, p. 331–342, 2018.

ANSON, N. M. et al. Effect of bioprocessing of wheat bran in wholemeal wheat breads on the colonic SCFA production in vitro and postprandial plasma concentrations in men. **Food Chemistry**, v. 128, n. 2, p. 404–409, 2011.

ANVISA. Agência Nacional de Vigilância Sanitária. **Resolução - RDC n° 269, de 22 de setembro de 2005**. Regulamento técnico sobre a ingestão diária recomendada (IDR) de proteína, vitaminas e minerais. **Diário Oficial da União**, Brasília, 23 set. 2005, Disponível em: <http://portal.anvisa.gov.br/documents/33916/394219/RDC_269_2005.pdf/2e95553c-a482-45c3-bdd1-f96162d607b3>. Acesso em: 5 nov. 2019.

ARAB, M. et al. Microencapsulation of microbial canthaxanthin with alginate and high methoxyl pectin and evaluation the release properties in neutral and acidic condition. **International Journal of Biological Macromolecules**, v. 121, p. 691–698, 2019.

BALLESTEROS, L. F. et al. Encapsulation of antioxidant phenolic compounds extracted from spent coffee grounds by freeze-drying and spray-drying using different coating materials. **Food Chemistry**, v. 237, p. 623–631, 2017.

BAN, Z. et al. Ginger essential oil-based microencapsulation as an efficient delivery system for the improvement of Jujube (*Ziziphus jujuba* Mill.) fruit quality. **Food Chemistry**, v. 306, p. 125628, 2020.

BAO, C. et al. The delivery of sensitive food bioactive ingredients: Absorption mechanisms, influencing factors, encapsulation techniques and evaluation models. **Food Research International**, v. 120, p. 130–140, 2019.

BILEK, S. E.; YILMAZ, F. M.; ÖZKAN, G. The effects of industrial production on black carrot concentrate quality and encapsulation of anthocyanins in whey protein hydrogels. **Food and Bioproducts Processing**, v. 102, p. 72–80, 2017.

BLANQUET, S. et al. A Dynamic artificial gastrointestinal system for studying the behavior of orally administered drug dosage forms under various physiological conditions. **Pharmaceutical Research**, v. 21, n. 4, p. 585–591, 2004.

BORA, A. F. M. et al. Application of microencapsulation for the safe delivery of green tea polyphenols in food systems: Review and recent advances. **Food Research International**, v. 105, p. 241–249, 2018.

CARVALHO, I. T.; ESTEVINHO, B. N.; SANTOS, L. Application of microencapsulated essential oils in cosmetic and personal healthcare products – a review. **International Journal of Cosmetic Science**, v. 38, p. 109–119, 2016.

CHAPEAU, A.-L. et al. Scale-up production of vitamin loaded heteroprotein coacervates and their protective property. **Journal of Food Engineering**, v. 206, p. 67–76, 2017.

CHURIO, O.; VALENZUELA, C. Development and characterization of maltodextrin microparticles to encapsulate heme and non-heme iron. **LWT - Food Science and Technology**, v. 96, p. 568–575, 2018.

CONCEIÇÃO, M. C. et al. Thermal and microstructural stability of a powdered gum derived from *Pereskia aculeata* Miller leaves. **Food Hydrocolloids**, v. 40, p. 104–114, 2014.

CUNHA, P. L. R. DA; PAULA, R. C. M. DE; FEITOSA, J. P. A. Polissacarídeos da biodiversidade brasileira: uma oportunidade de transformar conhecimento em valor econômico. **Química Nova**, v. 32, n. 3, p. 649–660, 2009.

DA CRUZ, M. C. R. et al. Assessment of physicochemical characteristics, thermal stability and release profile of ascorbic acid microcapsules obtained by complex coacervation. **Food Hydrocolloids**, v. 87, p. 71–82, 2019.

DAS PURKAYASTHA, M.; MANHAR, A. K. Nanotechnological Applications in Food Packaging, Sensors and Bioactive Delivery Systems. In: RANJAN, S.; DASGUPTA, N.; LICHTFOUSE, E. (Eds.). **Nanoscience in Food and Agriculture 2**. Cham: Springer International Publishing, 2016. p. 59–128.

DA SILVA, G. et al. Relative levels of dietary EPA and DHA impact gastric oxidation and essential fatty acid uptake. **The Journal of Nutritional Biochemistry**, v. 55, p. 68–75, 2018.

DE CASTRO CAMPOS PINTO, N. et al. *Pereskia aculeata*: A plant food with antinociceptive activity. **Pharmaceutical Biology**, v. 53, n. 12, p. 1780–1785, 2015.

DE SOUZA SIMÕES, L. et al. Micro- and nano bio-based delivery systems for food applications: In vitro behavior. **Advances in Colloid and Interface Science**, v. 243, p. 23–45, 2017.

DÉAT, E. et al. Combining the Dynamic TNO-Gastrointestinal Tract System with a Caco-2 Cell Culture Model: Application to the Assessment of Lycopene and α-Tocopherol Bioavailability from a Whole Food. **Journal of Agricultural and Food Chemistry**, v. 57, n. 23, p. 11314–11320, 2009.

DELLAPENNA, D. A decade of progress in understanding vitamin E synthesis in plants. **Journal of Plant Physiology**, v. 162, n. 7, p. 729–737, 2005.

DEVI, N. et al. Encapsulation of active ingredients in polysaccharide–protein complex coacervates. **Advances in Colloid and Interface Science**, v. 239, p. 136–145, 2017.

DORDJEVIĆ, V. et al. Trends in Encapsulation Technologies for Delivery of Food Bioactive Compounds. **Food Engineering Reviews**, v. 7, n. 4, p. 452–490, 2015.

EERMAN, K.; BRODATY, H. Tocopherol (vitamin E) in Alzheimer's disease and other neurodegenerative disorders. **CNS Drugs**, v. 18, n. 12, p. 807–825, 2004.

EKLUND-JONSSON, C. et al. Tempe Fermentation of Whole Grain Barley Increased Human Iron Absorption and In Vitro Iron Availability. **The Open Nutrition Journal**, v. 2, n. 1, p. 42–47, 2008.

ESFANJANI, A. F.; JAFARI, S. M.; ASSADPOUR, E. Preparation of a multiple emulsion based on pectin-whey protein complex for encapsulation of saffron extract nanodroplets. **Food Chemistry**, v. 221, p. 1962–1969, 2017.

EZHILARASI, P. N. et al. Nanoencapsulation Techniques for Food Bioactive Components: A Review. **Food and Bioprocess Technology**, v. 6, n. 3, p. 628–647, 2013.

FENG, J.-L. et al. Study on food-grade vitamin E microemulsions based on nonionic emulsifiers. **Colloids and Surfaces A: Physicochemical and Engineering Aspects**, v. 339, n. 1, p. 1–6, 2009.

GALÁN, I. et al. Effect of E-beam treatment on the bioaccessibility of folic acid incorporated to ready to eat meat products. **LWT - Food Science and Technology**, v. 59, n. 1, p. 547–552, 2014.

GANJU, S.; GOGATE, P. R. A review on approaches for efficient recovery of whey proteins from dairy industry effluents. **Journal of Food Engineering**, v. 215, p. 84–96, 2017.

GARCIA, J. A. A. et al. Phytochemical profile and biological activities of "Ora-pro-nobis" leaves (*Pereskia aculeata* Miller), an underexploited superfood from the Brazilian Atlantic Forest. **Food Chemistry**, v. 294, p. 302–308, 2019.

GONZÁLEZ-FERRERO, C.; IRACHE, J. M.; GONZÁLEZ-NAVARRO, C. J. Soybean protein-based microparticles for oral delivery of probiotics with improved stability during storage and gut resistance. **Food Chemistry**, v. 239, p. 879–888, 2018.

GUERRA-ROSAS, M. I. et al. Long-term stability of food-grade nanoemulsions from high methoxyl pectin containing essential oils. **Food Hydrocolloids**, v. 52, p. 438–446, 2016.

GURSUL, S.; KARABULUT, I.; DURMAZ, G. Antioxidant efficacy of thymol and carvacrol in microencapsulated walnut oil triacylglycerols. **Food Chemistry**, v. 278, p. 805–810, 2019.

HAKANSSON, A.; RAYNER, M. General Principles of Nanoemulsions Formation by High-Energy Mechanical Methods. In: JAFARI, S. M.; MCCLEMENTS, D. J. (Eds.). **Nanoemulsions:** Formulation, Applications, and Characterization. San Diego: Academic Press, 2018. p. 128–134.

HU, B.; HUANG, Q. Biopolymer based nano-delivery systems for enhancing bioavailability of nutraceuticals. **Chinese Journal of Polymer Science**, v. 31, n. 9, p. 1190–1203, 2013.

JAFARI, S. M. Chapter 1 - An Introduction to Nanoencapsulation Techniques for the Food Bioactive Ingredients. In: JAFARI, S. M. (Ed.). **Nanoencapsulation of Food Bioactive Ingredients**. London: Academic Press, 2017. p. 1–62.

JOYE, I. J.; DAVIDOV-PARDO, G.; MCCLEMENTS, D. J. Nanotechnology for increased micronutrient bioavailability. **Trends in Food Science & Technology**, v. 40, n. 2, p. 168–182, 2014.

JUNQUEIRA, L. A. et al. Rheological behavior and stability of emulsions obtained from *Pereskia aculeata* Miller via different drying methods. **International Journal of Food Properties**, v. 21, n. 1, p. 21–35, 2018.

JUNQUEIRA, L. A. et al. Effects of Change in PH and Addition of Sucrose and NaCl on the Emulsifying Properties of Mucilage Obtained from *Pereskia aculeata* Miller. **Food and Bioprocess Technology**, v. 12, n. 3, p. 486–498, mar. 2019.

KARACA, A. C.; LOW, N. H.; NICKERSON, M. T. Potential use of plant proteins in the microencapsulation of lipophilic materials in foods. **Trends in Food Science & Technology**, v. 42, n. 1, p. 5–12, 2015.

KELLY, P. Chapter 3 - Manufacture of whey protein products: concentrates, isolate, whey protein fractions and microparticulated. In: DEETH, H. C.; BANSAL, N. (Eds.). **Whey Proteins**. London: Academic Press, 2019. p. 97–122.

LAGO, A. M. T. et al. Ultrasound-assisted oil-in-water nanoemulsion produced from *Pereskia aculeata* Miller mucilage. **Ultrasonics Sonochemistry**, v. 50, p. 339–353, 2019.

LAM, R. S. H.; NICKERSON, M. T. Food proteins: A review on their emulsifying properties using a structure-function approach. **Food Chemistry**, v. 141, n. 2, p. 975–984, 2013.

LARSSON, M.; MINEKUS, M.; HAVENAAR, R. Estimation of the bioavailability of iron and phosphorus in cereals using a dynamic in vitro gastrointestinal model. **Journal of the Science of Food and Agriculture**, v. 74, n. 1, p. 99–106, 1997.

LEON, A. M.; AGUILERA, J. M.; PARK, D. J. Mechanical, rheological and structural properties of fiber-containing microgels based on whey protein and alginate. **Carbohydrate Polymers**, v. 207, p. 571–579, 2019.

LETCHFORD, K.; BURT, H. A review of the formation and classification of amphiphilic block copolymer nanoparticulate structures: micelles, nanospheres, nanocapsules and polymersomes. **European Journal of Pharmaceutics and Biopharmaceutics**, v. 65, n. 3, p. 259–269, 2007.

LI, Z. et al. New dynamic digestion model reactor that mimics gastrointestinal function. **Biochemical Engineering Journal**, v. 154, p. 107431, 2020.

LIMA, J. C. et al. Continuous fractionation of whey protein isolates by using supercritical carbon dioxide. **Journal of CO2 Utilization**, v. 30, p. 112–122, 2019.

LIMA JUNIOR, F. A. et al. Response surface methodology for optimization of the mucilage extraction process from *Pereskia aculeata* Miller. **Food Hydrocolloids**, v. 33, n. 1, p. 38–47, 2013.

LIN, Q. et al. Factors affecting the bioaccessibility of β-carotene in lipid-based microcapsules: Digestive conditions, the composition, structure and physical state of microcapsules. **Food Hydrocolloids**, v. 77, p. 187–203, 2018.

MADUREIRA, A. R. et al. Bovine whey proteins – Overview on their main biological properties. **Food Research International**, v. 40, n. 10, p. 1197–1211, 2007.

MARTEAU, P. et al. Survival of Lactic Acid Bacteria in a Dynamic Model of the Stomach and Small Intestine: Validation and the Effects of Bile. **Journal of Dairy Science**, v. 80, n. 6, p. 1031–1037, 1997.

MARTIN, A. A. et al. Chemical structure and physical-chemical properties of mucilage from the leaves of *Pereskia aculeata*. **Food Hydrocolloids**, v. 70, p. 20–28, 2017.

MARTINEVSKI, C. S. et al. Utilização de Bertalha (*Anredera cordifolia* (Ten.) Steenis) e Ora-pro-nobis (*Pereskia aculeata* Mill.) na elaboração de pães. **Brazilian Journal of Food and Nutrition**, v. 24, n. 3, p. 1–6, 2013.

MCCLEMENTS, D. J. **Food Emulsions:** Principles, Practice, and Techniques. 3rd ed. Boca Raton: CRC Press, 2015.

MCCLEMENTS, D. J. Encapsulation, protection, and delivery of bioactive proteins and peptides using nanoparticle and microparticle systems: A review. **Advances in Colloid and Interface Science**, v. 253, p. 1–22, 2018.

MCDONALD, S. W.; MACFARLANE, N. G. The mouth, stomach and intestines. **Anaesthesia & Intensive Care Medicine**, v. 19, n. 3, p. 128–132, 2018.

MERCÊ, A. L. R. et al. Complexes of arabinogalactan of *Pereskia aculeata* and Co2+, Cu2+, Mn2+, and Ni2+. **Bioresource Technology**, v. 76, n. 1, p. 29–37, 2001.

MINEKUS, M. et al. A Multicompartimental dynamic computer-controlled model simularting the stomach and small intestine. **Atla-Alternatives to Laboratory Animals**, v. 23, p. 197–209, 1995.

MINEKUS, M. The TNO in vitro model of the colon (TIM). In: VERHOECKX, K. et al. (Eds.). **The impact of food bioactives on gut health:** in vitro and ex vivo models. New York: Springer Open, 2015. p. 305–317.

MAPA. Ministério Da Agricultura Pecuária e Abastecimento. **Orientações para análise de rotulagem de produtos lácteos**. 2014. Disponível em: <http://www.agricultura.gov.br/assuntos/inspecao/produtos-animal/empresario/arquivos/MANUALROTULAGEMLEITE14082014.pdf>. Acesso em: 5 nov. 2019.

MOHAPATRA, S. et al. Enhanced reducing sugar production by saccharification of lignocellulosic biomass, *Pennisetum species* through cellulase from a newly isolated Aspergillus fumigatus. **Bioresource Technology**, v. 253, p. 262–272, 2018.

MORALES, G. A.; MOYANO, F. J. Application of an in vitro gastrointestinal model to evaluate nitrogen and phosphorus bioaccessibility and bioavailability in fish feed ingredients. **Aquaculture**, v. 306, n. 1, p. 244–251, 2010.

OLIVEIRA, N. L. et al. Development and characterization of biodegradable films based on *Pereskia aculeata* Miller mucilage. **Industrial Crops and Products**, v. 130, 2019.

OZKAN, G. et al. A review of microencapsulation methods for food antioxidants: Principles, advantages, drawbacks and applications. **Food Chemistry**, v. 272, p. 494–506, 2019.

OZTURK, B.; MCCLEMENTS, D. J. Progress in natural emulsifiers for utilization in food emulsions. **Current Opinion in Food Science**, v. 7, p. 1–6, 2016.

PERES, L. B. et al. Solid lipid nanoparticles for encapsulation of hydrophilic drugs by an organic solvent free double emulsion technique. **Colloids and Surfaces B: Biointerfaces**, v. 140, p. 317–323, 2016.

PETERA, B. et al. Characterization of arabinogalactan-rich mucilage from *Cereus triangularis cladodes*. **Carbohydrate Polymers**, v. 127, p. 372–380, 2015.

QI, P.; ONWULATA, C. Physical properties, molecular structures, and protein quality of texturized whey protein isolate: Effect of extrusion moisture content1. **Journal of Dairy Science**, v. 94, p. 2231–2244, 2011.

RAY, S.; RAYCHAUDHURI, U.; CHAKRABORTY, R. An overview of encapsulation of active compounds used in food products by drying technology. **Food Bioscience**, v. 13, p. 76–83, 2016.

REBOUL, E. Vitamin E Bioavailability: Mechanisms of Intestinal Absorption in the Spotlight. **Antioxidants**, v. 6, n. 4, p. 95–106, 2017.

REHMAN, A. et al. Pectin polymers as wall materials for the nano-encapsulation of bioactive compounds. **Trends in Food Science & Technology**, v. 90, p. 35–46, 2019.

RIBEIRO, A. M.; ESTEVINHO, B. N.; ROCHA, F. Microencapsulation of polyphenols - The specific case of the microencapsulation of *Sambucus Nigra* L. extracts - A review. **Trends in Food Science & Technology**, 2019. https://doi.org/10.1016/j.tifs.2019.03.011.

RIBNICKY, D. M. et al. Effects of a high fat meal matrix and protein complexation on the bioaccessibility of blueberry anthocyanins using the TNO gastrointestinal model (TIM-1). **Food Chemistry**, v. 142, p. 349–357, 2014.

ROJAS, V. M. et al. Formulation of mayonnaises containing PUFAs by the addition of microencapsulated chia seeds, pumpkin seeds and baru oils. **Food Chemistry**, v. 274, p. 220–227, 2019.

RUDKE, A. R. et al. Microencapsulation of ergosterol and *Agaricus bisporus* L. extracts by complex coacervation using whey protein and chitosan: Optimization study using response surface methodology. **LWT - Food Science and Technology**, v. 103, p. 228–237, 2019.

SAHA, D.; BHATTACHARYA, S. Hydrocolloids as thickening and gelling agents in food: a critical review. **Journal of Food Science and Technology**, v. 47, n. 6, p. 587–97, dez. 2010.

SAMAKRADHAMRONGTHAI, R. S. et al. Optimization of gelatin and gum arabic capsule infused with pandan flavor for multi-core flavor powder encapsulation. **Carbohydrate Polymers**, v. 226, p. 115262, 2019.

SHADDEL, R. et al. Double emulsion followed by complex coacervation as a promising method for protection of black raspberry anthocyanins. **Food Hydrocolloids**, v. 77, p. 803–816, 2018.

SHARIF, H. R. et al. Physicochemical stability of β-carotene and α-tocopherol enriched nanoemulsions: Influence of carrier oil, emulsifier and antioxidant. **Colloids and Surfaces A: Physicochemical and Engineering Aspects**, v. 529, p. 550–559, 2017.

SHARIPOVA, A. A. et al. Polymer–surfactant complexes for microencapsulation of vitamin E and its release. **Colloids and Surfaces B: Biointerfaces**, v. 137, p. 152–157, 2016.

SHISHIR, M. R. I. et al. Advances in micro and nano-encapsulation of bioactive compounds using biopolymer and lipid-based transporters. **Trends in Food Science & Technology**, v. 78, p. 34–60, 2018.

SOULIMAN, S. et al. A level A in vitro/in vivo correlation in fasted and fed states using different methods: Applied to solid immediate release oral dosage form. **European Journal of Pharmaceutical Sciences**, v. 27, n. 1, p. 72–79, 2006.

SOUZA, L. F. et al. *Pereskia aculeata* Muller (Cactaceae) Leaves: Chemical Composition and Biological Activities. **International Journal of Molecular Sciences**, v. 17, n. 9, 2016.

SOUZA, T. S. P. et al. Yogurt and whey beverages available in Brazilian market: Mineral and trace contents, daily intake and statistical differentiation. **Food Research International**, v. 119, p. 709–714, 2019.

SUHAG, Y.; NANDA, V. Optimisation of process parameters to develop nutritionally rich spray-dried honey powder with vitamin C content and antioxidant properties. **International Journal of Food Science and Technology**, v. 50, n. 8, p. 1771–1777, 2015.

TAKEITI, C. Y. et al. Nutritive evaluation of a non-conventional leafy vegetable (*Pereskia aculeata* Miller). **International Journal of Food Sciences and Nutrition**, v. 60, n. S1, p. 148–160, 2009.

TAN, S.; ZHONG, C.; LANGRISH, T. Pre-gelation assisted spray drying of whey protein isolates (WPI) for microencapsulation and controlled release. **LWT - Food Science and Technology**, v. 117, p. 108625, 2020.

TING, Y. et al. Using in vitro and in vivo models to evaluate the oral bioavailability of nutraceuticals. **Journal of Agricultural and Food Chemistry**, v. 63, n. 5, p. 1332–1338, 2015a.

TING, Y. et al. Viscoelastic emulsion improved the bioaccessibility and oral bioavailability of crystalline compound: a mechanistic study using in vitro and in vivo models**. Molecular Pharmaceutics**, v. 12, n. 7, p. 2229–2236, 6 jul. 2015b.

TSAI, M.-J.; WENG, Y.-M. Novel edible composite films fabricated with whey protein isolate and zein: Preparation and physicochemical property evaluation. **LWT - Food Science and Technology**, v. 101, p. 567–574, 2019.

URIOT, O. et al. Use of the dynamic gastro-intestinal model TIM to explore the survival of the yogurt bacterium Streptococcus thermophilus and the metabolic activities induced in the simulated human gut. **Food Microbiology**, v. 53, p. 18–29, 2016.

USCATEGUI, D. C. R.; VELÁSQUEZ, H. J. C.; VALENCIA, J. U. S. Concentrates of sugarcane juice and whey protein: Study of a new powder product obtained by spray drying of their combinations. **Powder Technology**, v. 333, p. 429–438, 2018.

VAN DE WIELE, T. R. et al. Comparison of five in vitro digestion models to in vivo experimental results: Lead bioaccessibility in the human gastrointestinal tract. **Journal of Environmental Science and Health - Part A**, v. 42, n. 9, p. 1203–1211, 2007.

VERWEI, M. et al. Predicted Serum Folate Concentrations Based on In Vitro Studies and Kinetic Modeling are Consistent with Measured Folate Concentrations in Humans. **The Journal of Nutrition**, v. 136, n. 12, p. 3074–3078, 2006.

VILLEMEJANE, C. et al. In vitro digestion of short-dough biscuits enriched in proteins and/or fibres using a multi-compartmental and dynamic system (2): Protein and starch hydrolyses. **Food Chemistry**, v. 190, p. 164–172, 2016.

WANG, B. et al. Microencapsulation of tuna oil fortified with the multiple lipophilic ingredients vitamins A, D3, E, K2, curcumin and coenzyme Q10. **Journal of Functional Foods**, v. 19, p. 893–901, 2015.

WEI, Z. et al. Ovotransferrin fibril–stabilized Pickering emulsions improve protection and bioaccessibility of curcumin. **Food Research International**, v. 125, p. 108602, 2019.

YADAV, J. S. S. et al. Food-grade single-cell protein production, characterization and ultrafiltration recovery of residual fermented whey proteins from whey. **Food and Bioproducts Processing**, v. 99, p. 156–165, 2016.

YAMASHITA, C. et al. Microencapsulation of an anthocyanin-rich blackberry (Rubus spp.) by-product extract by freeze-drying. **LWT - Food Science and Technology**, v. 84, p. 256–262, 2017.

YANG, Y.; MCCLEMENTS, D. J. Encapsulation of vitamin E in edible emulsions fabricated using a natural surfactant. **Food Hydrocolloids**, v. 30, n. 2, p. 712–720, 2013.

YE, Q.; GEORGES, N.; SELOMULYA, C. Microencapsulation of active ingredients in functional foods: From research stage to commercial food products. **Trends in Food Science & Technology**, v. 78, p. 167–179, 2018.

ZAMENI, A. et al. Effect of thermal and freezing treatments on rheological, textural and color properties of basil seed gum. **Journal of Food Science and Technology**, v. 52, n. 9, p. 5914–5921, 2015.

SEGUNDA PARTE – ARTIGO

EFFECT OF CARRIER OIL ON α-TOCOPHEROL ENCAPSULATION IN ORA-PRO-NOBIS (*Pereskia aculeata* Miller) MUCILAGE-WHEY PROTEIN ISOLATE MICROPARTICLES

Normas do Periódico: Food Hydrocolloids
ISSN: 0268-005X
(versão aceita)

Isabelle Cristina Oliveira Neves[a,b], Sérgio Henrique Silva[a], Natália Leite Oliveira[a], Amanda Maria Teixeira Lago[a], Natalie Ng[b], Arianna Sultani[b], Pedro Henrique Campelo[c], Lizzy Ayra Alcântara Veríssimo[a], Jaime Vilela de Resende[a*], Michael A. Rogers[b*]

[a]Department of Food Science, Federal University of Lavras, Lavras, MG, 37200-900, Brazil.
[b]Department of Food Science, University of Guelph, Guelph, ON N1G2W1, Canada.
[c]Faculty of Agrarian Science, Federal University of Amazonas, Manaus, AM, 69077-000, Brazil.

*Corresponding authors:
M.A. Rogers (e-mail address: mroger09@uoguelph.ca; tel. +01 519 924-4120 EXT. 54327)
J.V. de Resende (e-mail address: jvresende@dca.ufla.br; tel. +55 35 3829 1659)

ABSTRACT

Microparticles of whey protein isolate (WPI) and ora-pro-nobis mucilage (OPN) encapsulated α-tocopherol were made using long-chain unsaturated (e.g., canola oil (CA)) or medium-chain saturated oil (e.g., coconut oil (CO)) as the carrier oil. Microparticles were produced from CO- or CA-in-water emulsions by freeze-drying emulsions with various ratios of WPI/OPN. Before freeze dying, emulsions exhibited Newtonian or shear-thinning behavior. Drying yields for freeze-dried emulsions ranged between 74.1% to 87.1% w/w, depending on the biopolymers-to-oil ratio and varied depending on whether CA or CO was used as the carrier. WPI:OPN ratios (between 23:1 and 7:1) nor oil phase (e.g., CO or CA) significantly affected the physical properties (e.g., oil retention, water content, and activity) of the dried powder between treatments. Higher powder bulk density (0.22 $g \cdot cm^{-3}$) and encapsulation efficiency (79.8% w/w) were obtained from freeze-drying CO-, compared to CA-in-water emulsions and with higher concentrations of OPN. Over 35 days, α-tocopherol retention and degradation kinetics differed between CO and CA and was dependent on relative humidity. Bioaccessibility of encapsulated α-tocopherol was higher with WPI/OPN and CA (55.0±1.89%) compared to CO (42.4±1.78%), while the rate of α-tocopherol release and induction time for release were statically equal.

Keywords: Vitamin E; Canola oil; Coconut oil; Degradation kinetics; Isothermal behavior; Carrier oil; Bioaccessibility.

1. Introduction

Bioactive encapsulation in foods, cosmetics, and pharmaceuticals improves bioavailability and stability and as such has experienced a recent surge in interest (Koshani & Jafari, 2019; Rafiee, Nejatian, Daeihamed, & Jafari, 2019; Taheri & Jafari, 2019). Encapsulation protects bioactives from harsh storage conditions (i.e., exposure to oxygen, moisture, temperature, & light), inhospitable luminal conditions (i.e., presence of enzymes & acidic pH) while masking undesirable flavors and odors (Ballesteros, Ramirez, Orrego, Teixeira, & Mussatto, 2017). Improving bioavailability, especially for essential fat-soluble bioactives, is an active area of investigation due to their poor aqueous solubility in the luminal track hindering them from performing their biological function due to notoriously low bioaccessibility, the precursor to bioavailability (Amiri et al., 2018). Bioaccessibility refers to the amount of bioactive released from the food or encapsulates into the gastrointestinal (GI) luminal fluid that is then available to be transported across the epithelial layer of the GI tract. *In vitro* bioaccessibility is most accurately approximated by dynamically simulating the luminal conditions (i.e., peristaltic contractions, continuous gastric and intestinal emptying, pH, enzyme excretion and metabolite absorption) (AlHasawi et al., 2017; Bandali, Wang, Lan, Rogers, & Shapses, 2018; Convely, 1970; Minekus, 2015; Minekus, Marteau, Havenaar, & Huisintveld, 1995; Ting, Zhao, Xia, & Huang, 2015).

Encapsulation of hydrophobic and amphiphilic bioactives commonly utilizes emulsions, either as a precursor or final delivery vehicle, as they facilitate incorporation of hydrophobic regions of bioactives into the lipophilic dispersed phase and the hydrophilic region resides in the aqueous phase. Bioactive incorporation into emulsions improves loading efficiency and slows deteriorative reactions; thereby increasing both processing and storage stability (Carneiro, Tonon, Grosso, & Hubinger, 2013; Fioramonti, Rubiolo, & Santiago, 2017). Of particular interest herein, the role of carrier oil (CO or CA) on microparticle properties and bioaccessibility examines the effects of unsaturated versus saturated oil on bioactive stability and release in OPN. Canola oil is comprised primarily of long-chain, unsaturated fatty acids (Madankar, Dalai, & Naik, 2013), while coconut oil is high in medium-chain, saturated fatty acids (Beneš, Paruzel, Trhlíková, & Paruzel, 2017; Costa et al., 2016). These were selected as the lipid carrier due to the drastic difference in chemical composition which potentially alters encapsulation efficiency and bioaccessibility. Additional processing is required to convert oil-in-water loaded emulsions into microparticles.

Microencapsulation forms a protective boundary layer around bioactives which may be engineered to release bioactives via external triggers, such as pH, that control site specific release and disintegration (i.e., release) kinetics thereby reducing detrimental reactions capable of altering bioactive structure and thus eliminating biological activity (Tonon, Grosso, & Hubinger, 2011; Tyagi, Kaushik, Tyagi, & Akiyama, 2011). Numerous drying methodologies produce microparticles, however, for thermally labile bioactives, such as vitamin E (Vit E), freeze-drying is advantageous because of the low operating temperatures and pressures that slow oxidative deterioration (Arab et al., 2019; Ballesteros et al., 2017; da Cruz, Dagostin, Perussello, & Masson, 2019; da Rosa et al., 2013; Ezhilarasi, Karthik, Chhanwal, & Anandharamakrishnan, 2013; Gursul, Karabulut, & Durmaz, 2019; Khazaei, Jafari, Ghorbani, & Kakhki, 2014; Laokuldilok & Kanha, 2015; Martin, de Freitas, Sassaki, Evangelista, & Sierakowski, 2017; Ozkan, Franco, De Marco, Xiao, & Capanoglu, 2019; Pasrija, Ezhilarasi, Indrani, & Anandharamakrishnan, 2015; Sanchez, Baeza, & Chirife, 2015; Shaddel et al., 2018; Yamashita et al., 2017). α-tocopherol, the most biologically active form of Vit E, mitigates risks associated with cardiovascular disease, minimizes the effects of aging and reduces the likelihood of diseases initiated by free radicals (i.e., inflammation & cancers) (Reboul, 2017; Sharif et al., 2017). Unfortunately, throughout Western society, ultra-processed foods are rapidly displacing whole foods as the staple food (Reboul, 2017; Traber, 2014; Troesch, Hoeft, McBurney, Eggersdorfer, & Weber, 2012); and this change is in part responsible for consumers intaking less than the Recommended Dietary Allowance (RDA) for Vit E (EFSA Panel on Dietetic Products Nutrition and Allergies, 2015; Institute of Medicine, 2000). Further complicating the problem, instability, and insolubility of α-tocopherol lead to lower than expected bioavailability (Ye, Astete, & Sabliov, 2017). Research on storage stability and digestion kinetics of encapsulated Vit. E is critical to actualizing its benefits.

No one-fit solution exists to design microparticles as they can be engineered using lipids, proteins, surfactants, polysaccharides or any combination thereof. Although microencapsulation is possible using a single polymer, multi-component encapsulation is generally preferred because each polymer elicits different properties to the encapsulate. Blending polymers provides an exciting opportunity to more precisely engineer the final properties of the protective layers (Do, Hadji-Minaglou, Antoniotti, & Fernandez, 2015). The selection of the microparticle wall material depends on the encapsulating technique, physical properties of the core material, and cost (Alvarenga Botrel et al., 2012; Korma et al., 2019; Scholten, Moschakis, & Biliaderis, 2014). Raw materials derived from nature, such as polysaccharides and proteins, are preferred by consumers, as they are generally recognized as

safe (GRAS), affordable and biodegradable (Rehman et al., 2019). Research and development of raw materials with 'clean' ingredient labels are sought-after by industry to completely or partially replace synthetic ingredients applied to foods and beverages (Adjonu, Doran, Torley, & Agboola, 2014; Ozturk & McClements, 2016; Yang & McClements, 2013).

Whey proteins present several desirable functional properties, such as emulsifying capacity, gelation and film-forming ability, as well as active surface properties (Kelly, 2019; Suhag & Nanda, 2015). Recent studies have shown utility of using whey proteins to encapsulate and controlled release of bioactives, because it forms a microparticle wall surrounding the lipid core, either as a single component or in combination with others, presenting high encapsulation yield and storage stability (Bilek, Yılmaz, & Özkan, 2017; Devi, Sarmah, Khatun, & Maji, 2017; Esfanjani, Jafari, & Assadpour, 2017; Shishir, Xie, Sun, Zheng, & Chen, 2018; Tan, Zhong, & Langrish, 2020). Recently, the emulsifying and stabilizing activity of *Pereskia aculeata* Miller, popularly known as ora-pro-nobis (OPN) mucilage has been investigated (Martin et al., 2017) for gel-forming capacity and emulsions stability (Conceição, Junqueira, Guedes Silva, Prado, & De Resende, 2014; Junqueira, Amaral, Oliveira, Prado, & de Resende, 2018; Lima Junior et al., 2013). Alone, OPN produces stable ultrasound-assisted nanoemulsions (Lago et al., 2019); but, no studies exploring the effects of carrier oil on OPN mucilage/whey protein isolate (WPI) blends on the microencapsulation of bioactive compounds have been reported to date. OPN is a non-toxic mucilage extracted from the Cactaceae family (Martin et al., 2017). OPN leaves have high concentrations of proteins attached to arabinogalactan chains composed by galactose, arabinose, rhaminose and galacturonic acid (Lima Junior et al., 2013; Martin et al., 2017). This work aims to characterize the physical properties, storage stability, and bioaccessibility of OPN mucilage/WPI microparticles containing α-tocopherol dispersed in CA or CO freeze-dryied oil-in-water emulsions.

2. Material e methods

2.1. Materials

Ethyl alcohol (95%), methanol (≧ 99.9%), hexane (≧ 95%), hydrochloric acid (37%), sodium hydroxide (97%, flakes), α-tocopherol (synthetic, ≧ 96%), sodium bicarbonate (≧ 99.7%), (hydroxypropyl)methylcellulose (HPMC, mol. Wt. ~ 86 kDa), bile extract porcine ((95% (50% cholic acid sodium salt and 50% deoxycholic acid sodium salt)), sodium chloride anhydrous (≧ 99%), potassium chloride anhydrous (≧ 99%), calcium chloride dihydrate (≧ 99%), lipase from porcine pancreas (type II, 30-90 units/mg protein using triacetin), pepsin

from porcine gastric (≧ 2500 units/mg protein), α-amylase from *Bacillus* sp. (type II-A, ≧ 1500 units/mg protein using biuret), pancreatin from porcine pancreas (4 x USP), trypsin from bovine pancreas (≧ 7500 BAEE units/mg solid) were obtained from Sigma Aldrich (MO, USA). Acetonitrile (≧ 99.9%) and petroleum ether (HPLC and GC grade) were purchased from Fisher Scientific (NJ, USA). Canola oil (Great Value, ON, CA) and coconut oil (Great Value, ON, CA) were acquired from local supermarkets. Whey protein isolate Lacprodan® DI-9213 was kindly donated by Arla Food Ingredients Group (Viby, Denmark) and is ≧ 90% protein dry matter, 0.2% lactose, 0.2% fat, 4.5% ash, 5.0% moisture.

2.2. OPN mucilage production

OPN leaves were collected (Lavras, MG, Brazil), placed in polyethylene bags and stored at −18 ºC (Metalfrio DA 420, SP, Brazil) until use. OPN extraction was performed by gridding 1 kg of leaves with 2.5 L of boiling water using an industrial blender (Metvisa LG10, SP, Brazil) for 10 min. The mixture was then heated to 75 °C using a thermostatic bath (Quimis q-215-2, SP, Brazil) for 6 hr. The blend was vacuum filtered (Primar MC 1284, SP, Brazil) using three layers of organza fabric. The fiber was removed by centrifugation of the filtrate (SP Labor, SP-701, SP, Brazil) (7 min, 4677 × *g*). The supernatant was diluted to make 1:3 (extract: ethanol, 95% purity); after the precipitate was collected, frozen at −75 °C (Coldlab, CL120-86V, SP, Brazil), and freeze-dried (−40 °C; 0.998 mbar; 5 days) (Edwards High Vacuum, L4KR, SP, Brazil). The powder (6.08±0.12% moisture; dry basis: 78.93±0.29% carbohydrate, 8.89±0.17% proteins, 9.99±0.03% ash, 1.68±0.16% lipids, 0.49±0.29% fiber) was hermetically packed and stored at 25 °C in vacuum desiccators until further use.

2.3. Titration and turbidity of WPI and OPN dispersions

Titratable acidity (MPT-2 autotitrator (Malvern Instruments, Worcestershire, UK)) for WPI (5.0% w/w) and OPN (0.1% w/w) used NaOH (1.0 mol·L^{-1}) and HCl (0.1 and 1.0 mol·L^{-1}) as titrants. Zeta potentials between pH 2.5 and 7.5, at 0.5 intervals, evaluated the overall surface charge of the biopolymers. Optical turbidity evaluated the formation of soluble and insoluble complexes to determine the optimum continuous phase pH for the emulsification step. 0.075/0.037% w/w WPI/OPN dispersion turbidity was measured between pH 2.5 and 7.5 using UV-spectroscopy (Ultrospec 3100 pro, Biochrom Ltd., Cambridge, UK) at λ = 600 nm (Doost et al., 2019). Concentration of 0.075% w/w for WPI and 0.037% w/w for OPN were used to avoid absorbance values > 1.0 (a.u.). Before titration, stock solutions were produced by

hydrating polymers overnight. The pH of all treatments was adjusted manually using HCl 1 $mol \cdot L^{-1}$ or NaOH 1 $mol \cdot L^{-1}$.

2.4. Emulsion preparation

Total solids concentration (wall material + oil) for emulsions was 20.0% w/w. The continuous phase combined WPI (11.5%, 11.0%, 10.5% w/w) and OPN mucilage (0.5%, 1.0%, 1.5% w/w). OPN concentration limits were selected according to previous findings (Lago et al., 2019). OPN mucilage was first dispersed in distilled water, heated to 80 °C and constantly agitated for 1 hr. WPI, at various concentrations (Table 1), was added to the OPN dispersion and stirred for 2 hr. Samples were hydrated overnight at 4 °C. The pH of the continuous phase was adjusted to 7.0±0.1. The dispersed lipid phase (8.0% w/w) was then prepared by mixing α-tocopherol (10.0% w/w of the lipid fraction) in either CA or CO and mixed using a magnetic stir bar (Fisher Scientific, ON, CA) for 30 min at 25 °C. The two phases were combined and pre-homogenized (Caframo 2002, Caframo Lab Solutions, ON, CA) at 1500 rpm for 5 min, at 25 °C. The pre-homogenized samples were then passed through a high-pressure homogenizer (EmulsiFlex-C5, Avestin, ON, CA), at 50 MPa, for 10 passes at 25 °C.

Table 1. Emulsions composition.

Treatment	Oil type	WPI (% w/w)	OPN (% w/w)	Identification
1	Canola	11.50	0.50	CA WPI:OPN (23:1)
2	Canola	11.00	1.00	CA WPI:OPN (11:1)
3	Canola	10.50	1.50	CA WPI:OPN (7:1)
4	Coconut	11.50	0.50	CO WPI:OPN (23:1)
5	Coconut	11.00	1.00	CO WPI:OPN (11:1)
6	Coconut	10.50	1.50	CO WPI:OPN (7:1)

WPI: whey protein isolate; OPN: ora-pro-nobis mucilage; CA: canola oil; CO: coconut oil.

2.5. Rheological assessment of emulsions

The flow profile for emulsions was obtained using the coaxial cylinder measurement system (CC27 12028, D = 13.331 mm; gap = 1.290 mm) coupled with a Physica MCR 301 rheometer (Anton Paar, Ostfildern, Germany) and thermostatic bath (Julabo F25, Julabo West Inc., PA, USA). Flow curves between 0.001 to 200 s^{-1} were obtained from three continuous 2 min shear rate ramps (upward, downward and upward) at 25 °C. To obtain fluid viscosity, both

Newton's (Eq. 1) and Power Law (Eq. 2) models were fitted to the second rising curve, representing steady-state flow (Steffe, 1996):

$$\tau = \mu\dot{\gamma} \quad (1)$$

$$\tau = K\dot{\gamma}^{n} \quad (2)$$

where τ is shear stress (Pa), μ is Newtonian viscosity (Pa·s), $\dot{\gamma}$ is shear rate (s^{-1}), K is the consistency index ($Pa \cdot s^{n}$), and n is the flow behavior index (dimensionless). The apparent viscosity at shear rate of 100 s^{-1} was reported. The rheological models were fitted by a non-linear regression fit using the Statistical Analysis System 9.1.2 software (SAS Institute Inc., Cary, U.S.A., 2008).

2.6. Average droplet diameter, polydispersity index and zeta potential

The polydispersity index (PDI) and average droplet diameter (d_i) of emulsions were obtained using a 1:250 (sample:deionized water) dilution factor to avoid multiple scattering effects using dynamic light scattering (Nanotrac Flex, Microtrac, PA, USA). The refractive indices of canola oil, coconut oil, and the aqueous phase were 1.47, 1.45 and 1.33, respectively. Zeta potential (Zetasizer Nano ZS, Malvern Instruments, Worcestershire, UK) was calculated using the Smoluchowski approximation from electrophoretic mobility (Delgado, González-Caballero, Hunter, Koopal, & Lyklema, 2007; Ravindran, Williams, Ward, & Gillies, 2018).

2.7. Microencapsulation of α-tocopherol by freeze-drying

Microparticles containing α-tocopherol were made in triplicate and obtained by freeze-drying the emulsions (Table 1). After freezing emulsions at −80 °C for 24 hr (Forma 900 series, Thermo Scientific, OH, USA) they were lyophilized (Genesis 35EL, Virtis, CA, USA) at 2.67 mbar, −40 °C, for 48 hr. The material was triturated using a porcelain mortar and pestle and the powder was stored in dark sealed containers. The drying yield (% w/w) was calculated as the powder content (g) obtained after freeze-drying divided by total solids (g) in the emulsion (Pellicer et al., 2019).

2.8. Powder analysis

2.8.1. Moisture content, water activity (a_w) and bulk density

The moisture content (%) was determined by gravimetric analysis (Gravity convection oven Precision 18, GCA Corporation, IL, USA) at 105 °C, until a constant weight was achieved (method 943.03, AOAC, 2012). Water activity was measured using an Aqualab Vapor Sorption Analyzer (Meter Group, WA, USA) at 25 °C. The bulk density (BD, g·cm^{-3}) was calculated by measuring the volume (V, cm^3) of 1.0 g (m, g) of non-compact powder placed in a 10 mL graduated cylinder, as described by Eq. 3 (Reboul, 2017; Sharif et al., 2017):

$$BD = \frac{m}{V} \tag{3}$$

2.8.2. Encapsulation efficiency and oil retention

The encapsulation efficiency and oil retention were performed as previously described (Silva, Zabot, & Meireles, 2015). Briefly, the surface oil content was determined by adding 15 mL hexane to 1.5 g of microparticles and vortexed for 2 min at 25 °C. The suspension was filtered using Whatman N° 1 filter paper (Ge Healthcare, Shanghai, China). The retentate was washed 3 times in 20 mL of hexane. Residual solvent was evaporated from the filter paper using gravity convection drying (Precision 18, GCA Corporation, IL, USA) at 60 °C until a constant weight was achieved. The non-encapsulated oil (SO, g) was determined by difference from the weight prior to and following hexane extraction. Total oil (TO, g) was measured by Soxhlet (Glas-Col RX, IN, USA) using the AOAC official method 991.36 (AOAC, 2012). Encapsulation efficiency (EE, % w/w) was calculated from Eq. 4:

$$EE\% = \left(\frac{TO - SO}{TO}\right) x100 \tag{4}$$

Oil retention (OR, %) was calculated from the ratio between total oil (TO, g) and initial oil weight used during emulsion preparation.

2.8.3. Scanning electron microscopy (SEM)

A small portion of each sample was placed on the SEM stubs coated with carbon (600 Ultra Fine Norton SandWetTM, Worcester, MA, USA). Samples were then placed in a vacuum sputter coater (Denton Vacuum Desk V, NJ, USA) and let equilibrate at a vacuum pressure of

9 x 10^{-5} KPa before sputter coating gold-palladium blend (20 nm thickness) onto the sample surface using a 20 mA deposition current. Powder morphology was imaged using FEI Quanta 250 FEG-SEM (Thermo Fisher Scientific, Oregon, USA) equipped with Schottky field emission gun and Everhart-Thornley detector for secondary electrons. Imaging was controlled by the xT Microscope Control software. An accelerating voltage of 10 kV was maintained throughout the microscopy.

2.8.4. Accelerated storage stability test

α-Tocopherol stability and bioaccessibility (section 2.9.) were assessed for CA WPI:OPN (23:1) and CO WPI:OPN (23:1). An accelerated storage stability test evaluated the chemical stability of α-tocopherol encapsulated microparticles (do Carmo et al., 2018). About 25 g of powder, in open Ziploc bags (165 mm x 149 mm), were stored at 60±1.0 °C (Isotemp 60 L Incubator Gravity, Thermo Fisher Scientific, Langenselbold, Germany) in either 21% relative humidity (RH) (saturated solution of NaOH) or 55% (saturated solution of NaCl) (Barbosa-Cánovas et al., 2007). Encapsulation efficiency (as described in section 2.8.2.) was tested once a week for 5 weeks as well as Fourier-Transform Infrared Spectroscopy (FT-IR) (section 2.8.6.) and α-tocopherol concentration (quantified using HPLC, as follows).

Microparticle α-tocopherol concentration was determined as previously reported by Hategekimana, Masamba, Ma, & Zhong (2015). Extracting α-tocopherol from the microparticle core was accomplished by dispersing 10 mg of powder in 5 mL of methanol/acetonitrile (97:3 v/v). The mixture was sonicated for three-20 min cycles. The dispersion was centrifuged (Sorvall LYNX 4000, Thermo Scientific, Langenselbold, Germany) at 1000 *x g* for 20 min and the supernatant was collected. α-tocopherol concentration was quantified using HPLC (Agilent 1100 Series, Agilent Technologies, Waldbronn, Germany) equipped with a diode array detector (DAD) (G1315B DAD detector, Agilent Technologies, Waldbronn, Germany) at 295 nm. A 20 µL sample was injected onto a C18 column (Agilent ZORBAX Eclipse Plus C18 Rapid Resolution 4.6 x 150 mm 3.5 µm and Eclipse Plus C18 guard column 4.6 x 12.5 mm 5 µm) maintained at 40 °C. The mobile phase (97:3 v:v methanol: acetonitrile) had an isocratic 1 mL·min^{-1} flow rate. Pure α-tocopherol, 10 mg·L^{-1} to 500 mg·L^{-1}, was used to generate a standard curve and fitted with a linear regression (y = 1.1403·x-1.0299, R^2 = 0.996).

α-Tocopherol retention (TR_{35}, dimensionless) was defined as the ratio between α-tocopherol concentration as a function of time (C_T, mg·L^{-1}) and its concentration immediately after powder production (C_0, mg·L^{-1}). Degradation of α-tocopherol follows first-order kinetics

(Syamila, Gedi, Briars, Ayed, & Gray, 2019), thus the half-life ($t_{1/2}$) was determined according to Eq. 5 and 6 (do Carmo et al., 2018):

$$kt = -ln\left(\frac{C_t}{C_0}\right) \quad (5)$$

$$t_{1/2} = \frac{ln2}{k} \quad (6)$$

where k (days^{-1}) is a first-order rate constant, t (days) is the storage period, and $t_{1/2}$ (days) is the time required to degrade 50% of the α-tocopherol.

2.8.5. Sorption isotherms

Sorption and desorption isotherms of 700 mg of microparticles were obtained at 25±0.1 ºC using an AquaLab Vapor Sorption Analyzer (VSA) (Decagon Devices, Inc. Pullman, WA, USA) in the dynamic vapor sorption (DVS) mode. Water activity ranged between 0.10 and 0.90 at 0.05 increments. Equilibrium was achieved when the rate of change in mass as a function of time (d_m/d_t) was < 0.05 over two consecutive measurements. To describe the sorption isotherm of α-tocopherol microparticles, the GAB (Guggenheim, Ander- son and de Boer) model (Eq. 7) (Timmermann, Chirife, & Iglesias, 2001) was fitted using a non-linear square fit (Statistica software version 8.0, (Statsoft, Inc., Tulsa, USA)). According to literature, this model accurately quantifies water sorption isotherms of foods (Lewicki, 1997) and must include a minimum of five water activities measurements (Aykın-Dinçer & Erbaş, 2018).

$$m = \frac{m_0 C k a_w}{(1 - k a_w)(1 - k a_w + C k a_w)} \quad (7)$$

where m is the equilibrium moisture content (g water/100 g dry basis); m_0 is the monolayer moisture content (g water/100 g dry basis); a_w is the water activity (dimensionless); C and k are model constants (dimensionless). The coefficient of determination (R^2) and the mean relative percentage deviation modulus (< 10%) was used to evaluate the quality of the adjustments (Arslan & Togˇrul, 2005).

2.8.6. Fourier transform infrared (FTIR) spectroscopy

The FTIR spectroscopy, equipped with an attenuated total reflection (ATR) cell (Pike Technologies, Madison, USA), assessed chemical degradation of α-tocopherol in WPI/OPN

microparticles (IRPrestige21, Shimadzu Corporation, Japan). Samples were placed on the ATR cell and scanned 40 times at a resolution of 4 cm^{-1} in the mid-IR region (600 to 4000 cm^{-1}).

2.9. Bioaccessibility − TIM-1 simulated digestion

The TNO intestinal model (TIM-1) is a dynamic, robotic simulate gastrointestinal system that mimics the stomach and upper intestinal compartments (i.e., duodenum, jejunum, and ileum), facilitating bioaccessibility studies under fed or fasted conditions (Minekus et al., 1995; Ribnicky et al., 2014; Samtlebe et al., 2018; Thilakarathna et al., 2016). This model has been widely validated and statistically correlates to *in vivo* human studies (Anson et al., 2011; Déat et al., 2009; Eklund-Jonsson, Sandberg, Hulthen, & Alminger, 2008; Larsson, Minekus, & Havenaar, 1997; Marteau, Minekus, Havenaar, & Huis In't Veld, 1997; Souliman, Blanquet, Beyssac, & Cardot, 2006; Van De Wiele et al., 2007; Verwei, Freidig, Havenaar, & Groten, 2006). The fed state protocol for the TIM-1 was used to assess the release profile of α-tocopherol from microparticles over a 6 hrs. To mimic human physiological conditions, these compartments were filled with preset solutions following a programmed protocol and included: hydrochloric acid (1.00 $mol \cdot L^{-1}$ HCl), sodium bicarbonate (1.00 $mol \cdot L^{-1}$ $NaHCO_3$), gastric solution (0.40% w/v HPMC and 0.04% w/v bile salts powder), small intestinal electrolyte solution (SIES, 5.00 $g \cdot L^{-1}$ NaCl, 0.60 $g \cdot L^{-1}$ KCl, and 0.25 $g \cdot L^{-1}$ $CaCl_2$), gastric enzyme solution (4.80 $g \cdot L^{-1}$ NaCl, 2.20 $g \cdot L^{-1}$ KCl, 0.22 $g \cdot L^{-1}$ $CaCl_2$, 20 $U \cdot mL^{-1}$ lipase, 4800 $U \cdot mL^{-}1$ pepsin and 47 $U \cdot mL^{-1}$ amylase), 7.00% w/v pancreatin solution and fresh porcine bile previously collect from a slaughterhouse (Conestoga Meats, Breslau, CA). TIM-1 compartments were maintained at 37±1 ºC during the simulated digestion and pH was dynamically controlled (Table 2). The rate of gastric emptying was preset with a half-time of 80 min (TNO, Zeist, The Netherlands).

Table 2. Preset pH values of the TIM-1 compartments.

Compartment	Predetermined pH levels
Duodenal	5.5
Jejunal	6.5
Ileal	7.4
Stomach (0 min)	6.5
Stomach (30 min)	4.2
Stomach (60 min)	2.9
Stomach (120 min)	2.0
Stomach (210 min)	1.7
Stomach (360 min)	1.7

The TIM-1 compartments were prefilled with starting residues to mimic *in vivo* fed-state gastrointestinal conditions. The gastric starting residue was composed of 5.0 g gastric enzyme solution and 5.0 g of gastric solution; the duodenal starting solution consisted of 15.0 g of SIES, 15.0 g of 7.0% w/v pancreatin, 30.0 g of fresh bile and 1 mL trypsin solution (2 mg·mL $SIES^{-1}$); the jejunal starting residue was 35.0 g SIES, 35.0 g 7.0% w/v pancreatin, and 70.0 g fresh bile; and the ileal starting residue consisted of 140.0 g SIES. The solution used to simulate the ileal fluid was SIES and the jejunal secretion was composed of 10% fresh porcine bile in SIES. Semi-permeable filters (0.05 μm capillary membranes, Spectrum Milikros modules M80S-300-01P, Repligen, Waltham, USA) were attached to the ileal and jejunal compartments in order to obtain the micellar fractions representing the bioaccessible α-tocopherol fraction.

The fed 'meal' contained 10.0 g α-tocopherol WPI/OPN microparticles, 130.0 g of gastric electrolyte solution (4.80 $g \cdot L^{-1}$ NaCl, 2.20 $g \cdot L^{-1}$ KCl, 0.22 $g \cdot L^{-1}$ $CaCl_2$), 100.0 g water and 11.0 mg of amylase. The meal was added to the gastric compartment containing 10.0 g of gastric starting residue. An additional 50.0 g of water was used to rinse the meal container and was added to the gastric compartment thus the total meal was 300 g. Filtrates containing the bioaccessible α-tocopherol were analyzed by HPLC (as described in the section 2.8.4) at 30, 60, 90, 120, 180, 240, and 300 min from the jejunal and ileal compartments and the ileal efflux.

Cumulative α-tocopherol bioaccessibility (sum of jejunum + ileum filtrates) as a function of time was fitted to the shifted-logistical model (Eq. 8) using a non-linear analysis (Graphpad Prism 6.0 (La Jolla, CA)) (AlHasawi et al., 2018; Speranza et al., 2013):

$$C(t) = \frac{C_{asymp}}{1 + e^{k(t_c - t)}} - \frac{C_{asymp}}{1 + e^{kt_c}} \quad (8)$$

where $C(t)$ (%) is the % α-tocopherol released as a function of time (t, min); C_{asymp} (%) is the maximum α-tocopherol bioaccessibility; k (min^{-1}) is a rate constant; and t_c (min) is the induction time, representing the time to release 50% of the total bioaccessible α-tocopherol content. This model satisfies the boundary condition that at t = 0 min, the bioaccessible α-tocopherol content is zero. Statistical significance between formulations for fitted bioaccessibility parameters was evaluated. All analyses were done in triplicate and expressed as mean ± standard deviation.

2.10. Statistical analysis

Analysis of Variance (ANOVA) determined statically significant differences (p < 0.05) between treatments for both the emulsions and powders. Tukey post-hoc or Student *t*-tests (p < 0.05) evaluated means and standard error.

3. Results and discussion

3.1. Optimization of solution and emulsion characteristics required for microparticle production

OPN and WPI were similarly charged (Fig. S.1A & B) and had minimum turbidity, corresponding to low OPN-WPI interactions, when combined (Fig. S.1C) at pH of 7; thus, it was selected as the optimal pH for further formulation. ζ-Potential of OPN was negative across all pH values (2.5 < pH < 7.5) with an extrapolated pI < pH = 2.5 (Fig. S.1B), and the pI for WPI was 5.30 (Fig. S.1A).

Flow behavior of emulsions, prior to freeze drying, was dependent on both biopolymer concentration and ratio as well as carrier oil (CO or CA). WPI:OPN (23:1) in both CO and CA showed Newtonian behavior and fitted to the Newton's law (p < 0.05 and R^2 > 0.998) (Table 3). Higher OPN concentrations (i.e., > 0.5% w/w (WPI:OPN 11:1 and 7:1)) were fitted to the Power law (p < 0.05 and R^2 > 0.997) (Table 3). The consistency index (K) and the apparent viscosity (η_{100}) significantly increased (p < 0.05) at higher OPN concentrations. K and η_{100} were highest for CA WPI:OPN (7:1), which contained 1.5% w/w OPN and CA, and agrees with previous reports (Junqueira et al., 2018; Lago et al., 2019). With total solids constant, higher OPN concentrations had higher viscosities attributed to the branched structure of OPN mucilage

which contains arabinogalactan chains (carbohydrate fraction) attached to proteins (Lago et al., 2019). In all cases, CA presented statistically higher ($p < 0.05$) μ, K and η_{100} values compared to those prepared with CO due to the higher viscosity of pure CA (μ = 0.061 Pa·s) compared to CO (μ = 0.050 Pa·s) when comparing treatments with similar encapsulating composition (Table 3). The pseudoplastic behavior, fit to the Power law, for both CO and CA presented higher apparent viscosity, K values, and lower n values ($p < 0.05$) for treatments containing 1.5% w/w OPN. Increased pseudoplasticity was observed with increasing OPN concentration (Table 3) which is consistent with similar studies (Anvari & Melito, 2017; López-Castejón, Bengoechea, Espinosa, & Carrera, 2019).

Table 3. Newton and Power law fitted rheological parameters of OPN /WPI/Oil-in-water emulsions.

Treatment	**Newton law**				
	μ (Pa·s)*	RMSE	R^2		
WPI:OPN (23:1)					
CA	0.009±0.000[a]	0.014	0.999		
CO	0.006±0.000[b]	0.016	0.998		
Treatment	**Power law**				
	K (Pa·s^n)*	n (-)*	RMSE	R^2	η_{100} (mPa·s)*
WPI:OPN (11:1)					
CA	0.036±0.001[b]	0.898±0.004[b]	0.008	0.999	22.750±0.041[b]
CO	0.019±0.002[a]	0.952±0.020[c]	0.016	0.999	16.330±0.874[a]
WPI:OPN (7:1)					
CA	0.076±0.004[d]	0.840±0.014[a]	0.100	0.997	38.667±2.509[c]
CO	0.053±0.002[c]	0.847±0.001[a]	0.024	0.999	26.183±1.007[b]

*Different letters in columns indicate significant statistical differences ($p < 0.05$) by Tukey test.
WPI: whey protein isolate; OPN: ora-pro-nobis mucilage; CA: canola oil; CO: coconut oil; RMSE: root-mean-square error; μ: Newtonian viscosity; K: consistency index; n: flow behavior index; η_{100}: apparent viscosity at 100 s^{-1}.

CA WPI:OPN (7:1) emulsions had a bimodal distribution of larger particle sizes as apparent by the elevated polydispersity index (PDI) (Table 4); and as such this wall material formulation was not considered for further bioaccessibility studies. At 1.5% w/w OPN and CA had larger droplets because of the high solution viscosity (Table 3). Higher emulsion viscosity hinders oil-droplet disruption during homogenized, requiring higher energy input to achieve a

monomodal distribution leading to significantly higher operating costs. Instability is also introduced with high biopolymer ratios and viscosities including: 1) restricted diffusion and interfacial adsorption of surface-active molecules, 2) associative-electrostatic interactions bridge binding leading to flocculation; 3) thermodynamic incompatibility between biopolymers leading to depletion flocculation; and 4) etc. (Akbas, Soyler, & Oztop, 2018; Dickinson, 2019; Juttulapa, Piriyaprasarth, Takeuchi, & Sriamornsak, 2017; Lago et al., 2019; McClements, 2015).

Table 4. Average droplet diameter (d_i) and ζ-potential results for emulsions prepared according to the continuous phase composition.

Treatment	d_i (nm)*	Volume (%)	PDI (-)*	ζ-potential (mV)*
WPI:OPN (23:1)				
CA	287.00±4.25^{a,b}	100.00	0.203±0.033^{a,b}	−50.08±0.68^{a}
CO	230.37±5.31^{a}	100.00	0.144±0.070^{a}	−49.63±0.41^{a}
WPI:OPN (11:1)				
CA	389.67±10.27^{b,c}	100.00	0.269±0.042^{a,b}	−44.21±0.61^{b}
CO	318.00±2.40^{a,b,c}	100.00	0.252±0.026^{a,b,c}	−45.12±0.28^{b}
WPI:OPN (7:1)				
CA_1	1608.33±177.45^{d}	52.77±5.72	0.443±0.036^{c}	−40.03±0.20^{d}
CA_2	355.33±71.35^{b,c}	47.23±5.72		
CO	402.67±13.69^{c}	100.00	0.364±0.082^{b,c}	−42.02±0.69^{c}

*Different letters in the column indicate significant statistical differences ($p < 0.05$) by Tukey test. WPI: whey protein isolate; OPN: ora-pro-nobis mucilage; CA: canola oil; CO: coconut oil; d_i: droplet diameter; PDI: polydispersity index.

All formulations were controlled at pH 7, above the pI for both WPI and OPN (Fig. S.1A & B), and had negative ζ-potentials (Table 4). Increasing OPN concentration coincided with significantly ($p < 0.05$) decreased ζ-potential, arising from counter-ions present in OPN mucilage which potentially shield electrostatic repulsion (as Na^{+}, K^{+}, Mg^{2+}, Ca^{+2}, Mn^{2+}) (Martin et al., 2017; McClements, 2015). Colloidal systems have considerable kinetic stability when ζ-potential is greater than +30 mV or less than −30 mV (Shanmugam & Ashokkumar, 2014). Thus, it is expected that treatments CA WPI:OPN (23:1) and CO WPI:OPN (23:1) would have higher stability considering also their smaller droplet size diameter (Table 4). An increase in ζ-potential magnitude for emulsions (Table 4) compared to biopolymers solutions (Fig. S.1A & B) may be attributed to exposure of charged sites during homogenization that, in the native

conformation, were shielded (Saricaoglu, Gul, Besir, & Atalar, 2018; Tabilo-Munizaga et al., 2019).

3.2. Microparticle characterization

Following microparticle production drying yield, moisture content, water activity (a_w), bulk density (BD), α-tocopherol encapsulation efficiency (EE) and oil retention (Table 5) were assessed to find the optimal formulation for assessing long-term stability and α-tocopherol bioaccessibility. Although drying yield varied between formulations, moisture content nor a_w statistically differed between treatments ($p > 0.05$) (Table 5). More importantly, a_w ranged between 0.198±0.002 to 0.205±0.006 which was desirable as it is sufficiently low to prevent degrative reactions (Caliskan & Dirim, 2016), microbial growth, and caking (Goyal et al., 2015); while above the optimal range for lipid oxidation in powders ($0.1 < a_w < 0.2$) (Frankel, 2012). The bulk density (BD) was between 0.15±0.00 and 0.22±0.01 $g \cdot cm^{-3}$ irrespective of the oil used, and formulations with low OPN concentrations had higher BD arising from viscosities (Table 3) and smaller oil droplet diameter (Table 4) in precursor emulsions. Upon freeze drying, the consequence is smaller pores through the dried structure resulting in finer powder when triturated (Aghbashlo, Mobli, Rafiee, & Madadlou, 2012). Irregularly sized and shaped microparticles result in external voids, hindering particles compaction and lower BD (Rajam & Anandharamakrishnan, 2015). Encapsulation efficiency (EE) reflects protection conferred to α-tocopherol against environmental conditions (Fioramonti et al., 2017). Formulations containing CO exhibited higher $EE\%$ than those prepared with CA (Table 5), regardless of the WPI/OPN ratio since CO is solid and CA is liquid at room temperature. For CA, there was a positive correlation between $EE\%$ and emulsion droplet size, which has been shown to minimize oil migration and amount of unencapsulated oil (Fioramonti et al., 2017; González, Martínez, Paredes, León, & Ribotta, 2016). Oil retention, described as mass of oil in the particle divided by precursor emulsion total solids, did not significantly differ between samples (Table 5), which others have reported (Silva, Azevedo, Cunha, Hubinger, & Meireles, 2016; Silva, Zabot, Cazarin, Maróstica, & Meireles, 2016).

Table 5. Physico-chemical parameters for the α-tocopherol microparticles produced by freeze-drying.

Treatment	Yield* (%)	Moisture* (%)	a_w*	BD * (g·cm^{-3})	EE * (% w/w)	OR * (%)
WPI:OPN (23:1)						
CA	87.06±1.71^{c}	2.45±0.09^{a}	0.199±0.001^{a}	0.20±0.00^{b}	74.12±0.41^{b}	77.87±0.48^{a}
CO	86.03±0.63^{c}	2.47±0.10^{a}	0.198±0.002^{a}	0.22±0.01^{c}	79.77±0.41^{d}	77.88±1.87^{a}
WPI:OPN (11:1)						
CA	79.64±1.28^{b}	2.46±0.10^{a}	0.205±0.006^{a}	0.18±0.00^{b}	73.05±0.72^{b}	79.93±1.09^{a}
CO	82.91±0.60^{bc}	2.41±0.12^{a}	0.201±0.001^{a}	0.19±0.01^{b}	79.31±0.48^{cd}	76.95±0.44^{a}
WPI:OPN (7:1)						
CA	74.43±0.31^{a}	2.41±0.11^{a}	0.203±0.005^{a}	0.16±0.00^{a}	67.26±0.21^{a}	79.33±0.58^{a}
CO	74.05±2.91^{a}	2.42±0.05^{a}	0.205±0.006^{a}	0.15±0.00^{a}	77.42±0.97^{c}	79.85±1.97^{a}

*Different letters in the column indicate significant statistical differences ($p < 0.05$) by Tukey test. WPI: whey protein isolate; OPN: ora-pro-nobis mucilage; CA: canola oil; CO: coconut oil; a_w: water activity; BD: bulk density; EE: encapsulation efficiency; OR: oil retention.

Higher OPN concentrations led to darker powders, as illustrated moving left to right across Fig. S2, which is expected since the OPN mucilage powder is dark (Oliveira et al., 2019). It is also apparent that rougher powder texture (Fig. 1) coincides with more viscous emulsions (Table 3), which is attributed to harder structures produced after freeze-drying and thus larger particles when titrated. Agglomerates in CA WPI:OPN (7:1) and its low EE% (67.26±0.21% w/w), suggests that free oil migrating from the core to surface is responsible for particle aggregation (Fioramonti et al., 2017). Porous, irregular continuous surfaces, similar to glass-like flakes previously reported for freeze-dried powders are observed herein (Fig. 1) (Chranioti, Chanioti, & Tzia, 2016; Fioramonti et al., 2017; Pellicer et al., 2019; Vardanega, Muzio, Silva, Prata, & Meireles, 2019). The undulating surface morphologies (Fig. 1C and 1F), reflect lower *EE%* with high OPN concentration (Table 5); while Fig. 1A and 1D have smoother surface morphology.

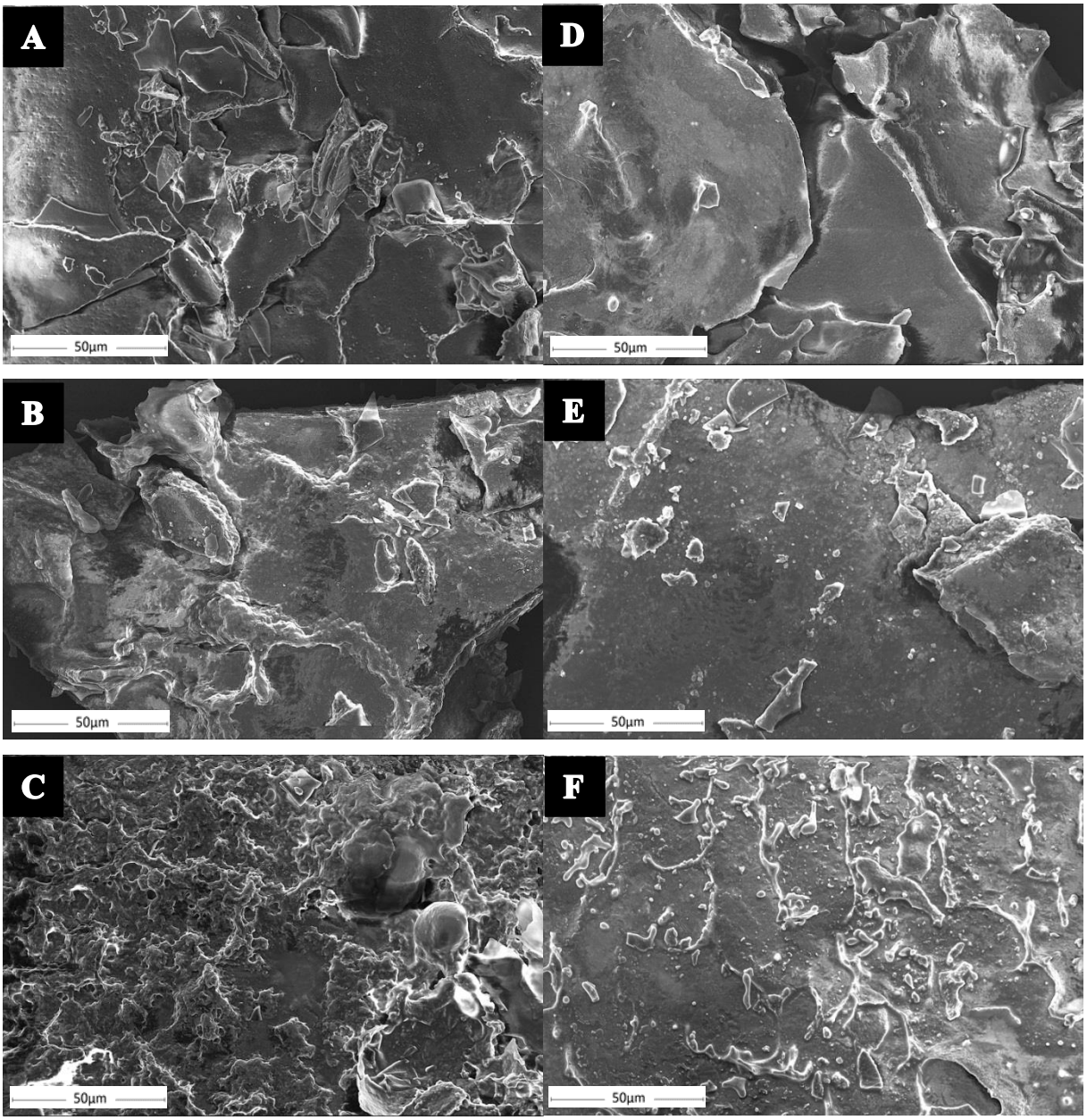

Figure 1. SEM images of freeze-dried α-tocopherol microparticles produced from WPI/OPN and CA or CO-in-water emulsions: CA WPI:OPN (23:1) (**A**); CA WPI:OPN (11:1) (**B**); CA WPI:OPN (7:1) (**C**); CO WPI:OPN (23:1) (**D**);CO WPI:OPN (11:1) (**E**); CO WPI:OPN (7:1) (**F**). Scale bars are provided on each micrograph.

3.3. Long-term microparticle stability

Based on the emulsion characteristics (e.g., low viscosity and monomodal particle size distribution) and physical properties (e.g., low moisture content and water activity, and higher drying yield, $EE\%$ and BD) of the microparticles, CA WPI:OPN (23:1) and CO WPI:OPN (23:1) were selected to test storage stability and α-tocopherol bioaccessibility. Microparticles entrained the oil phase as there was no significant difference in *EE%* indicated ($p > 0.05$) (Fig. 2A) over a 5-week accelerated self-stability test at 60 ºC and 21% (saturated NaOH solution)

or 55% (saturated NaCl solution) relative humidity. Both relative humidities are below the critical point (i.e., RH = 65%) where water absorption occurs at significantly faster rates (Fig. 2C & D).

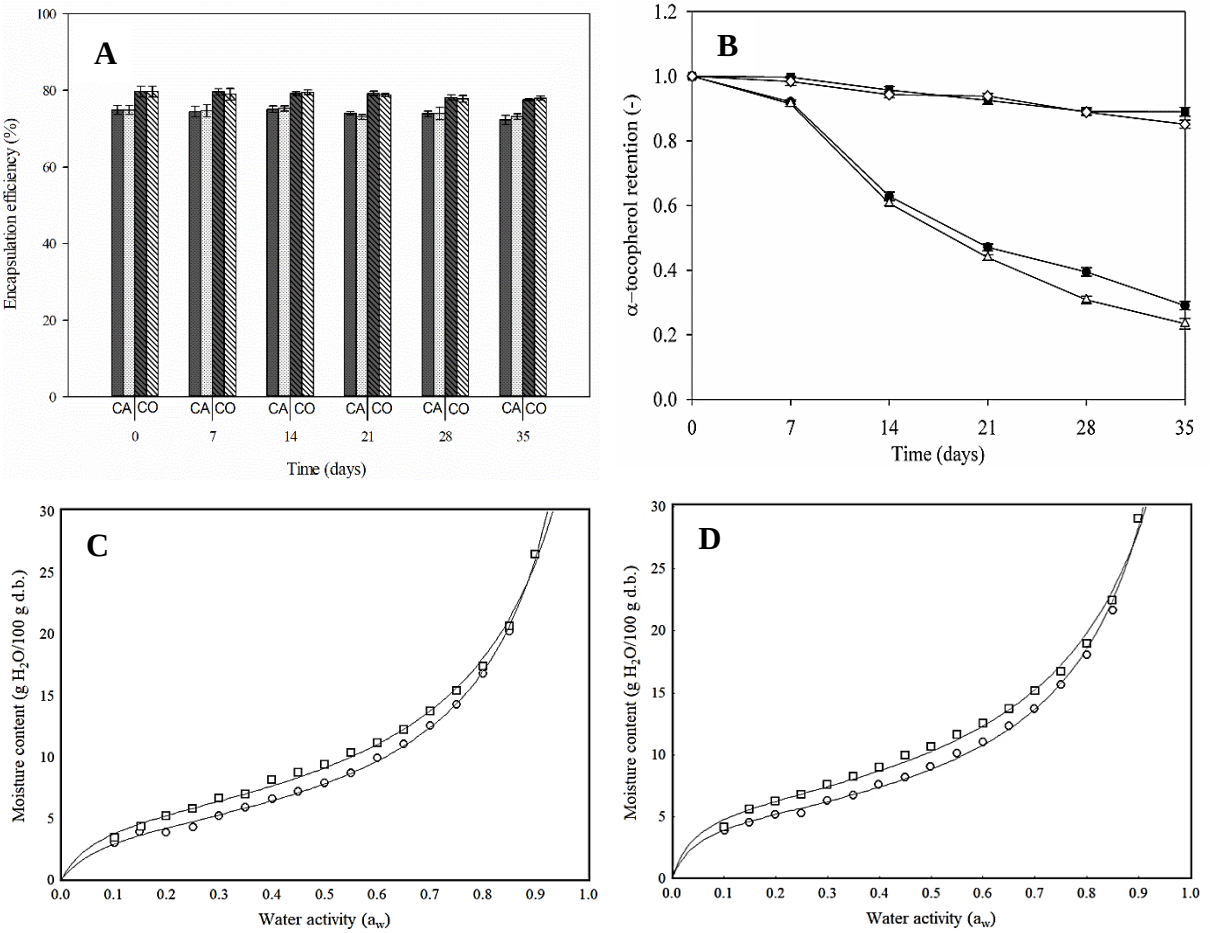

Figure 2. (A) Encapsulation efficiency (%) of α-tocopherol microparticles during storage, according to the relative humidity (21%, dark bars; 55%, light bars) and lipid phase (●, canola oil; \, coconut oil). **(B)** α-tocopherol retention throughout time for the treatments composed with: canola oil and stored in a RH = 21% (●); canola oil and stored in a RH = 55% (△); coconut oil and stored in a RH = 21% (■); coconut oil and stored in a RH = 55% (◇). Absorption (○) and desorption (□) isotherms and GAB model fit (line) for the treatments: CA WPI:OPN (23:1) **(C)**, and CO WPI:OPN (23:1) **(D)**.

Low initial moisture content of microparticles translates to improved stability (e.g., reduced rates of: microbial growth, enzymatic and non-enzymatic chemical reactions) contributing to extend the product shelf-life (Otálora, Carriazo, Iturriaga, Nazareno, & Osorio, 2015). α-tocopherol retention, after 35 days, was dependent on the lipid phase (Fig. 2B and Table 6). For CO containing microparticles α-tocopherol retention (TR_{35}) was > 87% at both 21 and 55 % RH. In contrast, CA microparticles had a significant decrease in TR_{35}, with values less than 30% of initial α-tocopherol microparticles concentration (Fig. 2B). CO is comprised primarily of saturated fatty acids that are less susceptible to oxidation (de Moura e Dias et al.,

2018). Also, higher TR_{35} for CO microparticles may be associated with tighter fatty acid chains packing resulting in more dense structures, which potentially mitigate oxygen permeability (Otálora et al., 2015; Wang et al., 2017). Microparticle α-tocopherol retention, as a fucntion of time, was fittecd to a first order equation ($0.949 < R^2 < 0.983$), to obtain the degradation rate constant, k (days^{-1}), and the time until half the α-tocopherol concentration has decreased, $t_{1/2}$ (days) (Table 6). Clearly, stability of α-tocopherol depended on carrier oil; CO had lower k values and higher $t_{1/2}$, compared to CA, which was independent of RH. These results concur with TR_{35} findings, suggesting α-tocopherol stability is improved when CO was the lipid carrier.

Table 6. α-Tocopherol retention after 35 days of storage and degradation rate constants of microparticles produced with CA or CO oil stored in different relative humididy, at 60 ºC.

Sample	TR_{35} (-)*,**	k (day^{-1}) *,**	$t_{1/2}$ (days) *,**	R^2
Canola oil (RH = 21%)	0.290±0.013^{A}	0.037±0.001^{A}	18.835±0.559^{A}	0.983
Canola oil (RH = 55%)	0.234±0.017^{B}	0.044±0.001^{B}	15.649±0.469^{B}	0.985
Coconut oil (RH = 21%)	0.890±0.014^{a}	0.004±0.000^{a}	179.804±18.740^{a}	0.949
Coconut oil (RH = 55%)	0.872±0.012^{a}	0.005±0.000^{a}	154.048±12.920^{a}	0.958

*Different capital superscripts in columns indicate significant difference ($p < 0.05$) for CA samples by *t* test. **Different lowercase letters in the column indicate significant difference ($p < 0.05$) for samples with CO by *t* test. RH: relative humidity; TR_{35}: α-tocopherol retention after 35 of storage; k: first order rate constant; $t_{1/2}$: half-life time.

Conversely, CA microparticle α-tocopherol degradation kinetics are dependent on RH ($p < 0.05$). Higher unsaturated fatty acids content of CA are prone oxidation, which accelerates in the presence of water (Vergara, Saavedra, Sáenz, García, & Robert, 2014). CA containing microparticles stored at RH = 21% had greater stability (k = 0.04±0.00 days^{-1} and $t_{1/2}$ = 18.83±0.56 days) compared to RH = 55% (k = 0.04±0.00 days^{-1} and $t_{1/2}$ = 15.65±0.47 days) implying that α-tocopherol is degraded to a greater extent when CA is used as the lipid carrier compared to CO. The less dense lipid core facilitates oxygen diffusion through the encapsulating matrix thereby accelerating α-tocopherol degradation by oxidation shortening shelf-life (Hategekimana et al., 2015). Irrespective of the carrier oil used, low water adsorption capacity was observed at low a_w, in contrast with a sharp increase in moisture content for a_w > 0.650; thus, materials have extended shelf-life when stored at RH < 65%. The GAB model accurately fit isotherms for the treatment prepared with CA (R^2 = 0.996 (adsorption curve) and 0.998 (desorption curve)) and for CO (R^2 = 0.997 (adsorption curve) and 0.994 (desorption

curve)). The monolayer moisture contents, predicted by the model, were 4.62 g H_2O/100 g d.b. and 5.01 g H_2O/100 g d.b. for the adsorption curves of microparticles with CA or CO, respectively. For the desorption curves CA and CO were 5.51 g H_2O/100 g d.b. and 6.06 g H_2O/100 g d.b., respectively. Similar monolayer moisture contents in both CO and CA α-tocopherol microparticles are expected due to identical encapsulation wall material composition. The monolayer moisture content, or water strongly adsorbed to protein and carbohydrate fractions of the WPI and OPN, represents the ideal water content required to produce chemically and microbiologically stable powders (Alpizar-Reyes et al., 2018). GAB constants, C, were 13.32 (adsorption isotherm) and 17.21 (desorption isotherm) for the microparticles containing CA, in comparison with 23.90 (adsorption isotherm) and 26.17 (desorption isotherm) for treatments with CO. This parameter is a measure of the energy involved in the water adsorption at the monolayer binding sites (De Sá Mendes et al., 2019; Téllez-Pérez, Sobolik, Montejano-Gaitán, Abdulla, & Allaf, 2015). Higher C values correlate to larger differences in enthalpy between the monolayer and multilayer molecules (Quirijns, Van Boxtel, Van Loon, & Van Straten, 2005). Higher C values obtained for microparticles containing CO suggest stronger water binding at the monolayer.

Finally, the GAB constant k was calculated to be 0.92 (adsorption isotherm) and 0.88 (desorption isotherm) for the treatment prepared with CA, while for microparticles containing CO it showed values equal to 0.92 (adsorption isotherm) and 0.87 (desorption isotherm). k is a measure of the energy of interaction between water molecules adsorbed at the monolayer and at a distant adsorption site (Alpizar-Reyes et al., 2018). More structured molecules in the multilayers (layers adjacent to the monolayer) have lower k values, while k values close to 1 implies the water molecules not included in the monolayer behavior, as free bulk water (Quirijns et al., 2005). k values were close to 1 suggesting fewer interactions between water and the encapsulating biopolymers. According to Lewicki (1997), isotherms are adequately described when C and k values are between $0.24 < k \leq 1$ and $5.65 \leq C \leq \infty$, as it ensures the predicted values do not differ from the real capacity of the monolayer more than ±15.5%. Besides, $k < 1$ and $C > 2$ are an indicative of Type-II sigmoid behavior (Brunauer, Emmett, & Teller, 1938), which accounts for the existence of multilayers arising due to colligative effects (i.e., water confined in capillaries) and surface water interactions (De Sá Mendes et al., 2019; Erbaş, Aykın, Arslan, & Durak, 2016).

WPI peaks, obtained with FTIR, at 1635 cm^{-1} (amide I) and 1525 cm^{-1} (amide II) (Fig. 3A) are related to peptide bond vibrations (-CO-NH) (Andrade et al., 2019; Tan, Ebrahimi, &

Langrish, 2019; Tan, Zhong, & Langrish, 2019). Peaks at 1442, 1384, 1228 and 628 cm^{-1} correspond with bending of -CH_2, streching of -COO^-, stretching -C-C vibrations and ring -C-H deformation (Esfanjani, Jafari, Assadpoor, & Mohammadi, 2015; Singh, Singh, Karthick, Tandon, & Prasad, 2018; Tan, Zhong, et al., 2019; Zhang, Peng, Ma, & Zeng, 2019). Peaks at 3050 and 2947 cm^{-1} are associated with aliphatic carbons -C-H(CH_2) and -C-H(CH_3) (Andrade et al., 2019; Botelho, Reis, Oliveira, & Sena, 2015). The region between 1200-900 cm^{-1}(stretching -C-C or -C-OH vibrations) is characteristic of carbohydrates, such as lactose present in WPI (Andrade et al., 2019; Darra et al., 2017). The broad peak between 3500-3100 cm^{-1} (stretching O-H band) suggests the presence of water, carbohydrate -O-H hydrogen bonds (Monrroy, García, Ríos, & García, 2017) or potentially stretching -N-H vibrations of amides (Conceição et al., 2014; Mól et al., 2019). Similar peaks were found in the spectrum obtained for OPN (Fig. 3B), which contains both proteins and carbohydrates, at 3360 cm^{-1} (stretching O-H vibrations), 2912 cm^{-1} (aliphatic carbons -C-H(CH_2) and -C-H(CH_3)), 1627 cm^{-1} (amide I), 1377 cm^{-1} (-COO^-), 1249 cm^{-1} (stretching -C-C vibrations) and 669 cm^{-1} (-C-H bending deformation). Peaks at 1317 and 1033 cm^{-1} are associated with amide III (stretching -C-N) from the oligopeptide covalent bonds (Tan, Zhong, et al., 2019), and stretching -C-O vibration of alcohols (Andrade et al., 2019). The peak at 806 cm^{-1} correspond with ring -C-H out-of-plane bending (Singh et al., 2018). FTIR spectra of OPN mucillage corresponds to previous reports of Conceição et al. (2014).

FTIR spectra of freeze-dried microparticles (Fig. 3C-F) maintained similar peaks as observed to WPI (Fig. 3A) and OPN (Fig. 3B). α-tocopherol exhibited absorbance bands at 3473 cm^{-1} (stretching -O-H), 2927 and 2868 cm^{-1} (asymmetric and symmetric stretching vibrations of –CH_2 and –CH_3), respectively (Che Man, Ammawath, & Mirghani, 2005). Absorbance at 1461 cm^{-1} coinsides with phenyl skeletal or methyl asymmetric bending, while 1378 cm^{-1} corresponds to methyl symmetric bending, 1262 cm^{-1} for –CH_2 stretching bending and 1086 cm^{-1} for plane bending of phenyl. These peaks are clearly present in microencapsulated of α-tocopherol in freeze-dried powders (Fig. 3C-F). Also, the presence of the bioactive is shown by the chromatograms of α-tocopherol encapsulated in CO WPI:OPN (23:1) (Figure S3) and in CA WPI:OPN (23:1) (Figure S4) microparticles.

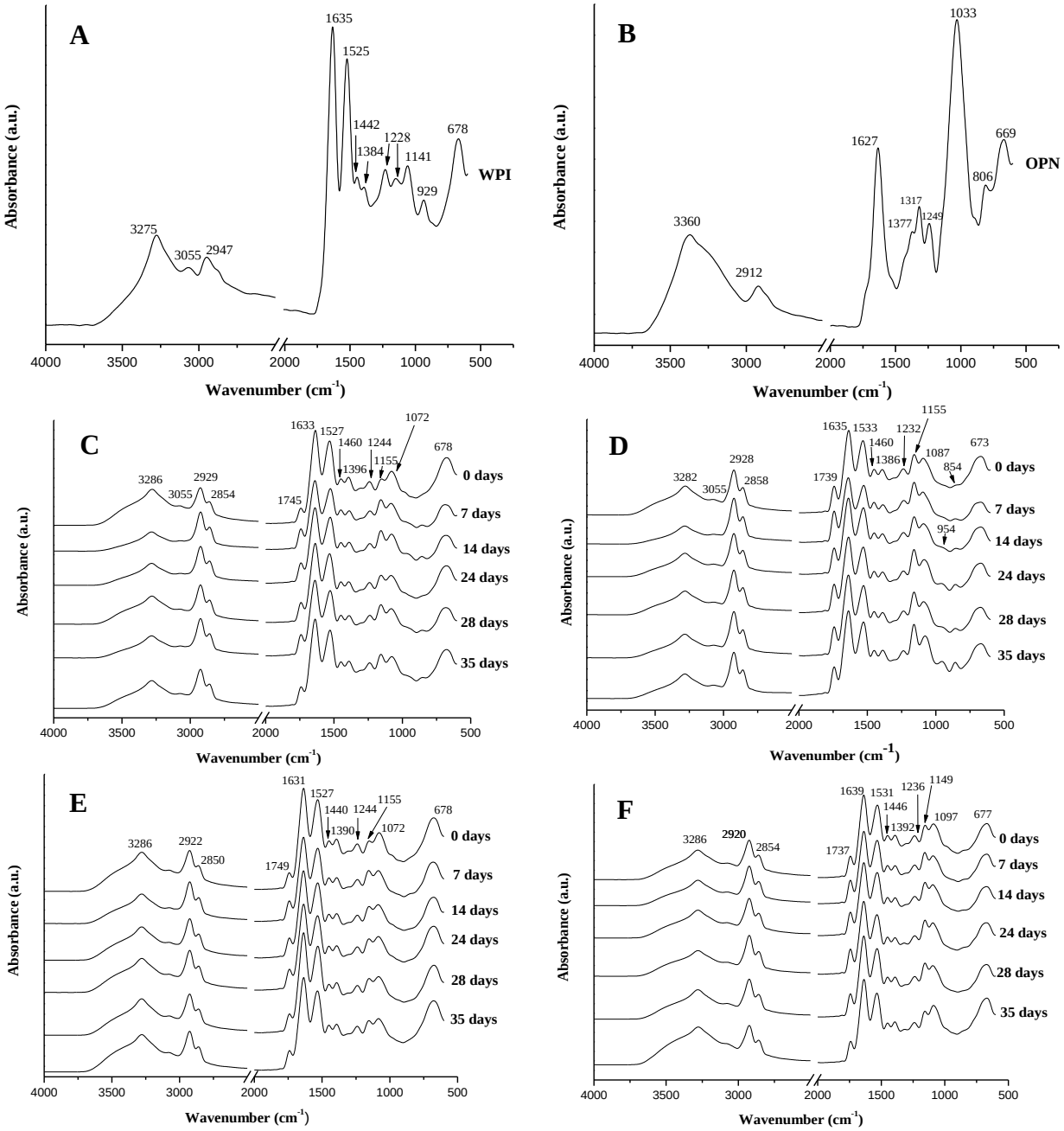

Figure 3. FTIR spectra of WPI (**A**); OPN (**B**); and freeze-dried α-tocopherol microparticles stored at low (21%, **C** and **E**) or high (55%, **D** and **F**) relative humidity, according to the oil carrier used (canola oil, **C** and **D**; coconut oil, **E** and **F**).

The lipid phase (CA or CO) presented vibrations at ~ 3008 cm^{-1} atributed to stretching of *cis* double bonds (-C=C-H), at 2920-2929 and 2850-2858 cm^{-1} representing asymmetrical and symmetrical -C-H stretching of aliphatic groups of organic fatty acids, and at 1737-1749 and 1244-1236 cm^{-1} (stretching -C=O of triglycerides or -C-O-C of esters, respectively). Peaks at 1460 cm^{-1} (bending vibrations of $-CH_2$ and $-CH_3$ aliphatic groups), 1386-1396 cm^{-1} rocking vibrations of -CH bonds of *cis*-disubstituted olefins in canola oil, at 1149-1155 cm^{-1} (stretching -C-O vibration of aliphatic esters) and at 1072-1092 cm^{-1} (stretching -CO band of ether linkages

or stretching -COH of alcohols) (Beneš et al., 2017; Khorasani, Ataei, & Neisiany, 2017; Mhaske, Condict, Dokouhaki, Katopo, & Kasapis, 2019; Ozulku, Yildirim, Toker, Karasu, & Durak, 2017; Talpur et al., 2015). FTIR spectra of samples with CO remained constant over 35 days of storage (Fig. 3E and 3F) indicatning α-tocopherol did not undergo degradation or oxidation, as previously predicted by the TR_{35} results and α-tocopherol retention (Fig. 2B). In contrast, samples with CA, observed peaks forming in time at 854 and 954 cm^{-1}, which were atributed to the formation of aromatic -CH bending vibrations and -C-O-C stretching epoxides (Khundamri, Aouf, Fulcrand, Dubreucq, & Tanrattanakul, 2019), indicating α-tocopherol is being converted to quinones via epoxide formation (Hategekimana et al., 2015).

3.4. TIM-1 simulated digestion

Microencapsulated powders of CA WPI:OPN (23:1) or CO WPI:OPN (23:1) and liquid formulations (CA and CA WPI:OPN (23:1) emulsions) each contained 2.5% w/w α-tocopherol was assessed using the TIM-1 simulated gastrointestinal tract (Fig. 4). Bioaccessiblilty herein represents the α-tocopherol released from the microencapsulates into the luminal fluid and is available for absorbtion (AlHasawi et al., 2018). Cumulative bioaccessbility followed sigmoidal trends, with a characteristic initial time period of ~ 60 min for microencapsulates and was higher for CA compared to CO (Fig. 4 jejunum + ileum). A non-linear shifted-logistical model was fitted (R^2 > 0.9828) to the sigmodial bioaccessibility curves to obtain the bioaccessible fraction (%), rate constant (min^{-1}) and induction time (min) (or a time to achieve half of the bioaccessible fraction) (Fig. 4 bottom row). The fitted total bioaccessibility from microencapsulates was 42.42±1.78% for CO, and 54.98±1.89% for CA. The α-tocopherol loaded CA OPN/WPI emulsion had a significantly lower bioaccessibility (i.e., 39.6±0.90%), compared to the microencapulated powder, demonstrating the utitlity of OPN/WPI encapsulates at improving bioactive stability and bioavailabity. Bioaccessibility for the control (α-tocopherol + CA) was lower than all other formulations (9.48±0.44%), illustrating the utility of hydrocolloids in emulsions and microparticles to enhance encapsulating of α-tocopherol microencapsulation.

The bioaccessible α-tocopherol fraction was greater for CA WPI:OPN (23:1) compared to CO WPI:OPN (23:1) microparticles. The long-chain fatty acids, higher in CA, are more hydrophobic with larger solubilization capacities for lipophilic substances compared to medium-chain fatty acids, which has previously been postulated to increase bioaccessibility (Verkempinck et al., 2018). Others have suggested that the 14 carbon, non-polar chain of α-

tocopherol may ineffectivly pack in micelles comprised of medium chain fatty acids (Yang & McClements, 2013). Higher bioactive bioaccessibility in CA versus CO result is in aggrement β-carotene and α-tocopherol bioaccessibility in treatments containing different chain length tryglycerides (Nagao, Kotake-Nara, & Hase, 2013; Yang & McClements, 2013). The rate constant (k) as well as the induction time (t_c) were statiscally similar ($p > 0.05$) for samples prepared with CA or CO (Fig. 4). The k and t_c were equal to 0.021±0.002 min^{-1} and 150.7±4.6 min when using CA, in comparison with 0.020±0.002 min^{-1} and 138.6±5.2 min for powders containing CO, respectively. For these parameters, the lipid carrier did not affect the α-tocopherol release from the core of the microparticle to the digestive medium. This result was attributed to the similar wall material composition for both samples, wich were disrupted in the same rate and throughout similar range of time.

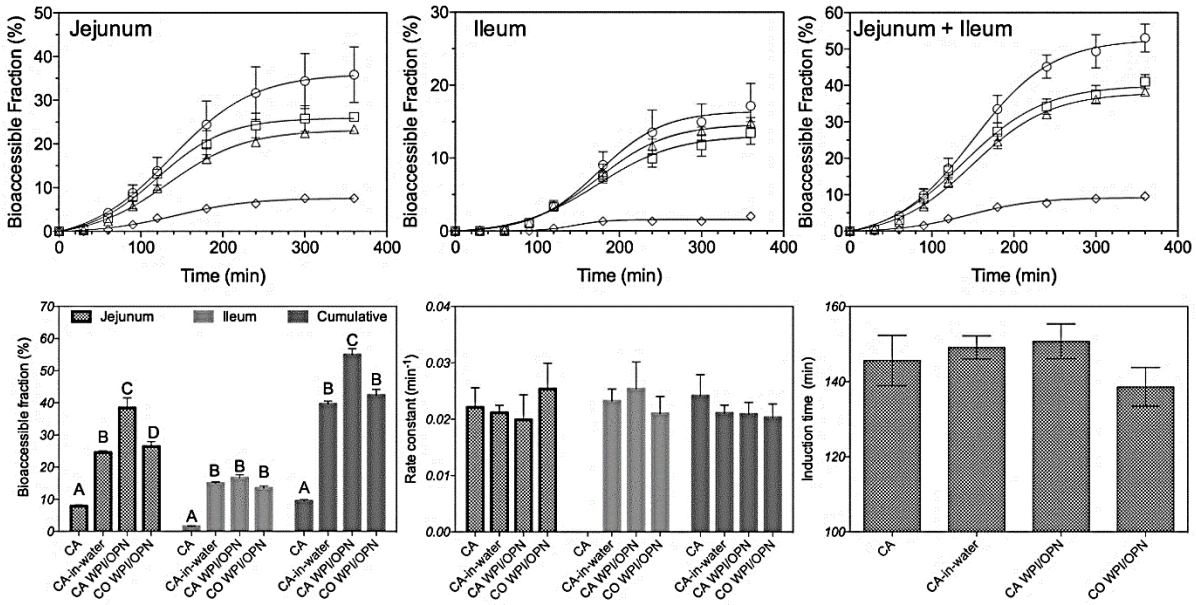

Figure 4. Cumulative bioaccessible fractions of α-tocopherol (%) obtained from the Jejunum, Ileum and combined, 2.5% w/w in all samples fed into the TIM, for CA (◇), CA WPI:OPN (23:1) (emulsion) (△), CA WPI:OPN (23:1) (○), CO WPI:OPN (23:1) (□). Fitted parameters from the shifted-logistical adjusted model to the cumulative bioaccessible fractions obtained from the Jejunum, Ileum and combined. Different letters indicate significant within groups. Fitted parameters that had no overlap between their 95% confidence intervals were considered statistically different.

4. Conclusion

Microparticles comprised on WPI and OPN obtained by freeze-drying canola or coconut oil-in-water emulsions effectively encapsulated α-tocopherol while maintaining high drying yields, low moisture contents and water activities. Microparticles obtained from emulsions with

higher OPN concentration had higher apparent viscosity, which translated to lower encapsulation efficiency and bulk density, and did not affect oil retention. α-tocopherol retention and degradation kinetics were greater affected when CA was the carrier compared to CO; this was attributed to higher unsaturated fatty acid content of CA, which has faster rates of α-tocopherol oxidation. OPN/WPI microparticles confer chemical and microbiological stability at RH < 65 % during accelerated shelf-life testing after 5 weeks at 60 °C Finally, total *in vitro* bioaccessibility of α-tocopherol, assesssed using the TIM-1 simulated digestive model, was significantly higher for CA due to the presence long-chain fatty acid chains which have been shown to improve α-tocopherol bioaccessibiltiy. The fitted shifted-logistical parameters, rate constant and induction time, were not influenced by carrier oil. It is concluded that the CO WPI:OPN (23:1) treatment was the one that presented the best performance for a possible industrial application, since it maintained high bioactive retention during the storage stability test and high bioaccessibility.

Declaration of interest

The authors declare there is no conflict of interest for this research.

Funding

This study was financially supported by the Coordenação de Aperfeiçoamento de Pessoal de Nível Superior – Brasil (CAPES) - Finance Code 001; Conselho Nacional de Desenvolvimento Científico e Tecnológico – Brasil (CNPq) (Grant numbers 478376/2013-8 and 308043/2015-4); and the Fundação de Amparo à Pesquisa do Estado de Minas Gerais – Brasil (FAPEMIG) (Grant numbers CAG - APQ-01308-12 and CAG - APQ-03851-16). Funding in Canada was received from the Canadian Foundation for Innovation, NSERC Discovery and Canada Research Chair programs.

Acknowledgments

The authors gratefully acknowledge support from funding agencies (CAPES, CNPq, FAPEMIG) for the financial support and the laboratory infra-structure provided by the Food Science Departments of the Federal University of Lavras (BR) and University of Guelph (CA).

M.A.R. also thankfully acknowledges support from Canadian Foundation for Innovation, NSERC Discovery and Canada Research Chair programs.

References

Adjonu, R., Doran, G., Torley, P., & Agboola, S. (2014). Whey protein peptides as components of nanoemulsions: A review of emulsifying and biological functionalities. *Journal of Food Engineering*, *122*(1), 15–27. https://doi.org/10.1016/j.jfoodeng.2013.08.034

Aghbashlo, M., Mobli, H., Rafiee, S., & Madadlou, A. (2012). Energy and exergy analyses of the spray drying process of fish oil microencapsulation. *Biosystems Engineering*, *111*(2), 229–241. https://doi.org/https://doi.org/10.1016/j.biosystemseng.2011.12.001

Akbas, E., Soyler, B., & Oztop, M. H. (2018). Formation of capsaicin loaded nanoemulsions with high pressure homogenization and ultrasonication. *LWT*, *96*, 266–273. https://doi.org/https://doi.org/10.1016/j.lwt.2018.05.043

AlHasawi, F. M., Fondaco, D., Ben-Elazar, K., Ben-Elazar, S., Fan, Y. Y., Corradini, M. G., … Rogers, M. A. (2017). In vitro measurements of luminal viscosity and glucose/maltose bioaccessibility for oat bran, instant oats, and steel cut oats. *Food Hydrocolloids*, *70*, 293–303. https://doi.org/https://doi.org/10.1016/j.foodhyd.2017.04.015

AlHasawi, F. M., Fondaco, D., Corradini, M. G., Ludescher, R. D., Bolster, D., Chu, Y. F., … Rogers, M. A. (2018). Gastric viscosity and sugar bioaccessibility of instant and steel cut oat/milk protein blends. *Food Hydrocolloids*, *82*, 424–433. https://doi.org/10.1016/j.foodhyd.2018.04.014

Alpizar-Reyes, E., Castaño, J., Carrillo-Navas, H., Alvarez-Ramírez, J., Gallardo-Rivera, R., Pérez-Alonso, C., & Guadarrama-Lezama, A. Y. (2018). Thermodynamic sorption analysis and glass transition temperature of faba bean (Vicia faba L.) protein. *Journal of Food Science and Technology*, *55*(3), 935–943. https://doi.org/10.1007/s13197-017-3001-1

Alvarenga Botrel, D., Vilela Borges, S., de Barros Fernandes, R., Dantas Viana, A., da Costa, J., & Reginaldo Marques, G. (2012). Evaluation of spray drying conditions on properties of microencapsulated oregano essential oil. *International Journal of Food Science & Technology*, *47*(11), 2289–2296. https://doi.org/10.1111/j.1365-2621.2012.03100.x

Amiri, S., Ghanbarzadeh, B., Hamishehkar, H., Hosein, M., Babazadeh, A., & Adun, P.

(2018). Vitamin E Loaded Nanoliposomes: Effects of Gammaoryzanol, Polyethylene Glycol and Lauric Acid on Physicochemical Properties. *Colloid and Interface Science Communications*, *26*, 1–6. https://doi.org/https://doi.org/10.1016/j.colcom.2018.07.003

Andrade, J., Pereira, C. G., Almeida Junior, J. C. de, Viana, C. C. R., Neves, L. N. de O., Silva, P. H. F. da, … Anjos, V. de C. dos. (2019). FTIR-ATR determination of protein content to evaluate whey protein concentrate adulteration. *Lwt*, *99*(September 2018), 166–172. https://doi.org/10.1016/j.lwt.2018.09.079

Anson, N. M., Havenaar, R., Vaes, W., Coulier, L., Venema, K., Selinheimo, E., … Haenen, G. R. M. M. (2011). Effect of bioprocessing of wheat bran in wholemeal wheat breads on the colonic SCFA production in vitro and postprandial plasma concentrations in men. *Food Chemistry*, *128*(2), 404–409. https://doi.org/https://doi.org/10.1016/j.foodchem.2011.03.043

Anvari, M., & Melito, H. S. J. (2017). Effect of fish gelatin-gum arabic interactions on structural and functional properties of concentrated emulsions. *Food Research International*, *102*, 1–7. https://doi.org/https://doi.org/10.1016/j.foodres.2017.09.085

AOAC. (2012). *Official methods of analysis of AOAC international.* (G. Horwitz & Latime, Eds.) (19th ed.). Washington, USA: AOAC International.

Arab, M., Hosseini, S. M., Nayebzadeh, K., Khorshidian, N., Yousefi, M., Razavi, S. H., & Mortazavian, A. M. (2019). Microencapsulation of microbial canthaxanthin with alginate and high methoxyl pectin and evaluation the release properties in neutral and acidic condition. *International Journal of Biological Macromolecules*, *121*, 691–698. https://doi.org/https://doi.org/10.1016/j.ijbiomac.2018.10.114

Arslan, N., & Togˇrul, H. (2005). Modelling of water sorption isotherms of macaroni stored in a chamber under controlled humidity and thermodynamic approach. *Journal of Food Engineering*, *69*(2), 133–145. https://doi.org/https://doi.org/10.1016/j.jfoodeng.2004.08.004

Aykın-Dinçer, E., & Erbaş, M. (2018). Drying kinetics, adsorption isotherms and quality characteristics of vacuum-dried beef slices with different salt contents. *Meat Science*, *145*, 114–120. https://doi.org/https://doi.org/10.1016/j.meatsci.2018.06.007

Ballesteros, L. F., Ramirez, M. J., Orrego, C. E., Teixeira, J. A., & Mussatto, S. I. (2017). Encapsulation of antioxidant phenolic compounds extracted from spent coffee grounds by freeze-drying and spray-drying using different coating materials. *Food Chemistry*, *237*, 623–631. https://doi.org/10.1016/j.foodchem.2017.05.142

Bandali, E., Wang, Y., Lan, Y., Rogers, M. A., & Shapses, S. A. (2018). The influence of

dietary fat and intestinal pH on calcium bioaccessibility: An: in vitro study. *Food and Function*, *9*(3), 1809–1815. https://doi.org/10.1039/c7fo01631j

Barbosa-Cánovas, G., Fontana Jr., A.J., Schmidt, S.J., T.P.L, 2007. Water Activity in Foods: Fundamentals and Applications. Iowa.

Beneš, H., Paruzel, A., Trhlíková, O., & Paruzel, B. (2017). Medium chain glycerides of coconut oil for microwave-enhanced conversion of polycarbonate into polyols. *European Polymer Journal*, *86*, 173–187. https://doi.org/10.1016/j.eurpolymj.2016.11.030

Bilek, S. E., Yılmaz, F. M., & Özkan, G. (2017). The effects of industrial production on black carrot concentrate quality and encapsulation of anthocyanins in whey protein hydrogels. *Food and Bioproducts Processing*, *102*, 72–80. https://doi.org/https://doi.org/10.1016/j.fbp.2016.12.001

Botelho, B. G., Reis, N., Oliveira, L. S., & Sena, M. M. (2015). Development and analytical validation of a screening method for simultaneous detection of five adulterants in raw milk using mid-infrared spectroscopy and PLS-DA. *Food Chemistry*, *181*, 31–37. https://doi.org/https://doi.org/10.1016/j.foodchem.2015.02.077

Brunauer, S., Emmett, P. H., & Teller, E. (1938). Adsorption of Gases in Multimolecular Layers. *Journal of the American Chemical Society*, *60*(2), 309–319. https://doi.org/10.1021/ja01269a023

Caliskan, G., & Dirim, S. N. (2016). The effect of different drying processes and the amounts of maltodextrin addition on the powder properties of sumac extract powders. *Powder Technology*, *287*, 308–314. https://doi.org/https://doi.org/10.1016/j.powtec.2015.10.019

Carneiro, H. C. F., Tonon, R. V., Grosso, C. R. F., & Hubinger, M. D. (2013). Encapsulation efficiency and oxidative stability of flaxseed oil microencapsulated by spray drying using different combinations of wall materials. *Journal of Food Engineering*, *115*(4), 443–451. https://doi.org/10.1016/j.jfoodeng.2012.03.033

Che Man, Y. B., Ammawath, W., & Mirghani, M. E. S. (2005). Determining α-tocopherol in refined bleached and deodorized palm olein by Fourier transform infrared spectroscopy. *Food Chemistry*, *90*(1–2), 323–327. https://doi.org/10.1016/j.foodchem.2004.05.059

Chranioti, C., Chanioti, S., & Tzia, C. (2016). Comparison of spray, freeze and oven drying as a means of reducing bitter aftertaste of steviol glycosides (derived from Stevia rebaudiana Bertoni plant) – Evaluation of the final products. *Food Chemistry*, *190*, 1151–1158. https://doi.org/https://doi.org/10.1016/j.foodchem.2015.06.083

Conceição, M. C., Junqueira, L. A., Guedes Silva, K. C., Prado, M. E. T., & De Resende, J. V. (2014). Thermal and microstructural stability of a powdered gum derived from Pereskia aculeata Miller leaves. *Food Hydrocolloids*, *40*, 104–114. https://doi.org/10.1016/j.foodhyd.2014.02.015

Convely, R. T. (1970). *Thermal stability of polymers*. New York: Marcel Dekker.

Costa, C. S. M. F., Fonseca, A. C., Moniz, J., Godinho, M., Serra, A. C., & Coelho, J. F. J. (2016). Soybean and coconut oil based unsaturated polyester resins : Thermomechanical characterization. *Industrial Crops & Products*, *85*, 403–411. https://doi.org/10.1016/j.indcrop.2016.01.030

Da Cruz, M. C. R., Dagostin, J. L. A., Perussello, C. A., & Masson, M. L. (2019). Assessment of physicochemical characteristics, thermal stability and release profile of ascorbic acid microcapsules obtained by complex coacervation. *Food Hydrocolloids*, *87*, 71–82. https://doi.org/https://doi.org/10.1016/j.foodhyd.2018.07.043

Da Rosa, C. G., Borges, C. D., Zambiazi, R. C., Nunes, M. R., Benvenutti, E. V., da Luz, S. R., … Rutz, J. K. (2013). Microencapsulation of gallic acid in chitosan, β-cyclodextrin and xanthan. *Industrial Crops and Products*, *46*, 138–146. https://doi.org/https://doi.org/10.1016/j.indcrop.2012.12.053

Darra, N. El, Rajha, H. N., Saleh, F., Al-Oweini, R., Maroun, R. G., & Louka, N. (2017). Food fraud detection in commercial pomegranate molasses syrups by UV–VIS spectroscopy, ATR-FTIR spectroscopy and HPLC methods. *Food Control*, *78*, 132–137. https://doi.org/https://doi.org/10.1016/j.foodcont.2017.02.043

De Moura e Dias, M., Pais Siqueira, N., Lopes da Conceição, L., Aparecida dos Reis, S., Xavier Valente, F., Maciel dos Santos Dias, M., … Gouveia Peluzio, M. do C. (2018). Consumption of virgin coconut oil in Wistar rats increases saturated fatty acids in the liver and adipose tissue, as well as adipose tissue inflammation. *Journal of Functional Foods*, *48*, 472–480. https://doi.org/https://doi.org/10.1016/j.jff.2018.07.036

De Sá Mendes, N., Santos, M. C. P., Santos, M. C. B., Cameron, L. C., Ferreira, M. S. L., & Gonçalves, É. C. B. A. (2019). Characterization of pepper (Capsicum baccatum) - A potential functional ingredient. *LWT*, *112*, 108209. https://doi.org/https://doi.org/10.1016/j.lwt.2019.05.107

Déat, E., Blanquet-Diot, S., Jarrige, J.-F., Denis, S., Beyssac, E., & Alric, M. (2009). Combining the Dynamic TNO-Gastrointestinal Tract System with a Caco-2 Cell Culture Model: Application to the Assessment of Lycopene and α-Tocopherol Bioavailability from a Whole Food. *Journal of Agricultural and Food Chemistry*, *57*(23), 11314–11320. https://doi.org/10.1021/jf902392a

Delgado, A. V., González-Caballero, F., Hunter, R. J., Koopal, L. K., & Lyklema, J. (2007). Measurement and interpretation of electrokinetic phenomena. *Journal of Colloid and Interface Science*, *309*(2), 194–224. https://doi.org/10.1016/j.jcis.2006.12.075

Devi, N., Sarmah, M., Khatun, B., & Maji, T. K. (2017). Encapsulation of active ingredients in polysaccharide–protein complex coacervates. *Advances in Colloid and Interface Science*, *239*, 136–145. https://doi.org/https://doi.org/10.1016/j.cis.2016.05.009

Dickinson, E. (2019). Strategies to control and inhibit the flocculation of protein-stabilized oil-in-water emulsions. *Food Hydrocolloids*, *96*, 209–223. https://doi.org/https://doi.org/10.1016/j.foodhyd.2019.05.021

Do Carmo, E. L., Teodoro, R. A. R., Félix, P. H. C., de Barros Fernandes, R. V., de Oliveira, É. R., Veiga, T. R. L. A., … Botrel, D. A. (2018). Stability of spray-dried beetroot extract using oligosaccharides and whey proteins. *Food Chemistry*, *249*, 51–59. https://doi.org/https://doi.org/10.1016/j.foodchem.2017.12.076

Do, T. K. T., Hadji-Minaglou, F., Antoniotti, S., & Fernandez, X. (2015). Authenticity of essential oils. *TrAC Trends in Analytical Chemistry*, *66*, 146–157. https://doi.org/https://doi.org/10.1016/j.trac.2014.10.007

Doost, A. S., Nasrabadi, M. N., Kassozi, V., Dewettinck, K., Stevens, C. V, & Meeren, P. Van Der. (2019). Pickering stabilization of thymol through green emulsification using soluble fraction of almond gum – Whey protein isolate nano-complexes. *Food Hydrocolloids*, *88*(October 2018), 218–227. https://doi.org/10.1016/j.foodhyd.2018.10.009

EFSA Panel on Dietetic Products Nutrition and Allergies. (2015). Scientific Opinion on Dietary Reference Values for vitamin E as α-tocopherol. *EFSA Journal*, *13*(7), 4149. https://doi.org/10.2903/j.efsa.2015.4149

Eklund-Jonsson, C., Sandberg, A.-S., Hulthen, L., & Alminger, M. L. (2008). Tempe Fermentation of Whole Grain Barley Increased Human Iron Absorption and In Vitro Iron Availability. *The Open Nutrition Journal*, *2*(1), 42–47. https://doi.org/10.2174/1874288200802010042

Erbaş, M., Aykın, E., Arslan, S., & Durak, A. N. (2016). Adsorption behaviour of bulgur. *Food Chemistry*, *195*, 87–90. https://doi.org/https://doi.org/10.1016/j.foodchem.2015.06.050

Esfanjani, A. F., Jafari, S. M., Assadpoor, E., & Mohammadi, A. (2015). Nano-encapsulation of saffron extract through double-layered multiple emulsions of pectin and whey protein concentrate. *Journal of Food Engineering*, *165*, 149–155. https://doi.org/https://doi.org/10.1016/j.jfoodeng.2015.06.022

Esfanjani, A. F., Jafari, S. M., & Assadpour, E. (2017). Preparation of a multiple emulsion based on pectin-whey protein complex for encapsulation of saffron extract nanodroplets. *Food Chemistry*, *221*, 1962–1969. https://doi.org/https://doi.org/10.1016/j.foodchem.2016.11.149

Ezhilarasi, P. N., Karthik, P., Chhanwal, N., & Anandharamakrishnan, C. (2013). Nanoencapsulation Techniques for Food Bioactive Components: A Review. *Food and Bioprocess Technology*, *6*(3), 628–647. https://doi.org/10.1007/s11947-012-0944-0

Fioramonti, S. A., Rubiolo, A. C., & Santiago, L. G. (2017). Characterization of freeze-dried flaxseed oil microcapsules obtained by multilayer emulsions. *Power Technology*, *319*, 238–244.

Frankel, E. N. (2012). *Lipid Oxidation* (2nd ed.). Cambridge: Woodhead Publishing Limited.

González, A., Martínez, M. L., Paredes, A. J., León, A. E., & Ribotta, P. D. (2016). Study of the preparation process and variation of wall components in chia (Salvia hispanica L.) oil microencapsulation. *Powder Technology*, *301*, 868–875. https://doi.org/https://doi.org/10.1016/j.powtec.2016.07.026

Goyal, A., Sharma, V., Sihag, M. K., Tomar, S. K., Arora, S., Sabikhi, L., & Singh, A. K. (2015). Development and physico-chemical characterization of microencapsulated flaxseed oil powder: A functional ingredient for omega-3 fortification. *Powder Technology*, *286*, 527–537. https://doi.org/https://doi.org/10.1016/j.powtec.2015.08.050

Gursul, S., Karabulut, I., & Durmaz, G. (2019). Antioxidant efficacy of thymol and carvacrol in microencapsulated walnut oil triacylglycerols. *Food Chemistry*, *278*, 805–810. https://doi.org/https://doi.org/10.1016/j.foodchem.2018.11.134

Hategekimana, J., Masamba, K. G., Ma, J., & Zhong, F. (2015). Encapsulation of vitamin E: Effect of physicochemical properties of wall material on retention and stability. *Carbohydrate Polymers*, *124*, 172–179. https://doi.org/10.1016/j.carbpol.2015.01.060

Institute of Medicine. (2000). *Dietary Reference Intakes for Vitamin C, Vitamin E, Selenium, and Carotenoids*. Washington, DC: The National Academies Press. https://doi.org/10.17226/9810

Junqueira, L. A., Amaral, T. N., Oliveira, N. L., Prado, M. E. T., & de Resende, J. V. (2018). Rheological behavior and stability of emulsions obtained from Pereskia aculeata Miller via different drying methods. *International Journal of Food Properties*, *21*(1), 21–35. https://doi.org/10.1080/10942912.2018.1437177

Juttulapa, M., Piriyaprasarth, S., Takeuchi, H., & Sriamornsak, P. (2017). Effect of high-pressure homogenization on stability of emulsions containing zein and pectin. *Asian Journal of Pharmaceutical Sciences*, *12*(1), 21–27. https://doi.org/https://doi.org/10.1016/j.ajps.2016.09.004

Kelly, P. (2019). Chapter 3 - Manufacture of Whey Protein Products: Concentrates, Isolate, Whey Protein Fractions and Microparticulated. In H. C. Deeth & N. Bansal (Eds.), *Whey Proteins* (pp. 97–122). Academic Press. https://doi.org/https://doi.org/10.1016/B978-0-12-812124-5.00003-5

Khazaei, K. M., Jafari, S. M., Ghorbani, M., & Kakhki, A. H. (2014). Application of maltodextrin and gum Arabic in microencapsulation of saffron petal's anthocyanins and evaluating their storage stability and color. *Carbohydrate Polymers*, *105*, 57–62. https://doi.org/https://doi.org/10.1016/j.carbpol.2014.01.042

Khorasani, S. N., Ataei, S., & Neisiany, R. E. (2017). Microencapsulation of a coconut oil-based alkyd resin into poly(melamine–urea–formaldehyde) as shell for self-healing purposes. *Progress in Organic Coatings*, *111*(May), 99–106. https://doi.org/10.1016/j.porgcoat.2017.05.014

Khundamri, N., Aouf, C., Fulcrand, H., Dubreucq, E., & Tanrattanakul, V. (2019). Bio-based flexible epoxy foam synthesized from epoxidized soybean oil and epoxidized mangosteen tannin. *Industrial Crops and Products*, *128*, 556–565. https://doi.org/https://doi.org/10.1016/j.indcrop.2018.11.062

Korma, S. A., Wei, W., Ali, A. H., Abed, S. M., Zheng, L., Jin, Q., & Wang, X. (2019). Spray-dried novel structured lipids enriched with medium-and long-chain triacylglycerols encapsulated with different wall materials: Characterization and stability. *Food Research International*, *116*, 538–547. https://doi.org/https://doi.org/10.1016/j.foodres.2018.08.071

Koshani, R., & Jafari, S. M. (2019). Ultrasound-assisted preparation of different nanocarriers loaded with food bioactive ingredients. *Advances in Colloid and Interface Science*, *270*, 123–146. https://doi.org/https://doi.org/10.1016/j.cis.2019.06.005

Lago, A. M. T., Neves, I. C. O., Oliveira, N. L., Botrel, D. A., Minim, L. A., & de Resende, J. V. (2019). Ultrasound-assisted oil-in-water nanoemulsion produced from *Pereskia aculeata* Miller mucilage. Ultrasonics Sonochemistry, 50, 339–353. https://doi.org/https://doi.org/10.1016/j.ultsonch.2018.09.036

Laokuldilok, T., & Kanha, N. (2015). Effects of processing conditions on powder properties of black glutinous rice (Oryza sativa L.) bran anthocyanins produced by spray drying and freeze drying. *LWT - Food Science and Technology*, *64*(1), 405–411. https://doi.org/https://doi.org/10.1016/j.lwt.2015.05.015

Larsson, M., Minekus, M., & Havenaar, R. (1997). Estimation of the bioavailability of iron and phosphorus in cereals using a dynamic in vitro gastrointestinal model. *Journal of the Science of Food and Agriculture*, *74*(1), 99–106. https://doi.org/10.1002/(SICI)1097-0010(199705)74:1<99::AID-JSFA775>3.0.CO;2-G

Lewicki, P. P. (1997). The applicability of the GAB model to food water sorption isotherms. *International Journal of Food Science and Technology*, *32*(6), 553–557. https://doi.org/10.1111/j.1365-2621.1997.tb02131.x

Lima Junior, F. A., Conceição, M. C., Vilela de Resende, J., Junqueira, L. A., Pereira, C. G., & Torres Prado, M. E. (2013). Response surface methodology for optimization of the mucilage extraction process from Pereskia aculeata Miller. *Food Hydrocolloids*, *33*(1), 38–47. https://doi.org/10.1016/j.foodhyd.2013.02.012

López-Castejón, M. L., Bengoechea, C., Espinosa, S., & Carrera, C. (2019). Characterization of prebiotic emulsions stabilized by inulin and β-lactoglobulin. *Food Hydrocolloids*, *87*, 382–393. https://doi.org/https://doi.org/10.1016/j.foodhyd.2018.08.024

Madankar, C. S., Dalai, A. K., & Naik, S. N. (2013). Green synthesis of biolubricant base stock from canola oil. *Industrial Crops & Products*, *44*, 139–144. https://doi.org/10.1016/j.indcrop.2012.11.012

Marteau, P., Minekus, M., Havenaar, R., & Huis In't Veld, J. H. J. (1997). Survival of Lactic Acid Bacteria in a Dynamic Model of the Stomach and Small Intestine: Validation and the Effects of Bile. *Journal of Dairy Science*, *80*(6), 1031–1037. https://doi.org/https://doi.org/10.3168/jds.S0022-0302(97)76027-2

Martin, A. A., de Freitas, R. A., Sassaki, G. L., Evangelista, P. H. L., & Sierakowski, M. R. (2017). Chemical structure and physical-chemical properties of mucilage from the leaves of Pereskia aculeata. *Food Hydrocolloids*, *70*, 20–28. https://doi.org/10.1016/j.foodhyd.2017.03.020

McClements, D. (2015). *Food Emulsions: Principles, practices and techniques* (3rd ed.). Boca Raton: CRC Press. https://doi.org/10.1201/b18868

Mhaske, P., Condict, L., Dokouhaki, M., Katopo, L., & Kasapis, S. (2019). Quantitative analysis of the phase volume of agarose-canola oil gels in comparison to blending law predictions using 3D imaging based on confocal laser scanning microscopy. *Food Research International*, *In press*, 108529. https://doi.org/10.1016/j.foodres.2019.108529

Minekus, M. (2015). The TNO in vitro model of the colon (TIM). In K. Verhoeckx, P. Cotter, I. López-Expósito, C. Kleiveland, T. Lea, A. Mackie, … H. Wichers (Eds.), *The Impact of Food Bioactives on Gut Health: In Vitro and Ex Vivo Models* (pp. 305–317). New York: Springer Open. https://doi.org/10.1007/978-3-319-16104-4_26

Minekus, Mans, Marteau, P., Havenaar, R., & Huisintveld, J. H. J. (1995). A Multicompartimental Dynamic Computer-controlled Model Simularting the Stomach and Small Intestine. *Atla-Alternatives to Laboratory Animals*, *23*, 197–209. https://doi.org/10.1038/s41596-018-0119-1

Mól, P. C. G., Veríssimo, L. A. A., Minim, L. A., Boscolo, M., Gomes, E., & da Silva, R. (2019). Production and capture of β-glucosidase from Thermoascus aurantiacus using a tailor made anionic cryogel. *Process Biochemistry*, *82*, 75–83. https://doi.org/https://doi.org/10.1016/j.procbio.2019.03.029

Monrroy, M., García, E., Ríos, K., & García, J. R. (2017). Extraction and Physicochemical Characterization of Mucilage from Opuntia cochenillifera (L.) Miller . *Journal of Chemistry*, *2017*, 1–9. https://doi.org/10.1155/2017/4301901

Nagao, A., Kotake-Nara, E., & Hase, M. (2013). Effects of Fats and Oils on the Bioaccessibility of Carotenoids and Vitamin E in Vegetables. *Bioscience, Biotechnology, and Biochemistry*, *77*(5), 1055–1060. https://doi.org/10.1271/bbb.130025

Oliveira, N. L., Rodrigues, A. A., Oliveira Neves, I. C., Teixeira Lago, A. M., Borges, S. V., & de Resende, J. V. (2019). Development and characterization of biodegradable films based on Pereskia aculeata Miller mucilage. *Industrial Crops and Products*, *130*. https://doi.org/10.1016/j.indcrop.2019.01.014

Otálora, M. C., Carriazo, J. G., Iturriaga, L., Nazareno, M. A., & Osorio, C. (2015). Microencapsulation of betalains obtained from cactus fruit (Opuntia ficus-indica) by spray drying using cactus cladode mucilage and maltodextrin as encapsulating agents. *Food Chemistry*, *187*, 174–181. https://doi.org/10.1016/j.foodchem.2015.04.090

Ozkan, G., Franco, P., De Marco, I., Xiao, J., & Capanoglu, E. (2019). A review of microencapsulation methods for food antioxidants: Principles, advantages, drawbacks and applications. *Food Chemistry*, *272*, 494–506. https://doi.org/10.1016/j.foodchem.2018.07.205

Ozturk, B., & McClements, D. J. (2016). Progress in natural emulsifiers for utilization in food emulsions. *Current Opinion in Food Science*, *7*, 1–6. https://doi.org/https://doi.org/10.1016/j.cofs.2015.07.008

Ozulku, G., Yildirim, R. M., Toker, O. S., Karasu, S., & Durak, M. Z. (2017). Rapid detection of adulteration of cold pressed sesame oil adultered with hazelnut, canola, and sunflower oils using ATR-FTIR spectroscopy combined with chemometric. *Food Control*, *82*, 212–216. https://doi.org/10.1016/j.foodcont.2017.06.034

Pasrija, D., Ezhilarasi, P. N., Indrani, D., & Anandharamakrishnan, C. (2015). Microencapsulation of green tea polyphenols and its effect on incorporated bread quality. *LWT - Food Science and Technology*, *64*(1), 289–296. https://doi.org/https://doi.org/10.1016/j.lwt.2015.05.054

Pellicer, J. A., Fortea, M. I., Trabal, J., Rodríguez-López, M. I., Gabaldón, J. A., & Núñez-Delicado, E. (2019). Stability of microencapsulated strawberry flavour by spray drying, freeze drying and fluid bed. *Powder Technology*, *347*, 179–185. https://doi.org/https://doi.org/10.1016/j.powtec.2019.03.010

Quirijns, E. J., Van Boxtel, A. J. B., Van Loon, W. K. P., & Van Straten, G. (2005). Sorption isotherms, GAB parameters and isosteric heat of sorption. *Journal of the Science of Food and Agriculture*, *85*(11), 1805–1814. https://doi.org/10.1002/jsfa.2140

Rafiee, Z., Nejatian, M., Daeihamed, M., & Jafari, S. M. (2019). Application of curcumin-loaded nanocarriers for food, drug and cosmetic purposes. *Trends in Food Science & Technology*, *88*, 445–458. https://doi.org/https://doi.org/10.1016/j.tifs.2019.04.017

Rajam, R., & Anandharamakrishnan, C. (2015). Spray freeze drying method for microencapsulation of Lactobacillus plantarum. *Journal of Food Engineering*, *166*, 95–103. https://doi.org/https://doi.org/10.1016/j.jfoodeng.2015.05.029

Ravindran, S., Williams, M. A. K., Ward, R. L., & Gillies, G. (2018). Understanding how the properties of whey protein stabilized emulsions depend on pH, ionic strength and calcium concentration, by mapping environmental conditions to zeta potential. *Food Hydrocolloids*, *79*, 572–578. https://doi.org/https://doi.org/10.1016/j.foodhyd.2017.12.003

Reboul, E. (2017). Vitamin E Bioavailability: Mechanisms of Intestinal Absorption in the Spotlight. *Antioxidants*, *6*(4), 95–106. https://doi.org/10.3390/antiox6040095

Rehman, A., Ahmad, T., Aadil, R. M., Spotti, M. J., Bakry, A. M., Khan, I. M., … Tong, Q. (2019). Pectin polymers as wall materials for the nano-encapsulation of bioactive compounds. *Trends in Food Science & Technology*, *90*, 35–46. https://doi.org/https://doi.org/10.1016/j.tifs.2019.05.015

Ribnicky, D. M., Roopchand, D. E., Oren, A., Grace, M., Poulev, A., Lila, M. A., … Raskin, I. (2014). Effects of a high fat meal matrix and protein complexation on the bioaccessibility of blueberry anthocyanins using the TNO gastrointestinal model (TIM-1). *Food Chemistry*, *142*, 349–357. https://doi.org/https://doi.org/10.1016/j.foodchem.2013.07.073

Samtlebe, M., Denis, S., Chalancon, S., Atamer, Z., Wagner, N., Neve, H., … Hinrichs, J. (2018). Bacteriophages as modulator for the human gut microbiota: Release from dairy food systems and survival in a dynamic human gastrointestinal model. *LWT*, *91*, 235–241. https://doi.org/https://doi.org/10.1016/j.lwt.2018.01.033

Sanchez, V., Baeza, R., & Chirife, J. (2015). Comparison of monomeric anthocyanins and colour stability of fresh, concentrate and freeze-dried encapsulated cherry juice stored at 38 °C. *Journal of Berry Research*, *5*(4), 243–251. https://doi.org/10.3233/JBR-150106

Saricaoglu, F. T., Gul, O., Besir, A., & Atalar, I. (2018). Effect of high pressure homogenization (HPH) on functional and rheological properties of hazelnut meal proteins obtained from hazelnut oil industry by-products. *Journal of Food Engineering*, *233*, 98–108. https://doi.org/10.1016/j.jfoodeng.2018.04.003

Scholten, E., Moschakis, T., & Biliaderis, C. G. (2014). Biopolymer composites for engineering food structures to control product functionality. *Food Structure*, *1*(1), 39–54. https://doi.org/https://doi.org/10.1016/j.foostr.2013.11.001

Shaddel, R., Hesari, J., Azadmard-Damirchi, S., Hamishehkar, H., Fathi-Achachlouei, B., & Huang, Q. (2018). Double emulsion followed by complex coacervation as a promising method for protection of black raspberry anthocyanins. *Food Hydrocolloids*, *77*, 803–816. https://doi.org/https://doi.org/10.1016/j.foodhyd.2017.11.024

Shanmugam, A., & Ashokkumar, M. (2014). Ultrasonic preparation of stable flax seed oil emulsions in dairy systems – Physicochemical characterization. *Food Hydrocolloids*, *39*, 151–162. https://doi.org/https://doi.org/10.1016/j.foodhyd.2014.01.006

Sharif, H. R., Goff, H. D., Majeed, H., Liu, F., Nsor-Atindana, J., Haider, J., … Zhong, F. (2017). Physicochemical stability of β-carotene and α-tocopherol enriched nanoemulsions: Influence of carrier oil, emulsifier and antioxidant. *Colloids and Surfaces A: Physicochemical and Engineering Aspects*, *529*, 550–559. https://doi.org/10.1016/j.colsurfa.2017.05.076

Shishir, M. R. I., Xie, L., Sun, C., Zheng, X., & Chen, W. (2018). Advances in micro and nano-encapsulation of bioactive compounds using biopolymer and lipid-based transporters. *Trends in Food Science & Technology*, *78*, 34–60. https://doi.org/https://doi.org/10.1016/j.tifs.2018.05.018

Silva, E. K., Azevedo, V. M., Cunha, R. L., Hubinger, M. D., & Meireles, M. A. A. (2016). Ultrasound-assisted encapsulation of annatto seed oil: Whey protein isolate versus modified starch. *Food Hydrocolloids*, *56*, 71–83. https://doi.org/https://doi.org/10.1016/j.foodhyd.2015.12.006

Silva, E. K., Zabot, G. L., Cazarin, C. B. B., Maróstica, M. R., & Meireles, M. A. A. (2016). Biopolymer-prebiotic carbohydrate blends and their effects on the retention of bioactive compounds and maintenance of antioxidant activity. *Carbohydrate Polymers*, *144*, 149–158. https://doi.org/https://doi.org/10.1016/j.carbpol.2016.02.045

Silva, E. K., Zabot, G. L., & Meireles, M. A. A. (2015). Ultrasound-assisted encapsulation of annatto seed oil: Retention and release of a bioactive compound with functional activities. *Food Research International*, *78*, 159–168. https://doi.org/https://doi.org/10.1016/j.foodres.2015.10.022

Singh, S., Singh, H., Karthick, T., Tandon, P., & Prasad, V. (2018). Phase transition analysis of V-shaped liquid crystal: Combined temperature-dependent FTIR and density functional theory approach. *Spectrochimica Acta Part A: Molecular and Biomolecular Spectroscopy*, *188*, 561–570. https://doi.org/https://doi.org/10.1016/j.saa.2017.07.043

Souliman, S., Blanquet, S., Beyssac, E., & Cardot, J.-M. (2006). A level A in vitro/in vivo correlation in fasted and fed states using different methods: Applied to solid immediate release oral dosage form. *European Journal of Pharmaceutical Sciences*, *27*(1), 72–79. https://doi.org/https://doi.org/10.1016/j.ejps.2005.08.006

Speranza, A., Corradini, M. G., Hartman, T. G., Ribnicky, D., Oren, A., & Rogers, M. A. (2013). Influence of Emulsifier Structure on Lipid Bioaccessibility in Oil–Water Nanoemulsions. *Journal of Agricultural and Food Chemistry*, *61*(26), 6505–6515. https://doi.org/10.1021/jf401548r

Steffe, J. F. (1996). *Rheological Methods in Food Process Engineering* (second). East Lansing: Freeman Press. https://doi.org/10.1016/0260-8774(94)90090-6

Suhag, Y., & Nanda, V. (2015). Optimisation of process parameters to develop nutritionally rich spray-dried honey powder with vitamin C content and antioxidant properties. *International Journal of Food Science and Technology*, *50*(8), 1771–1777. https://doi.org/10.1111/ijfs.12841

Syamila, M., Gedi, M. A., Briars, R., Ayed, C., & Gray, D. A. (2019). Effect of temperature, oxygen and light on the degradation of β-carotene, lutein and α-tocopherol in spray-dried spinach juice powder during storage. *Food Chemistry*, *284*, 188–197. https://doi.org/https://doi.org/10.1016/j.foodchem.2019.01.055

Tabilo-Munizaga, G., Villalobos-Carvajal, R., Herrera-Lavados, C., Moreno-Osorio, L., Jarpa-Parra, M., & Pérez-Won, M. (2019). Physicochemical properties of high-pressure treated lentil protein-based nanoemulsions. *Lwt*, *101*(November 2018), 590–598. https://doi.org/10.1016/j.lwt.2018.11.070

Taheri, A., & Jafari, S. M. (2019). Gum-based nanocarriers for the protection and delivery of food bioactive compounds. *Advances in Colloid and Interface Science*, *269*, 277–295. https://doi.org/https://doi.org/10.1016/j.cis.2019.04.009

Talpur, M. Y., Hassan, S. S., Sherazi, S. T. H., Mahesar, S. A., Kara, H., Kandhro, A. A., & Sirajuddin. (2015). A simplified FTIR chemometric method for simultaneous determination of four oxidation parameters of frying canola oil. *Spectrochimica Acta - Part A: Molecular and Biomolecular Spectroscopy*, *149*, 656–661. https://doi.org/10.1016/j.saa.2015.04.098

Tan, S., Ebrahimi, A., & Langrish, T. (2019). Smart release-control of microencapsulated ingredients from milk protein tablets using spray drying and heating. *Food Hydrocolloids*, *92*(February), 181–188. https://doi.org/10.1016/j.foodhyd.2019.02.006

Tan, S., Zhong, C., & Langrish, T. (2019). Microencapsulation of pepsin in the spray-dried WPI (whey protein isolates) matrices for controlled release. *Journal of Food Engineering*, *263*(June), 147–154. https://doi.org/10.1016/j.jfoodeng.2019.06.005

Tan, S., Zhong, C., & Langrish, T. (2020). Pre-gelation assisted spray drying of whey protein isolates (WPI) for microencapsulation and controlled release. *LWT*, *117*, 108625. https://doi.org/https://doi.org/10.1016/j.lwt.2019.108625

Téllez-Pérez, C., Sobolik, V., Montejano-Gaitán, J. G., Abdulla, G., & Allaf, K. (2015). Impact of Swell-Drying Process on Water Activity and Drying Kinetics of Moroccan Pepper (Capsicum annum). *Drying Technology*, *33*(2), 131–142. https://doi.org/10.1080/07373937.2014.936556

Thilakarathna, S. H., Rogers, M., Lan, Y., Huynh, S., Marangoni, A. G., Robinson, L. E., & Wright, A. J. (2016). Investigations of in vitro bioaccessibility from interesterified stearic and oleic acid-rich blends. *Food and Function*, *7*(4), 1932–1940. https://doi.org/10.1039/c5fo01272d

Timmermann, E. O., Chirife, J., & Iglesias, H. A. (2001). Water sorption isotherms of foods and foodstuffs: BET or GAB parameters? *Journal of Food Engineering*, *48*(1), 19–31. https://doi.org/https://doi.org/10.1016/S0260-8774(00)00139-4

Ting, Y., Zhao, Q., Xia, C., & Huang, Q. (2015). Using in vitro and in vivo models to evaluate the oral bioavailability of nutraceuticals. *Journal of Agricultural and Food Chemistry*, *63*(5), 1332–1338. https://doi.org/10.1021/jf5047464

Tonon, R. V, Grosso, C. R. F., & Hubinger, M. D. (2011). Influence of emulsion composition and inlet air temperature on the microencapsulation of flaxseed oil by spray drying. *Food Research International*, *44*(1), 282–289. https://doi.org/https://doi.org/10.1016/j.foodres.2010.10.018

Traber, M. G. (2014). Vitamin E Inadequacy in Humans: causes and consequences. *Advances in Nutrition: An International Review Journal*, *5*, 503–514. https://doi.org/10.3945/an.114.006254.deficiency

Troesch, B., Hoeft, B., McBurney, M., Eggersdorfer, M., & Weber, P. (2012). Dietary surveys indicate vitamin intakes below recommendations are common in representative Western countries. *British Journal of Nutrition*, *108*(4), 692–698. https://doi.org/10.1017/S0007114512001808

Tyagi, V. V, Kaushik, S. C., Tyagi, S. K., & Akiyama, T. (2011). Development of phase change materials based microencapsulated technology for buildings: A review. *Renewable and Sustainable Energy Reviews*, *15*(2), 1373–1391. https://doi.org/https://doi.org/10.1016/j.rser.2010.10.006

Van De Wiele, T. R., Oomen, A. G., Wragg, J., Cave, M., Minekus, M., Hack, A., … Sips, A. J. A. M. (2007). Comparison of five in vitro digestion models to in vivo experimental results: Lead bioaccessibility in the human gastrointestinal tract. *Journal of Environmental Science and Health - Part A Toxic/Hazardous Substances and Environmental Engineering*, *42*(9), 1203–1211. https://doi.org/10.1080/10934520701434919

Vardanega, R., Muzio, A. F. V, Silva, E. K., Prata, A. S., & Meireles, M. A. A. (2019). Obtaining functional powder tea from Brazilian ginseng roots: Effects of freeze and spray drying processes on chemical and nutritional quality, morphological and redispersion properties. *Food Research International*, *116*, 932–941. https://doi.org/https://doi.org/10.1016/j.foodres.2018.09.030

Vergara, C., Saavedra, J., Sáenz, C., García, P., & Robert, P. (2014). Microencapsulation of pulp and ultrafiltered cactus pear (Opuntia ficus-indica) extracts and betanin stability during storage. *Food Chemistry*, *157*, 246–251. https://doi.org/10.1016/j.foodchem.2014.02.037

Verkempinck, S. H. E., Salvia-Trujillo, L., Moens, L. G., Carrillo, C., Van Loey, A. M., Hendrickx, M. E., & Grauwet, T. (2018). Kinetic approach to study the relation between in vitro lipid digestion and carotenoid bioaccessibility in emulsions with different oil unsaturation degree. *Journal of Functional Foods*, *41*(December 2017), 135–147. https://doi.org/10.1016/j.jff.2017.12.030

Verwei, M., Freidig, A. P., Havenaar, R., & Groten, J. P. (2006). Predicted Serum Folate Concentrations Based on In Vitro Studies and Kinetic Modeling are Consistent with Measured Folate Concentrations in Humans. *The Journal of Nutrition*, *136*(12), 3074–3078. https://doi.org/10.1093/jn/136.12.3074

Wang, S., Shi, Y., Tu, Z., Zhang, L., Wang, H., Tian, M., & Zhang, N. (2017). Influence of soy lecithin concentration on the physical properties of whey protein isolate-stabilized emulsion and microcapsule formation. *Journal of Food Engineering*, *207*, 73–80. https://doi.org/https://doi.org/10.1016/j.jfoodeng.2017.03.020

Yamashita, C., Chung, M. M. S., dos Santos, C., Mayer, C. R. M., Moraes, I. C. F., & Branco, I. G. (2017). Microencapsulation of an anthocyanin-rich blackberry (Rubus spp.) by-product extract by freeze-drying. *LWT*, *84*, 256–262. https://doi.org/https://doi.org/10.1016/j.lwt.2017.05.063

Yang, Y., & McClements, D. J. (2013). Vitamin E bioaccessibility: Influence of carrier oil type on digestion and release of emulsified α-tocopherol acetate. *Food Chemistry*, *141*(1), 473–481. https://doi.org/10.1016/j.foodchem.2013.03.033

Ye, F., Astete, C. E., & Sabliov, C. M. (2017). Entrapment and delivery of α-tocopherol by a self-assembled, alginate-conjugated prodrug nanostructure. *Food Hydrocolloids*, *72*, 62–72. https://doi.org/https://doi.org/10.1016/j.foodhyd.2017.05.032

Zhang, Z. H., Peng, H., Ma, H., & Zeng, X. A. (2019). Effect of inlet air drying temperatures on the physicochemical properties and antioxidant activity of whey protein isolate-kale leaves chlorophyll (WPI-CH) microcapsules. *Journal of Food Engineering*, *245*(August 2018), 149–156. https://doi.org/10.1016/j.jfoodeng.2018.10.011

Supplementary information

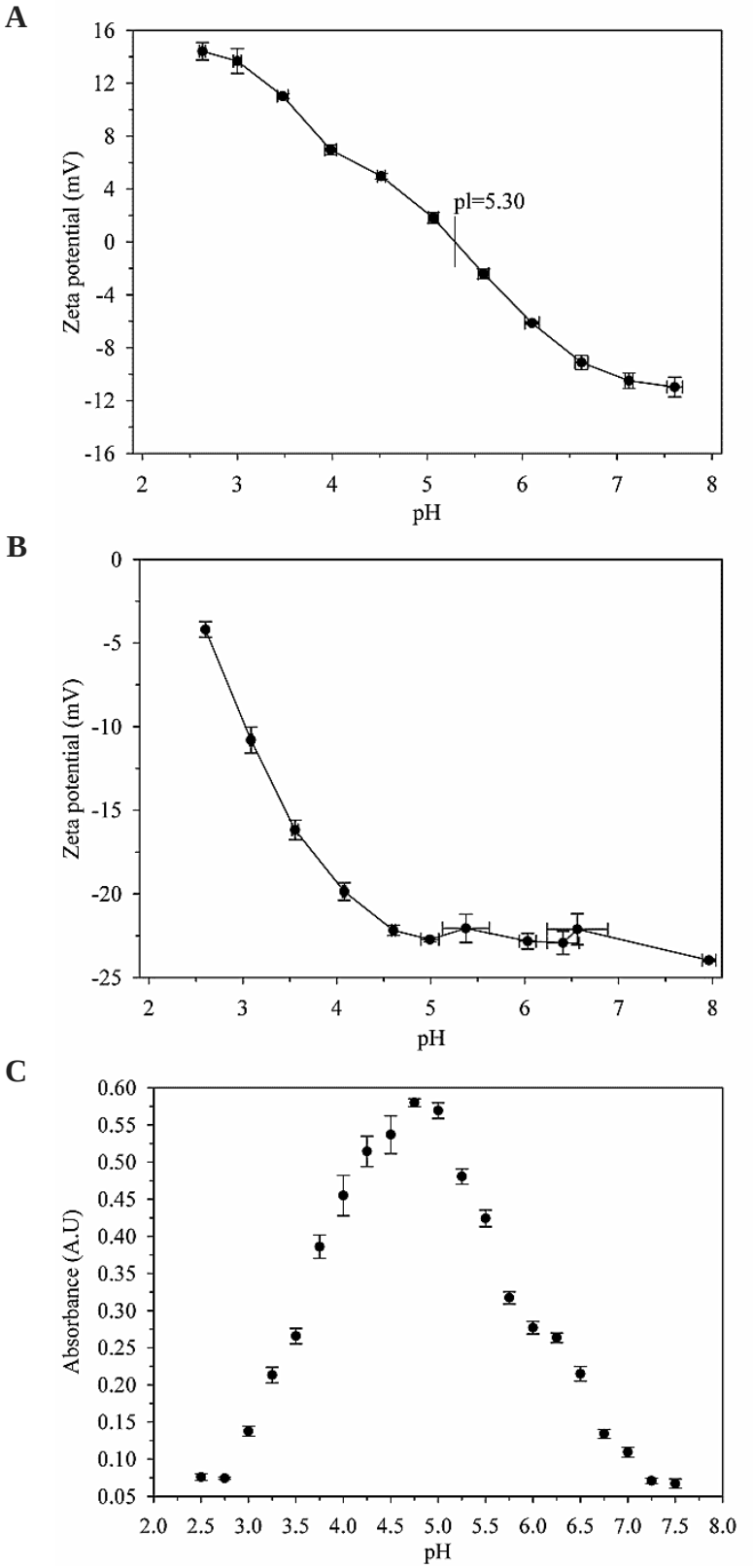

Figure S1. ζ-potential as function of pH for WPI (**A**) and OPN (**B**). Continuous phase absorption, at 600 nm, of 0.075/0.037 % w/w WPI/OPN dispersion (**C**).

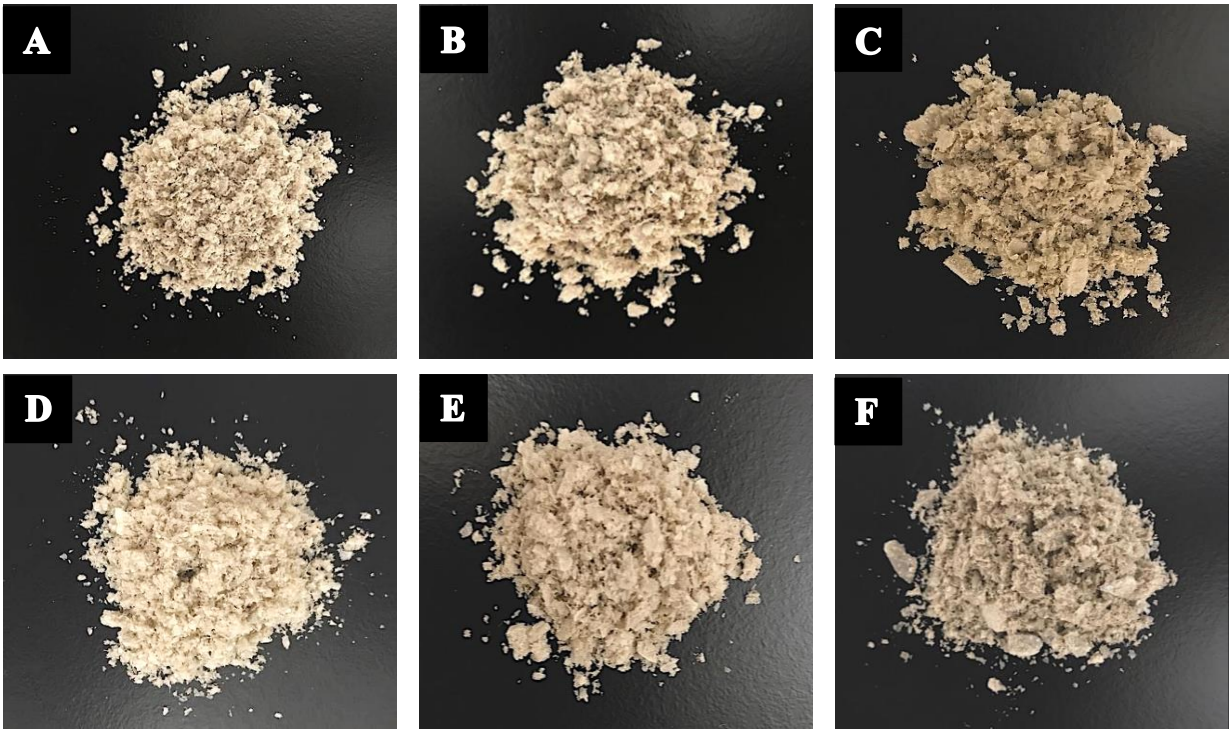

Figure S2. Freeze-dried α-tocopherol microparticles produced from WPI/OPN and CA or CO, according to treatments: CA WPI:OPN (23:1) (**A**); CA WPI:OPN (11:1) (**B**); CA WPI:OPN (7:1) (**C**); CO WPI:OPN (23:1) (**D**); CO WPI:OPN (11:1) (**E**); CO WPI:OPN (7:1) (**F**).

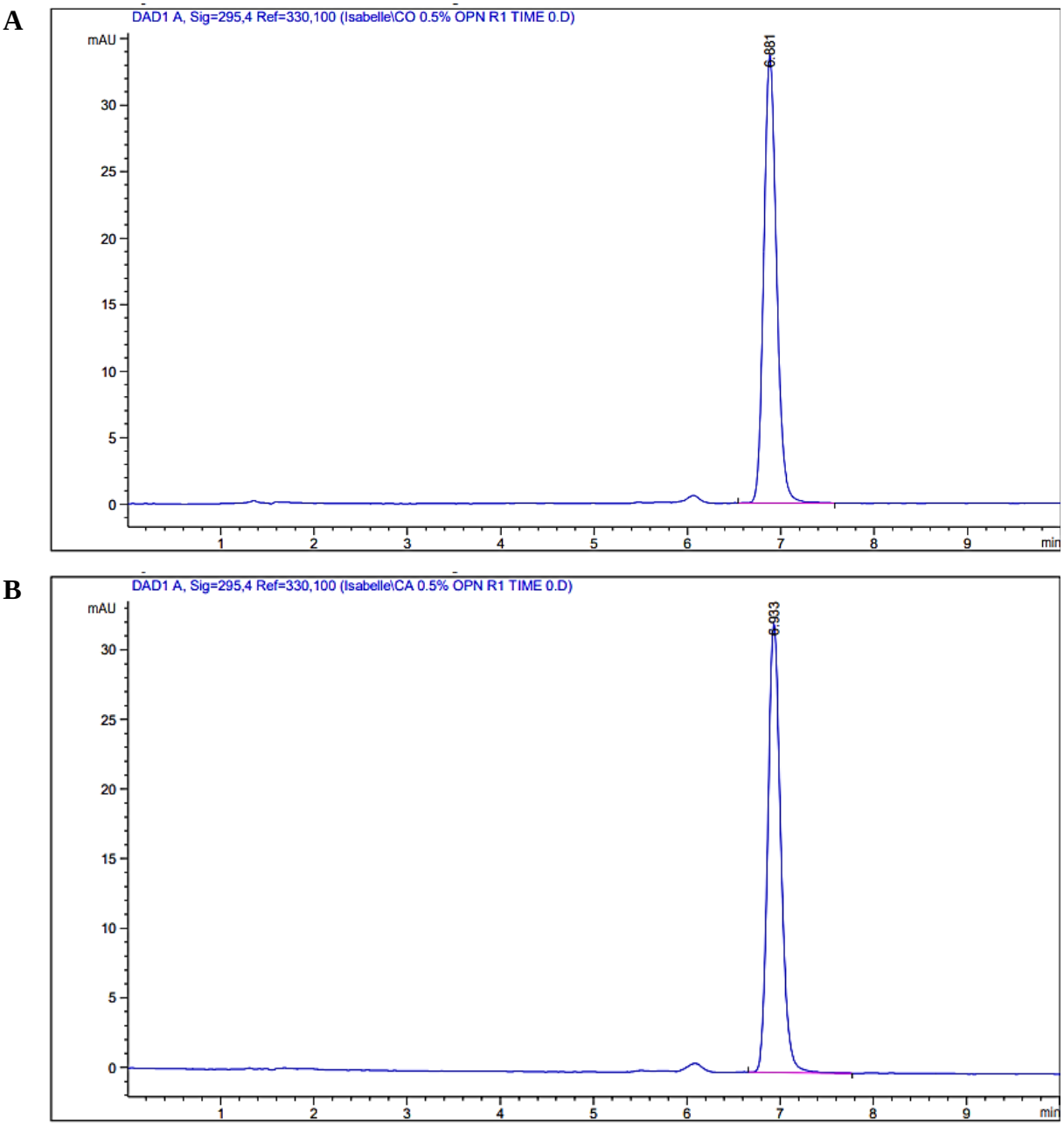

Figure S3. Chromatogram of α-tocopherol encapsulated in CO WPI:OPN (23:1) (**A**) and CA WPI:OPN (23:1) (**B**) microparticles.